5-20-2011

Determining biological roles of four unique Vernicia fordii acyl-CoA Binding Proteins

Steven Pastor
University of New Orleans

Determining biological roles of four unique *Vernicia fordii* acyl-CoA Binding Proteins

A Thesis

Submitted to the Graduate Faculty of the
University of New Orleans
in partial fulfillment of the
requirements for the degree of

Master of Science
in
Biological Sciences

by

Steven Pastor

B.S. University of New Orleans, 2008

May 2011

Acknowledgement

I would like to give special thanks to Dr. Jay Shockey for inviting me into his lab where I learned more about science then I could have imagined. He was very patient and guided me through what can sometimes be an arduous process of research. I especially appreciate all of the well-thought out feedback and that I was always placed into a position to succeed in order to obtain my goals. He never once denied discussing anything related to coursework, lab work, or even life and always understood that sometimes, certain things are important and need to be placed in the proper perspective. He has unparalleled foresight and a keen ability to adjust when things aren't producing as they should, like any great biologist would.

Thanks to the rest of the lab as well, as without them and their input, I would have had a difficult time staying motivated. I thank Ms. Catherine Mason, who was invaluable in her help on a daily basis with regard to not just laboratory techniques but helping me keep my sanity when things don't work. Also, thanks to Ms. Dorselyn Chapital for her guidance and someone I could count on for extra tools and some added fun on the side.

I really appreciate the efforts and attention to the entire process, from classwork to graduation processes and thesis work of Dr. Mary Clancy. Without her, none of this would be possible as she really was an irreplaceable asset both as a professor and a person. She was fantastic to talk to and always had a calm demeanor and a professional yet easy-going way of dealing with any situation. She helped me throughout undergraduate coursework and proved that she was without a doubt, one of the most valuable people anyone could have on their side in any situation.

I would also like to thank Dr. Wendy Schluchter for her additional aid and fantastic advice, especially as someone who helped me get my graduate studies started. Her guidance also

spread from my undergraduate career and into my graduate studies. She is a not only a great professor, but is very organized and always answers in a timely manner. She is incredibly helpful and has a passion and purpose in all of her duties.

Thanks to the University of New Orleans as a whole for all of the help I received throughout my long career, spanning from undergraduate studies into the end of my graduate research. The university went through a lot of changes since I started, some good and some bad, but it proved its resilience despite some of the extreme hardships the school had to endure. It will always be a large portion of my life that I dedicated to the university and it is appreciated.

Lastly, I would like to thank my family, for without their words, motivation, and input, I never would have finished. Thanks to my Mom, Kay Pastor, and my sisters, Lori and Erin, for their willingness to stand by me when things were going well and when things were frustrating. Their ardent backing of me always pushed me to do my best. Rest in peace to my father, Rodney Pastor, who I miss and appreciate all he taught me in life.

Table of Contents

List of Figures v

Abstract vii

Introduction 1

Materials and Methods 38

Results 56

Discussion 89

References 115

Vita 123

List of Figures

Figure number	*Figure Title*	*Page*
Figure 1-1.	Identification of Fatty Acids	11
Table 1-2.	*At*ACBPs compared to *Vf*ACBPs	24
Figure 1-3.	Pictures of an infected tung tree	31
Figure 1-4.	*Vf*ACBP3a hydropathy plot	33
Figure 1-5.	*Vf*ACBP3b hydropathy plot	33
Figure 1-6.	*At*ACBP3 hydropathy plot	34
Figure 1-7.	Eukaryotic soluble ACBPs	35
Figure 2-1.	Genome walking primers	40
Figure 2-2.	5'RACE primers	42
Figure 2-3.	5'RACE nested primers	42
Figure 2-4.	3'RACE primers	44
Figure 2-5.	3'RACE nested primers	44
Figure 2-6.	Full-length PCR primers	44
Figure 2-7.	Illustration of the split ubiquitin system	49
Figure 2-8.	Vector pB9	51
Figure 2-9.	Vector pEB218	52
Figure 2-10.	Vector pEB220	52
Figure 2-11.	Vector pE29	53
Figure 2-12.	Vector pB110	53
Figure 3-1.	BLAST of *Vf*ACBP3a and *Vf*ACBP3b	60-61

Figure 3-2.	BLAST of *Vf*ACBP3a and *Vf*ACBP3b	61
Figure 3-3.	Tung ACBP6 and ACBP3a critical binding residues	62
Figure 3-4.	qPCR: *Vf*DGAT2 and *Vf*FADX	64
Figure 3-5.	qPCR: *Vf*ACBP3a	65
Figure 3-6.	qPCR: *Vf*ACBP3b	65
Figure 3-7.	qPCR: *Vf*ACBP4	66
Figure 3-8.	qPCR: *Vf*ACBP6	66
Figure 3-9.	Expression data of *Vf*ACBPs and *Vf*DGAT2 and *Vf*FADX	68
Figure 3-10.	Split-ubiquitin plate results	70
Figure 3-11.	Split-ubiquitin interactions of the *Vf*ACBPs	71-73
Figure 3-12.	β-Galactosidase Assay results	74-75
Figure 3-13.	Bulk T_2 generation scatter plots	77
Figure 3-14.	*Vf*FADX transformed lines (*Vf*ACBP6)	78
Figure 3-15.	*Vf*FADX transformed lines (*Vf*ACBP3a)	79
Figure 3-16.	Wild type *Arabidopsis thaliana* plant lines (*Vf*ACBP3a)	82
Figure 3-17.	Wild type *Arabidopsis thaliana* plant lines (*Vf*ACBP6)	83
Figure 3-18.	Average values of *Vf*ACBP3a and *Vf*ACBP6 plant lines	85
Figure 3-19.	Brown and red seeds (*Vf*ACBP3a)	86
Figure 3-20.	Brown and red seeds (*Vf*ACBP6)	87

Abstract

High-value industrial oils are essential for many processes and have great economic and environmental impacts. The tung tree produces a high-value seed oil. Approximately 80% of tung oil is α-eleostearic acid, which has a high degree of unsaturation thus giving it properties as a drying oil. The identification of the biological components in tung is imperative to further the knowledge of its processes. Four unique tung acyl-CoA binding proteins, *Vf*ACBP3a, *Vf*ACBP3b, *Vf*ACBP4, and *Vf*ACBP6 were identified and the genes encoding them were cloned and analyzed to determine their biological roles. The *Vf*ACBPs were observed to be similar to other organisms' ACBPs, especially *Arabidopsis thaliana.* In addition, each gene was expressed in all tung tissues. They were shown to interact with *Vf*DGAT1 and *Vf*DGAT2, two known components of tung lipid metabolism. Finally, *Vf*ACBP3a and *Vf*ACBP6 were expressed in the seeds of transgenic plants to study the effects of *Vf*ACBP expression on seed lipid fatty acid content.

Keywords: acyl-CoA binding protein, *Vernicia fordii*, *Arabidopsis thaliana*, lipid biosynthesis, lipid metabolism, eleostearic acid, tung, Kennedy pathway, biofuel, industrial feedstocks, qPCR, split ubiquitin

Introduction

Alternate energy sources and their economic impacts

Fossil fuels power nearly everything in the modern world. Coal and natural gas power plants generate large amounts of electricity, distributed through countries by massive power grids. Gasoline and diesel are used as the primary energy sources for many vehicles. Ships, planes, rockets, motorcycles, and virtually everything else that moves uses some form of fossil fuel. The supply of fossil fuels on the planet is a finite resource, and is quickly dwindling, causing concerns about controlling steady supplies. At the same time, environmental concerns about fossil fuels are growing steadily. It is estimated that roughly 21.3 billion tons of carbon dioxide are generated by fossil fuels each year, with only about half of that absorbed by natural processes (ISTA Mielke GmbH Hamburg, 2002).

Fuel is necessary for everyday activities and extremely important for specific activities. Alternative fuel sources could alleviate the usage of current fuel sources without interruption of necessary processes. Some of the more popular forms of alternative energy include but are not limited to: solar energy, wind energy, hydroelectric energy, tidal energy and biomass. The positive aspects of alternative energy sources must outweigh the negatives greatly and provide a monetary advantage over current petroleum usage and main sources of energy. Determining whether alternative fuels provide advantages over the fossil fuels they displace requires thorough investigations into the inputs and outputs for their production and use life cycles over short and long periods of time.

In the most general sense, an alternative fuel is any substance that can be utilized in place of conventional fuels (Metzger, et. al., 2006). There has been much concern over creation and implementation of alternative fuels into current applications. Alternative fuels must provide

some specific benefits in order to replace any of the conventional fuels currently in use. In order to be a viable substitute for a fossil fuel, an alternative fuel should not only exceed any potential environmental benefits over the fossil fuel it replaces, but be at least economically competitive with it, and be producible in large quantities to make an impact on the high energy demands of modern societies. In addition, it must provide a net energy gain over the energy sources used to produce it.

There has been a growing interest in biofuels recently, which has largely been driven by rising energy prices, increasing energy imports, concerns about petroleum supply, and an increased recognition of the environmental consequences of fossil fuel uses. The production of biofuels, many of which are derived from biomass, require energy to grow crops and convert them to biofuels. These energy demands can have negative environmental impacts through movement and usage of agricultural chemicals, especially nitrogen, phosphorus, and various pesticides from farms to other regions of the environment (Biermann, et. al., 2000).

The usage of fossil energy may present more issues than simply deciding how cost-effective they are or characterizing their emissions. For example, there are environmental costs which cannot be captured in market prices, meaning a biofuel's impacts on society depends on not only cost-competitive properties, but also its environmental costs, influences, and benefits. This could mean that subsidizing biofuels that are typically economically uncompetitive can be justified if their environmental impacts are much less than for current alternatives. There was no biofuel that was cost competitive with any of the petroleum-based fuels without subsidy in 2005 (FAOSTAT, 2007). Ethanol's net production cost in 2005 was $0.46 per energy equivalent liter of gasoline (FAOSTAT, 2007), versus gasoline prices which averaged $0.44 per liter (FAOSTAT, 2007). Similarly, another biofuel, soybean oil, had an estimated production cost of

$0.55 per energy equivalent liter of diesel (FAOSTAT, 2007), compared to diesel prices that averaged $0.46 per liter (FAOSTAT, 2007). Since 2005, petroleum prices have risen (FAOSTAT, 2007), and this seems to have improved the cost competitiveness of biofuels. Again though, if biofuels prove to not be as cost competitive as expected, their production may still be profitable due to large subsidies. For example, the United States government provides subsidies of $0.20 per energy equivalent liter for ethanol and $0.29 for biodiesel (FAOSTAT, 2007). The producers of biodiesel and ethanol can also benefit from subsidies that lower corn and soybean prices.

One of the underlying issues with the utilization of biofuels is the effect it has on food sources. For example, in 2005, 14.3% of the United States' harvested corn was processed to produce 1.48×10^{10} liters of ethanol (FAOSTAT, 2007). This is energetically equivalent to 1.72% of the United States' usage of gasoline (FAOSTAT, 2007). Likewise, soybean oil, which made up 1.5% of the United States' soybean harvest in 2005, was used to produce 2.56×10^{8} liters of biodiesel, which was only 0.09% of Unites States' use of diesel (FAOSTAT, 2007). These results illustrate how little both soybean oil and corn oil contribute to gasoline and diesel usage in America; thus even devoting all sources to biodiesel and ethanol production would not offset production completely. Due to the fossil energy that is needed to produce ethanol and biodiesel, this devotion would allow for a net energy gain equal to only 2.4% and 2.9% of United States gasoline and diesel consumption respectively (FAOSTAT, 2007). Given this information, it is currently unrealistic to ascertain the maximal rates of biofuel supply since crops utilized in the process are integral in human and livestock consumption.

Within the next 50 years, the global demand for food is expected to increase (Gunstone, et. al., 2006), while the global demand for transport fuels is expected to increase even more

quickly compared to that of food (Metzger, et. al., 2006). Thus, it is imperative to provide any renewable energy supplies that would not cause adverse environmental impacts and, perhaps just as importantly, do not compete with food supply. As previously mentioned, biofuels from food sources can meet only a small portion of transportation energy needs and biofuels that are not food-based may be of greater importance over the long term. For example, there are biofuels such as synfuel hydrocarbons that can be produced with minimal agricultural requirements and lands with minimal pesticides, fertilizers, and fossil energy inputs, or even produced from agricultural residues (Durrett, et. el., 2008). These have the potential to provide fuel supplies with increased environmental benefits relative to petroleum or food-based biofuels.

The general impacts of oilseed crops

For thousands of years, oilseed crops, which are grown primarily for the oil contained in the seeds, have been produced to serve as food sources for humans and livestock, and as such, the fatty acid composition of storage oils is tailored towards the necessities of human and animal nutrition (Ohlrogge, Browse, 1995). There are a variety of nontraditional plant species; however, that accumulate large amounts of unusual fatty acids stored in their seed oils that have potential uses in industrial applications (Dyer, et. al., 2002). The identification of genes that are responsible for the synthesis, accumulation, and storage of these exotic fatty acids has made possible the production of oleochemicals in the seed oils of transgenic crops. Unfortunately, expression of certain transgenes has met with very limited success due to the low accumulation of the desired fatty acids (Dyer, et. al., 2002). As it stands, multiple genes will be required in order to efficiently synthesize and accumulate exotic fatty acids in transgenic hosts.

The tung tree

Tung is a subtropical tree with very limited agronomic characteristics, meaning, it has difficulty growing unless there are very specific accommodations made for its growth, and thus there is interest in producing tung-specific drying oils in more conventional, easier to grow, oilseed crops (Duke, 1979). The tung tree (*Vernicia fordii)* accumulates α-eleostearic acid, a trienoic fatty acid with conjugated double bonds (9*cis*, 11*trans*, 13*trans* octadecatrienoic acid; see Figure 1-1 for nomenclature and structures of fatty acids), utilized for industrial applications (Duke, 1983). As alluded to previously, a fatty acid that is industrially important is highly important in studies for transgenic crops aiming to provide alternatives to the traditional industrial energy sources. Currently, U.S. industries import the majority of tung oil from South America and China, and both the quality and price of the oil can fluctuate appreciably (FAOSTAT, 2007). Methods have to be developed for converting regular vegetable oils into industrial drying oils; such methods would have the potential to create new markets for vegetable oils while defining the minimal sets of genes that are necessary for the efficient accumulation of industrially-important fatty acids in transgenic hosts.

Usages of the tung tree

For the most part, tung has been known to be cultivated primarily for its oil (Duke, 1983). The oil that is pressed from tung seeds makes an exceptionally efficient wood finish. Tung oil dries quickly to form a tough, glossy, waterproof surface on the object it is coating. Tung oil is also used as a drying agent for paints and varnishes; as waterproofing for paper, cloth, and ceramic products; and in the manufacture of linoleum, oilcloth, inks, resins, artificial leather, lubricants, brake linings, and cleaning and polishing compounds. It is also used in coatings for food containers and electronic parts (Brown, Keeler, 2005). Interestingly, during World War II,

the Chinese developed a way to process tung oil to supplement gasoline, as a blended mixture, for motor fuel (Brown, Keeler, 2005). Although it is toxic, tung oil has been used to treat skin conditions and constipation (Brown, Keeler, 2005). In addition, tung extracts have recently shown potential as termite control compounds (Brown, Keeler, 2005).

With regard to this study, the most relevant piece of information is that tung produces a unique fatty acid in large quantity: α-eleostearic acid (Brown, Keeler, 2005). General properties of fatty acids and an exhaustive description of eleostearic acid will be described.

A visual description of the tung tree

Vernicia fordii, which is a species of the genus *Vernicia* in the spurge (Euphorbiaceae) family, is a round-crowned deciduous tree that has the potential to grow to roughly 30-40 ft (9.1-12.2 m) in size, but usually stays half that size upon completion of its growth cycle (Brown, Keeler, 2005). The flowers open before the leaves come out in early spring. It has several round-tipped ivory petals on its flowers that are streaked with orange. They are borne in long-stemmed clusters that consist of dozens of flowers (Duke, 1983). On the majority of the trees, all but one in each cluster are staminate male flowers. When the female flowers are pollinated, they develop into 2-3 in (5.1-7.6 cm) hard, round, green or purple-green fruits that can contain upwards of 1-15 seeds, but usually have about five on average. They ripen in the fall as the foliage turns yellow color (Duke, 1983).

Locations of the tung tree's growth

A large contingency of tung trees come from the subtropical foothills of western China (Duke, 1979). The trees are cultivated in China, Argentina, Paraguay, and, to a lesser extent, Africa and the southeastern region of the United States. There are many naturalized populations in the southeastern U.S. around abandoned commercial tung oil groves in the vicinities of

Tallahassee, Gainesville, and Marianna, Florida; in Bogalusa, Louisiana; and in Poplarville, Mississippi (Brown, Keeler, 2005).

A general description of Fatty acids

A fatty acid is a multiple-linked hydrocarbon that possesses a carboxyl (-COOH) group at one of its ends. The majority of fatty acids are straight-chain compounds containing an even number of carbon atoms (Rigaudy, Klesney, 1979). Their carbon chain-lengths can range anywhere from 2 to 80 but commonly are found in the 12 to 24 range (Rigaudy, Klesney, 1979). Fatty acids may be divided into four distinct classes, depending upon their chain length. Those which contain chain lengths of 2 to 6 are termed short-chain, 8 to 10 are termed medium-chain, 12 to 18 are termed long-chain, and greater than 20 are termed very long-chain fatty acids (Gunstone, Harwood, 2006). The physical and biological properties of fatty acids are highly dependent upon chain length. In addition, chain length is a crucial parameter in acyl chain contribution to membrane structure and stability (Gunstone, Harwood, 2006). As fatty acyl chain length is increased, melting point is increased while solubility is decreased. This effect results from the weak apolar interactions that determine how the membrane can interact with its surrounding environment. As an example, the restricted solubility of lipids in the surrounding aqueous milieu is dictated by the tendency of acyl chains to remain associated with one another as opposed to associating with the aqueous environment (Gunstone, Harwood, 2006). Similarly, responses to temperature fluctuations are modulated by the extent to which thermal influences allow the acyl chains to dissociate from one another and assume a much more randomized structure (Gunstone, Harwood, 2006).

There are two general types of fatty acids: saturated or unsaturated. Saturated fatty acids do not contain carbon-carbon double bonds, meaning they are saturated with hydrogen, as

opposed to unsaturated fatty acids that typically have anywhere from one to three double bonds (Christie, 1986). Some fatty acids may also contain additional functional groups such as hydroxyl, epoxy, conjugated, acetylenic, and many others that also may play specific roles in their conformations and functions (Christie, W.W., 1993). One of the more prominent abilities of fatty acids in a cell is to maintain the fluidity of a membrane. One of the major strategies that is incorporated by a cell in order to maintain membrane fluidity at physiological temperatures, is to change the composition of membrane phospholipids by adjusting the ratio of saturated to unsaturated fatty acids (Christie, W.W., 1993). Many times, unsaturated fatty acids can have profound effects on the fluidity and function of biological membranes. In a variety of organisms, unsaturated fatty acid homeostasis can be achieved by feedback regulation (Aguilar and de Mendoza, 2006). In the majority of plant tissues, approximately 75% of the fatty acids they contain are unsaturated (Aguilar and de Mendoza, 2006).

Saturated fatty acids are straight chains, with free rotation about the carbon-carbon double bonds. This property allows them to pack closely together and produce a membrane that is virtually solid at low temperatures, adversely impacting membrane fluidity and thus a cell's survival. When a more loosely packed membrane structure is more advantageous, the rigidity of the lengthy saturated acyl chains can be contravened by acyl chains with double bonds (Gunstone, Harwood, 2006). A carbon-carbon double bond in unsaturated fatty acids is introduced by a desaturase reaction and produces a bend in the carbon chain. Upon the introduction of a double bond of cis (Latin for "on the same side") geometric configuration, a bend of the chain is introduced that moves the straight chain approximately 30° away from the original linearity of the saturated chain (Gunstone, Harwood, 2006). Also, double bonds are non-rotating and restrict any acyl chain movement (Gunstone, Harwood, 2006). The result is that Van

der Waals forces expand the distance between chains, thereby decreasing the potential for any chain to chain interactions (Gunstone, Harwood, 2006). Furthermore, around the double bond, some charge concentration can increase the polarity of the acyl chain (Gunstone, Harwood, 2006). While double bonds have the potential to cause bends or curved shapes within the biological membrane, the extent to which they do this is poorly understood. Physical and biochemical data, however, have clearly shown that unsaturated acids decrease membrane rigidity and melting point (Gunstone, Harwood, 2006).

The introduction of additional bends in the fatty acid chain can occur due to multiple desaturase reactions. The membrane bilayer or lipid body containing the fatty acid cannot pack into a regular structure due to the bends introduced into the hydrocarbon backbone, which allows the membrane to remain more fluid at low temperatures (Hamilton, 2007). The most prominent strategy that is employed by the cell in order to ensure that membranes remain sufficiently fluid to maintain cellular function at any temperature is to change the ratio of saturated to unsaturated fatty acids (Hamilton, 2007). An increase in temperature is followed by an increase in saturated with a concomitant decrease in unsaturated fatty acids, while decreasing temperatures results in an increase in the amount of unsaturated with a decrease in saturated fatty acids in cell membranes (Gunstone, Harwood, 2006).

The acyl chain length and both the number and positions of double bonds, heavily influence the fluidity, permeability and stability of biological membranes within membrane phospholipids. As such, fatty acids are named using these parameters since the physiological properties of unsaturated fatty acids are heavily dependent upon the length and position of double bonds (IUPAC Compendium of Chemical Terminology, 1997). To name fatty acids, two numbers separated by a colon, for example, 18:1, denotes the number of carbon atoms (the

number before the colon) followed by the number double bonds (the number after the colon). In addition to the number system other naming conventions are also used, since bond position and orientation are important contributors to the physiological properties of fatty acids. The carbons that are counted from the carboxyl (-COOH) end of the fatty acid are deemed to be in the delta (Δ) position, while those that are counted back from the terminal carbon are deemed to be in the omega (ω) position (IUPAC Compendium of Chemical Terminology, 1997). The delta (Δ) nomenclature is assigned to the position of an individual double bond, or the specificity of an enzyme that is inserting it. The (n-) nomenclature is used to designate a fatty acid within a family of structurally related acids. There is also still a wide use of the (ω-) designation in order to designate the position of a double bond from the methyl end. As an example of this, linoleic acid (18:2 ω-6), is an 18-carbon chain containing 2 double bonds, that has the first double bond in the sixth position from the methyl end. Also, linoleic acid can be designated as $18{:}2\Delta^{9,12}$ to indicate that there are 2 double bonds, one at the 9^{th} and one at the 12th carbon position, counting from the carboxyl end of the fatty acid (IUPAC Compendium of Chemical Terminology, 1997). The double bonds are in the cis-configuration in most naturally occurring fatty acids, and thus it is assumed that all double bonds are cis, and separated by a single methylene group, unless noted otherwise (IUPAC Compendium of Chemical Terminology, 1997). Using linoleic acid as an example again, it is described by $18{:}2cis\Delta^{9,12}$ to illustrate both the position and orientation of the double bonds. Figure 1-1 illustrates an example of a fatty acid along with some naming conventions.

(A)

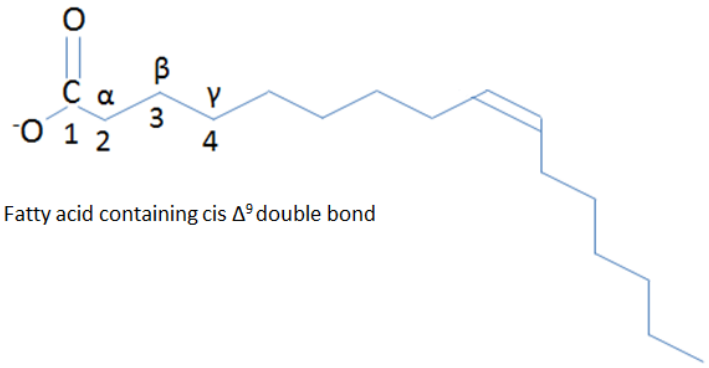

(B)

Non-polar Polar

$CH_3(CH_2)_N–COO^-$

(C)

14:0	Myristic acid
16:0	Palmitic acid
18:0	Stearic acid
$18:1cis\Delta^{9}$	Oleic acid
$18:2cis\Delta^{9,12}$	Linoleic acid
$18:3cis\Delta^{9,12,15}$	Linolenic acid
$20:4cis\Delta^{5,8,11,14}$	Arachidonic acid

Figure 1-1. Identification of fatty acids. Part A illustrates the basic structure of a fatty acid through oleic acid, a monounsaturated fatty acid containing a *cis* double bond at the ninth carbon, as an example. Part B illustrates the amphipathic nature of a fatty acid. Part C lists many of the common fatty acids; the first three being saturated and the last four being unsaturated.

Tung seed oil

The tung produces fruit once a year during the summer months, and the large seeds of these fruit contain roughly 50% dry weight oil (Brown, Keeler, 2005). As mentioned earlier, this oil consists of about 80% eleostearic acid (wt/wt total fatty acids) which is a trienoic fatty acid with conjugated double bonds (Duke, 1983). This conjugated bond system can be easily

oxidized, resulting in the polymerization of the oil and also results in the formation of tough resistant films (Brown, Keeler, 2005). Tung oil also contains smaller amounts of oleic, linoleic and palmitic acids (Duke, 1983). Eleostearic acid also occurs as a beta acid (9, 11, 13 all *trans*), typically due to irradiation of the alpha form of the acid (Cahoon, et. al., 2006).

Biosynthetic pathways

Cell membranes are comprised of phospholipids, each of which contains two fatty acids. In addition, fatty acids are also used for protein modifications. Fatty acid metabolism, therefore, consists of catabolic processes which generate energy and primary metabolites from fatty acids, along with anabolic processes that create biologically important molecules from fatty acids and other dietary carbon sources (Browse, Sommerville, 1991).

Plants synthesize a very large variety of fatty acids; however, only a few of these are major and common constituents (Napier, 2007). Generally speaking, long chain fatty acids are synthesised *de novo* from smaller precursors that are ultimately derived from photosynthate (Gurr, et. al., 2002). There are two enzyme systems that are incorporated: acetyl-CoA carboxylase and fatty acid synthase (Gurr, et. al., 2002). This synthesis produces end products that are usually palmitate and stearate with the latter predominating in many plants by as much as 2-3 times that of palmitate (Gurr, et. al., 2002). Most stearate is desaturated by a stromal acyl-acyl carrier protein desaturase to form oleic acid (Whittle, et. al., 2005). The long chain acids can be subjected to elongation, desaturation, and further modifications or processes (Gurr, et. al., 2002). As opposed to acetyl-CoA carboxylase and fatty acid synthase, which are soluble enzymes, the elongases are membrane-bound and are situated in the endoplasmic reticulum (Gunstone, Harwood, 2006). Recently, the details of such reactions have begun to be elucidated

at the molecular level (Gunstone et. al., 2006). The elongases are coded by FAE genes while the desaturases are coded by FAD genes (Gunstone, Harwood, 2006).

As for the tung tree, some plants can produce unusual fatty acids in their seed oils, many of which having industrial applications. These include hydroxyl fatty acids, cyclopropane fatty acids, epoxy fatty acids and conjugated unsaturated fatty acids, to name a few (Gunstone, Harwood, 2006). It is important to mention that these unusual fatty acids accumulate preferentially in triacylglycerols (TAGs) and are essentially excluded from membrane acyl lipids, presumably because they would disrupt or impair function (Gunstone et. al., 2006).

Triacylglycerols (TAGs)

Almost all of the commercially important fats and oils of both animal and plant origin consist almost exclusively of the simple lipid class, triacylglycerols (Baud, Lepiniec, 2010). This is inclusive of all the vegetable oils, like those from corn, olive, palm, and sunflower, and the animal fats, like tallow, lard and butter, as well as many commercial products such as margarines. The more prominent animal triacylglycerols are either fats from adipose tissue or the milk fats, where their main function may be energy storage, but some triacylglycerols may confer more dynamic roles (Baud, Lepiniec, 2010). An example of these triacylglycerols would be those of blood plasma or the liver. Likewise, in plants, seed oils provide an energy source and structural fatty acids for the developing embryo (Biermann, et. al., 2000).

More specifically, triacylglycerols consist of the trihydric alcohol glycerol that is esterified with long-chain fatty acids. Upon the esterification of the three primary hydroxyl groups with different fatty acids, there results a triacylglycerol that can be asymmetric and thus can display optical activity, although this activity is usually far too low to be measured (Li-Beisson, et. al., 2010). Problems arise in the application of the conventional D/L or R/S systems

that designate enantiomers without ambiguity (as with simple molecules), due to the complexity of the mixtures of triacylglycerols that are found throughout nature (Li-Beisson, et. al., 2010). These problems can be circumvented; however, if the stereochemistry of triacylglycerols and that of other glycerolipids is described by the stereospecific numbering system, termed *sn*, as recommended by the IUPAC-IUB (IUPAC Compendium of Chemical Terminology, 1997).

Biosynthesis of triacylglycerols

All eukaryotic organisms, along with some prokaryotes, have the capability to synthesize TAGs and how this synthesis occurs has been studied extensively in plants and animals (Mu and Høy, 2004, Murphy, 2001). There are many different cell types and organs that are able to synthesize TAGs. In animals, the predominant organs that participate in this synthesis with the greatest activity are the liver and intestines; however, most of the body stores TAGs in adipose tissue (Murphy, 2001). Within all types of cells, TAGs are stored as cytoplasmic lipid droplets, also known as fat globules, oil bodies, lipid particles, or adiposomes. These are encased by a monolayer of phospholipids and hydrophobic proteins, including perilipins in adipose tissue or oleosins in seeds. These lipid droplets can be distinguished as distinctive organelles, complete with their own unique metabolic pathways and enzymes. Mycobacteria and yeast have similar lipid inclusions (Kohlwein, 2010). Lipids mainly function as a store of energy and a reserve of essential fatty acids, but they may also exist as a measure of protection to enable the eradication of the excess of biologically active and potentially harmful lipids including free fatty acids, diacylglycerols (DAGs), cholesterol esters and coenzyme A esters (Murphy, 2001).

Two principal biosynthetic pathways for TAG synthesis have been elucidated, the sn-glycerol-3-phosphate pathway, also known as the Kennedy pathway, which predominates in adipose tissue and the liver, and a monoacylglycerol pathway located in the intestines (Coleman

and Lee, 2004). A third pathway has been recognized in a few animal tissues and maturing plant seeds, in which a diacylglycerol transferase (DAG:DAG transacylase) is involved (Coleman and Lee, 2004). Of these three pathways, perhaps the most important is the *sn*-glycerol-3-phosphate pathway, which was first described by Professor Eugene Kennedy and colleagues in the 1950s (Coleman and Lee, 2004). More than 90% of the liver TAGs are produced by the Kennedy pathway (Schittmayer and Birner-Gruenberger, 2009).

In this pathway, the major source of the glycerol backbone is believed to be *sn*-glycerol-3-phosphate, which is assembled by the catabolism of glucose via glycolysis, or to a lesser degree by the activity of glycerol kinase on free glycerol (Coleman and Lee, 2004). There is evidence, however, that a portion of the glycerol is produced in a *de novo* fashion by glyceroneogenesis through pyruvate (Coleman and Lee, 2004).

After these events, all subsequent reactions take place in the endoplasmic reticulum (Coleman and Lee, 2004). Initially, a fatty acid coenzyme A ester esterifies *sn*-glycerol-3-phosphate in a reaction that is catalyzed by glycerol-3-phosphate acyltransferase (GPAT) at the *sn*-1 position to form lysophosphatidic acid. Lysophosphatidic acid is then acylated by an acylglycerophosphate acyltransferase in the *sn*-2 position, leading to the formation of an important intermediate in the biosynthesis of all glycerolipids: phosphatidic acid (Coleman and Lee, 2004).

The removal of the phosphate group is catalyzed by the enzyme phosphatidic acid phosphohydrolase (PAP). The importance of PAP is also illustrated in its ability to produce diacylglycerols as key intermediates in the biosynthetic production of phosphatidylcholine and phosphatidylethanolamine (Murphy, 2001). In direct opposition to the processes involved in and responsible for the biosynthesis of phospholipids in mammals, much of the phosphatase activity

culminating in the biosynthesis of triacylglycerol resides in three inter-related cytoplasmic proteins, termed lipin-1, lipin-2, and lipin-3 (Murphy, 2001). Each of the lipins is specific for certain tissues, and each seems to have distinct expression and functions. Lipin-1 (PAP1), however, is responsible for all the PAP activity in adipose tissue and skeletal muscle. In response to elevated levels of fatty acids within cells, lipin-1 is translocated to the endoplasmic reticulum from the cytoplasmic compartment of cells. Lipin-1 requires Mg^{2+} ions and is inhibited by N-ethylmaleimide, as opposed to the membrane-bound activity responsible for synthesizing diacylglycerols as a phospholipid intermediate. The latter is independent of Mg^{2+} ion concentration and is also not sensitive or reactive to the inhibitor (Coleman and Lee, 2004).

Lastly, the resulting 1,2-diacyl-*sn*-glycerol is acylated by a diacylglycerol acyltransferase (DGAT) to lead to form triacyl-sn-glycerol (Coleman and Lee, 2004). The glycerol-3-phosphate acyltransferase has the lowest specific activity of these enzymes, so this step is potentially rate-limiting (Coleman and Lee, 2004). Moreover, DGAT is the enzyme that is dedicated to the formation of triacylglycerols, making DGAT an attractive anti-obesity target for the pharmaceutical industry (Mu and Høy, 2004).

In the third and less well-known biosynthetic pathway, the synthesis of triacylglycerols is dependent upon an acyl-CoA independent transacylation among two racemic diacylglycerols (Zammit, et. al., 2008). This reaction is catalyzed by a diacylglycerol transacylase, and was first observed in intestinal microvillus cells (Zammit, et. al., 2008). The two diacylglycerol enantiomers engage equally in the reaction for the transfer of a fatty acyl group with the propagation of triacylglycerols along with a 2-monoacyl-sn-glycerol. Seed oils have been observed to contain a similar reaction to these processes (Zammit, et. al., 2008).

The synthesis of triacylglycerols in plants

Within plant seeds, fatty acid storage occurs in the embryo or endosperm tissues as triacylglycerols (TAGs) within lipid droplets. These lipid droplets reside in close vicinity with glyoxysomes (peroxisomes) (Dugail and Hajduch, 2007). The vast majority of the enzymes that are necessary to oxidize fatty acids produced from the TAGs via acetyl-CoA to four-carbon compounds comes from glyoxysomes. These organelles also supply structural elements, well before seedlings develop the ability to photosynthesize (Dugail and Hajduch, 2007).

The synthesis of triacylglycerols occurs in developing seeds by way of the Kennedy pathway, as described above. There is an accumulation of oil droplets in the endoplasmic reticulum by mechanisms that are currently not well understood (Coleman and Lee, 2004). These oil droplets are surrounded by a monolayer of proteins and phospholipids, which in *Arabidopsis* include the oleosins, a caleosin, a steroleosin, an aquaporin, and a glycosylphosphatidylinositol-anchored protein (Voelker and Kinney, 2001). Lipases are activated upon germination, and lipolysis lipid breakdown initiates at the surface of oil bodies. It is at these oil bodies that the oleosins, which are the most prominent structural proteins, assist in the docking of lipases. There have been many lipases that have been cloned from many species of plants (Schittmayer and Birner-Gruenberger, 2009). These lipases are prototypical α/β-hydrolases, containing a conserved catalytic triad of serine, histidine, and aspartic acid or glutamic acid. This class of proteins is capable of hydrolyzing triacylglycerols but not phospholipids or galactolipids. Perhaps the most important lipase is the sugar-dependent lipase 1 (SDP1) (Schittmayer and Birner-Gruenberger, 2009). It is a patatin-like lipase that is very much like the mammalian adipose triacylglycerol lipase, and it is found on the surface of the oil body. SDP1 is mostly active mainly against triacylglycerols for the purpose of generating diacylglycerols, but has been

suggested to work in concordance with mono- and diacylglycerol lipases to propagate glycerol and free fatty acids. It is not known how the products are transported to the peroxisomes for further metabolic processes, and these transport processes are controlled by a specific regulatory network. As an aside, in plants, the oil droplets in the anthers of flowers produce the lipids and oleosins that are capable of coating and stabilizing pollen (Schittmayer and Birner-Gruenberger, 2009).

Lipid droplets' size and triacylglycerol content in many yeast vary in the different stages of growth and development (Kohlwein, 2010). The majority of the biosynthetic and catabolic enzymes that participate in the metabolism of triacylglycerols are conserved among yeast and mammals, and yeast currently prove to be the most useful model for research involving the homeostasis of triacylglycerols (Kohlwein, 2010).

Lipid biosynthesis in tung

This study is focused on the identification and functional analysis of the enzymes and other proteins that are involved in tung oil biosynthesis, specifically acyl-coA binding proteins (ACBPs) as will be discussed. All of the enzymes and cofactors required for the synthesis of polyunsaturated fatty acid components in tung oil, including eleostearic acid, have been identified. This large list of enzymes includes of an oleate desaturase (*FAD2*), a diverged *FAD2* (*FADX*), three isoforms of ω-3 fatty acid desaturase (*FAD3*), four isoforms of cytochrome b_5, and two isoforms of NADH cytochrome b_5 reductase (Shockey, et. al., 2006). In earlier work it was shown that the expression of the tung *FADX* in transgenic *Arabidopsis*, tobacco, or yeast cells only resulted in accumulation of a small percentage of eleostearic acid compared to other fatty acids produced (Shockey, et. al., 2006). Given this low accumulation, it is obvious that additional enzymes will be necessary for the synthesis and high-yield accumulation of eleostearic

acid in seed oils that are transgenically produced. In addition, the full-length or partial gene sequences have been identified for the primary acyltransferases that may channel eleostearic acid into storage oils: *GPAT, LPAAT, DGAT1, DGAT2,* and *PDAT.* Full-length *Arabidopsis* counterparts for these enzymes have also been obtained. There have also been several isoforms of long chain acyl-CoA synthetases (*LACS*) and acyl-CoA binding proteins (*ACBP*s) that have been cloned as well. The goal of this study is to study the role of ACBPs in developing tung seeds. These tung-derived enzymes may show preferential incorporation of eleostearic acid into storage oils in comparison to orthologous proteins from *Arabidopsis* or yeast cells.

Acyl-CoA Binding Proteins (ACBPs)

It has long been known that lipids are important in many biological processes. In order to deliver their functions, some of them require transport within and between subcellular compartments during lipid metabolism (Faergeman, et. al., 2007). In plant cells, lipid-transfer proteins (LTPs) and acyl-CoA-binding proteins (ACBPs) have been identified as potential candidates for the transfer of lipids within the cell (Burton, et. al., 2005). LTPs are small proteins, roughly 9 kDa, while the various isoforms of ACBPs in plants range from 10 to 73 kDa in size (Burton, et. al., 2005). Many eukaryotes studied were found to contain the 10-kDa small, soluble ACBP (Yurchenko, et. al., 2009, Xiao, et. al., 2009, Mogensen, et. al., 1987, Schjerling, et. al., 1996, Taskinen, et. al., 2007). There is also evidence of several larger ACBPs, many of which have yet to be characterized, while others are better studied (Chye, et. al., 1999, Chye, et. al., 2000, Leung, et. al., 2006). Currently, there is a shortage of information on many of these larger proteins with acyl-CoA-binding domains available from the data mining of sequenced genomes (Burton, et. al., 2005). A total of 30 plant *ACBP* gene sequences have been published (Faergeman, et. al., 2007).

Acyl-Coenzyme A binding protein (ACBP) is named after the protein's ability to bind specifically to CoA esters of fatty acids (Burton, et. al., 2005). ACBP, is known to be found in some prokaryotes (Alves-Bezerra, et. al., 2010), some species of yeast (Schjerling, et. al., 1996), and in animals (Larsen, et. al., 2006, Mandrup et. al., 1991, Taskinen, et. al., 2007) and plants (Chye, et. al., 1998, Yurchenlo, et. al., 2009, Xiao, et. al., 2009). The biological function of ACBP is not well known; however, analysis of the yeast gene has illustrated that ACBP may participate as a housekeeping gene, thus suggesting that ACBP appears to be important for essential biochemical functions in cells (Schjerling, et. al., 1996). In addition, the nuclear magnetic resonance (NMR) structures of the bovine ACBP have been determined for both the apo-protein and for the ACBP complexed with palmitoyl-CoA (Andersen et. al., 1991).

Long chain acyl-CoA esters function as important intermediates in the synthesis of lipids and the degradation of fatty acids (Faergeman, Knudsen, 2009). Aside from this role as intermediates, long chain acyl-CoA esters have been implicated in both regulation of intermediary metabolism and the regulation of gene expression (Faergeman, Knudsen, 2009). Long chain acyl-CoA esters are amphipathic molecules which partition into phospholipid vesicles (Faergeman, Knudsen, 2009). They are believed to inhibit many cellular functions and a host of enzymes at low concentrations (Faergeman, Knudsen, 2009). Thus, a specific and specialized acyl-CoA pool former and transporter is necessary for the function of long chain acyl-CoAs as intermediates in the metabolism of lipids and as signaling molecules (Faergeman, Knudsen, 2009). ACBP is found to fulfill this role in the cytoplasm of the cell (Post-Beittenmiller, et. al., 1992).

The majority of the eukaryotic ACBPs that have been investigated are low molecular weight, about ~10 kDa, cytosolic proteins that are highly conserved in their amino acid

sequences among many species (Burton, et. al., 2005, Xiao and Chye, 2009). There have been several ACBP homologues that were identified in all four eukaryotic kingdoms, Animalia, Plantae, Fungi and Protista, in addition to eleven species of eubacteria (Yurchenko, et. al., 2009, Xiao, et. al., 2009, Mogensen, et. al., 1987, Schjerling, et. al., 1996, Taskinen, et. al., 2007, Burton et. al., 2005). It is important to note that most of the bacteria that contain ACBPs have been shown to be pathogenic to plants or animals, suggesting that their pathogens may have acquired a host ACBP via horizontal gene transfer (Burton, et. al., 2005). ACBPs appeared very early in plant evolution, implying that there is a very important role of ACBPs in acyl-CoA metabolism in plant species (Faergeman, et. al., 2007).

The acyl-CoA-binding domain is well-conserved in each ACBP and allows it to bind acyl-CoA esters (Xiao and Chye, 2009). This has been observed in *in vitro* binding assays, like the Lipidex assay, where recombinant ACBPs have been observed to bind CoA esters (Leung, et. al., 2006). Recombinant *Arabidopsis* ACBPs that have been expressed in *Escherichia coli*, have been utilized to establish the function of the acyl-CoA binding domain through the usage of site-directed mutagenesis followed by *in vitro* binding assays (Leung, et. al., 2006, Xiao and Chye, 2009). A few of the *Arabidopsis* ACBPs have also been observed to bind phospholipids in filter binding assays (Chen, et. al., 2008). An example of this is a recombinant ACBP6 that binds phosphatidylcholine (PC) (Chen, et. al., 2008). The recombinant *Arabidopsis* ACBPs show certain preferences for various acyl-CoA esters and phospholipids in *in vitro* binding assays (Chen, et. al., 2008, Leung, et. al., 2006, Xiao, Chye, 2009). Because of this, it has been hypothesized that different subclasses of ACBPs in *Arabidopsis* do not have redundant functions (Leung, et. al., 2006).

Acyl-CoA binding to a single binding site on ACBP has been demonstrated by several *in vitro* studies (Chen, et. al., 2008, Leung, et. al., 2006, Xiao, Chye, 2009, Andersen, et. al., 1991, Faergeman et. al., 1996). It has been calculated that the stoichiometric values for hexadecanoyl-CoA binding by bovine and rat ACBP were approximately 1 mol/mol (Andersen, et. al., 1991). The ACBP binding site is arranged in such a manner that only acyl-CoA esters and not any other certain types of ligand can bind strongly (Andersen, et. al., 1991). Therefore, both the acyl chain and CoA portions are necessary for the correct orientation and the strong interaction between the ligand and the ACBP (Andersen, et. al., 1991). Consequently, ACBP binds specifically to acyl-CoA esters as opposed to free fatty acids, free CoA, ATP, NADH, NADPH, GABA, palmitoyl carnitine, or cholesterols (Andersen, et. al., 1991, Faergeman et. al., 1996).

ACBPs from different organisms each specifically bind to acyl-CoA esters via a one-to-one binding process (Andersen, et. al., 1991, Faergeman et. al., 1996). ACBPs cannot bind free fatty acids; however, they can bind Coenzyme A alone (Faergeman et. al., 1996). The 3' phosphate of ribose of the CoA moiety has been observed to contribute up to 40% of the complete binding energy (Andersen, et. al., 1991), thus indicating that the head group of the CoA performs an important role in dictating the specificity for the binding capacity of the acyl-CoA esters (Faergeman et. al., 1996).

Through multiple *in vitro* experiments, ACBP's ability to perform as an intracellular acyl-CoA transporter and pool former has been demonstrated (Knudsen, et. al., 2000, Kader, 1996, Xiao and Chye, 2009). It is capable of acting as a powerful protector of acetyl-CoA carboxylase, acyl-CoA synthetase, and adenylate translocase against the inhibition provided by long chain acyl-CoA esters (Knudsen, et. al., 2000). In addition, ACBP may be capable of

mediating intermembrane acyl-CoA transport and has the ability to protect long chain acyl-CoA esters from the hydrolysis of cellular acyl-CoA hydrolases (Knudsen, et. al., 2000).

Arabidopsis thaliana acyl-CoA binding proteins

In *Arabidopsis*, six genes encode ACBPs (Xiao and Chye, 2009). They are designated as ACBP1 through ACBP6 (Xiao and Chye, 2009). ACBP1 and ACBP2 are membrane-associated proteins (Chye, et. al., 2000), ACBP3 is extracellularly-targeted (Leung, et. al., 2006), and ACBP4 and ACBP5 are cytosolic proteins containing kelch-motifs (Li, et. al., 2008). Acyl-CoA-binding domains in all 6 ACBPs have been observed to bind long-chain acyl-CoA esters *in vitro*, with varying affinities, perhaps suggestive of their non-overlapping roles in plant lipid metabolism (Xiao and Chye, 2009). These ACBPs are mostly conserved at the acyl-CoA-binding domain and range in size from 10.4 to 73.1 kD (Xiao and Chye, 2009). C-terminal ankyrin repeats in ACBP1 and ACBP2 and kelch motifs in ACBP4 and ACBP5, can potentially mediate protein-protein interactions, while N-terminal transmembrane domains in ACBP1 and ACBP2 target them to the endoplasmic reticulum (ER) and the plasma membrane (PM) (Chye, et. al., 2000).

Vernicia fordii acyl-CoA binding proteins

To date, there have been 4 unique acyl-CoA binding proteins identified in *Vernicia fordii*, which have been named based upon the *Arabidopsis thaliana* nomenclature adapted by Chye and her colleagues (Xiao and Chye, 2009). The *Vernicia fordii* ACBPs include *Vf*ACBP3a, *Vf*ACBP3b, *Vf*ACBP4, and *Vf*ACBP6. These were named as such due to sequence similarities to the *Arabidopsis* ACBPs. This similarity was found by utilizing the BLAST search engine comparing the sequences obtained for the *V. fordii* ACBPs to the sequences of the *A. thaliana* ACBPs. To date, there have been no known studies or elucidation of the sequences of the tung

ACBPs. The purpose of this study is to elucidate the roles of ACBPs in tung. Figure 1-2 shows both the naming conventions of *Vernicia fordii* ACBPs and *Arabidopsis thaliana* ACBPs as determined by Chye.

A. thaliana	Base Pairs	Localization	*V. fordii*	Base Pairs	Localization
ACBP1	1014	Plasma membrane and ER	ACBP1		
ACBP2	1062	Plasma membrane and ER	ACBP2		
ACBP3	1086	Extracellular	ACBP3a ACBP3b	819 1125	Extracellular? Extracellular?
ACBP4	2004	Cytoplasm	ACBP4	1995	
ACBP5	1944	Cytoplasm and Peroxisome	ACBP5		
ACBP6	276	Cytoplasm	ACBP6	276	Cytoplasm

Table 1-2. *Arabidopsis thaliana* Acyl-CoA Binding Proteins (ACBPs) as compared to *Vernicia fordii* ACBPs.

Comparison of plant ACBPs

Arabidopsis thaliana ACBPs have various structural features that not only provide a unique way to identify each one but also determine their functions. ACBP1 and ACBP2, of which there are currently no known tung counterparts, contain ankyrin repeats (Chye, et. al., 2000), which are 33-residue motifs in proteins consisting of two alpha helices separated by loops that are amongst the most common protein-protein interaction motifs in nature (Chye et. al., 2000).

Dr. M. L. Chye observed enhanced cold acclimation provided to *Arabidopsis thaliana* via a reduction in ACBP1 but not in ACBP2, 338 amino acids and 334 amino acids with molecular weights of 37.5 and 38.5 kDa respectively, despite the sequence homology (Identities = 258/349 (74%), Positives = 294/349 (85%)) (Chye et. al., 2000). ACBP1 contains an amino-terminal transmembrane domain that targets it to the plasma membrane and the endoplasmic reticulum. The function of ACBP1 was analyzed by overexpression in transgenic *Arabidopsis* plants. Five-week-old wild-type, *acbp1* mutant, and ACBP1-complemented plants were grown at 23°C and then subjected to freezing treatment ranging from -4°C to -12°C. The plants were then thawed

overnight at 4°C and recovered in a growth chamber (16-h-light [23°C]/8-h-dark [21°C] photoperiods) for 7 days. *At*ACBP1 overexpressors showed reduction in several species of diunsaturated phosphatidylcholine (PC), prompting an investigation into whether they were altered in response to freezing stress. *At*ACBP1 overexpressors demonstrated increased freezing sensitivity accompanied by a decrease in PC and an increase in phosphatidic acid (PA), while *acbp1* mutant plants showed enhanced freezing tolerance associated with PC accumulation and PA reduction. It was also shown that the binding of a recombinant eukaryotic *At*ACBP (ACBP1) to PA, indicating the possibility of enhanced PA interaction in ACBP1 overexpressors.

Since phospholipase Dα1 (PLDα1) promotes the hydrolysis of PC to PA, *PLDα1* expression was examined and was observed to be higher in *At*ACBP1 overexpressors than in *Atacbp1* mutant plants. In contrast, the expression of PLDδ, which plays a positive role in freezing tolerance, declined in the *At*ACBP1 overexpressors but increased in *acbp1* mutant plants. Since *At*ACBP1 is localized to the endoplasmic reticulum and plasma membrane, it may regulate the expression of PLDα1 and PLDδ by maintaining a membrane-associated PA pool through its ability to bind PA. Moreover, both genotypes showed no alterations in proline and soluble sugar content or in cold-regulated (*COR6.6* and *COR47*) gene expression, suggesting that the *At*ACBP1-mediated response is PLD associated and is independent of osmolyte accumulation (Chye et. al., 2008).

Arabidopsis thaliana ACBP2 was observed to interact with farnesylated protein 6 (*At*FP6), which has a metal-binding motif (M/LXCXXC). Yeast two-hybrid analysis and *in vitro* assays showed that an *At*ACBP2 derivative lacking ankyrin repeats did not interact with *At*FP6, indicating that the ankyrin repeats mediate protein–protein interaction. Fluorescent-tagged *At*ACBP2 and *At*FP6 transiently co-expressed in tobacco were both targeted to the plasma

membrane. Reverse transcriptase polymerase chain reaction and northern blot analyses revealed that *At*FP6 mRNA was induced by cadmium (Cd(II)) in *A. thaliana* roots. Assays using metal-chelate affinity chromatography demonstrated that *in vitro* translated *At*ACBP2 and *At*FP6 bound lead (Pb(II)), Cd(II) and copper (Cu(II)). Consistently, assays using fluorescence analysis confirmed that (His)6-*At*FP6 bound Pb(II), as does (His)6-*At*ACBP2. *Arabidopsis thaliana* plants overexpressing *At*ACBP2 or *At*FP6 were more tolerant to Cd(II) than wild-type plants. Plasma membrane-localized *At*ACBP2 and *At*FP6 may mediate Pb(II), Cd(II) and Cu(II) transport in *A. thaliana* roots. In addition, (His)6-*At*ACBP2 binds [^{14}C]linoleoyl-CoA and [^{14}C]linolenoyl-CoA, the precursors for phospholipid repair following lipid peroxidation under heavy metal stress at the plasma membrane. *At*ACBP2-overexpressing plants were more tolerant of hydrogen peroxide than wild-type plants, further supporting a role for *At*ACBP2 in post-stress membrane repair. (Chye, et. al., 2009).

Again, both of these ACBPs were localized to the ER and plasma membrane. Targeting of ACBPs to the ER would potentially be compatible with a role in TAG metabolism in oil bodies of seeds. *De novo* fatty acid synthesis occurs in the plastid and while subsequent lipid synthesis and storage processes occur in the cytoplasm and ER, it may be reasonable to wonder if a tung ACBP similar to *At*ACBP1 or *At*ACBP2 in *Arabidopsis* could play a of role in the processes involved in the channeling and accumulation of eleostearic acid-containing intermediates, especially since ACBPs across many organisms have been shown to bind fatty acyl-CoA esters with great affinity (Larsen, et. al., 2006, Mandrup et. al., 1991, Schjerling, et. al., 2006, Taskinen, et. al., 2007). These fatty acyl-CoA esters play a large role in lipid biosynthesis, elongation, channeling, and accumulation processes. Perhaps comparable ACBPs in tung provide similar measures as listed here for the *Arabidopsis* ACBP1 and ACBP2 as well.

It would be interesting to analyze, if a tung ACBP1 equivalent were found, if its expression was downregulated in colder weather while upregulated in warm weather in tung, so as to provide similar freezing tolerance benefits and potentially allow for some benefit in the seed development process that occurs in the hot mid-summer months. Tung ACBP2, on the other hand, may prove useful in the tolerance of cadmium, or other metals if it contains an ankyrin repeat like *Arabidopsis* ACBP2 that allows for protein-protein interactions.

*At*ACBP3 is a 362 amino acid and 39.2 kDa protein. To determine the localization of AtACBP3, it was expressed as *At*ACBP3-red fluorescent protein (DsRed2) from the CaMV 35S promoter. *At*ACBP3-DsRed was localized extracellularly in transiently expressed tobacco BY-2 cells and onion epidermal cells. In addition, through Lipidex binding assays, it was observed to bind [^{14}C]arachidonyl-CoA with high affinity in comparison to [^{14}C]palmitoyl-CoA and [^{14}C]oleoyl-CoA binds arachidonyl-CoA. Although arachidonyl-CoA is not known to be synthesized by the plant, it nonetheless is commercially available and would represent a polyunsaturated fatty acid for in vitro tests. However, further binding assays did not indicate any occurrence of competitive binding with linolenoyl-CoA, a polyunsaturated fatty acid present in plants. To identify the residues functional in the binding, five mutants with single amino acid substitutions in the acyl-CoA-binding domain of (His)6-*At*ACBP3 and (His)6-*At*ACBP1 (which also binds [14C]arachidonyl-CoA) were generated by site-directed mutagenesis (Leung, et. al., 2006). Binding assays with arachidonyl-CoA revealed that replacement of a conserved R residue (R150A in *At*ACBP1 and R284A in *At*ACBP3), disrupted binding (Leung, et. al., 2006). In contrast, other substitutions in *At*ACBP1 (Y126A, K130A, K152A and Y171A) and in *At*ACBP3 (F260A, K264A, K286A and Y305A) did not affect arachidonyl-CoA binding, unlike their equivalents in (His)6-*At*ACBP2, (His)6-*At*ACBP4, and (His)6-*At*ACBP5, which had altered

binding to palmitoyl-CoA or oleoyl-CoA (Leung, et. al., 2006). Since R and Y residues have been implicated to be critical in binding carboxylic acid moieties of arachidonic acid in mouse prostaglandin endoperoxide synthase-2 (Rowlinson et al. 1999), R150 and R284, the only conserved R residues within the acyl-CoA-binding domains in ACBP1 and ACBP3, respectively, were subjected to site-directed mutagenesis and were shown to impair arachidonyl-CoA binding. Their equivalent in ACBP2 (R160) is also conserved and (His)6-*At*ACBP2 binds arachidonyl-CoA as well as it binds palmitoyl-CoA (Leung et al. 2004). The lack of this R equivalent in *At*ACBP4 and *At*ACBP5 could be the reason for their inability to bind arachidonyl-CoA. It is predicted that this R residue, critical in arachidonyl-CoA binding, likely governs *At*ACBP1 and *At*ACBP3 functions *in planta* (Leung, et. al., 2006).

Further investigations on *At*ACBP3 show its upregulation upon dark treatment and in senescing rosettes. Transgenic *Arabidopsis thaliana* overexpressing *At*ACBP3 displayed accelerated leaf senescence, whereas an *Atacbp3* T-DNA insertional mutant and *At*ACBP3 RNA interference transgenic *Arabidopsis* lines were delayed in dark-induced leaf senescence. Acyl-CoA and lipid profiling revealed that the overexpression of *At*ACBP3 led to an increase in acyl-CoA and phosphatidylethanolamine (PE) levels, whereas *At*ACBP3 downregulation reduced PE content. Significant losses in phosphatidylcholine (PC) and phosphatidylinositol, and gains in phosphatidic acid (PA), lysophospholipids, and oxylipin-containing galactolipids (arabidopsides) were evident in 3-week-old dark-treated and 6-week-old premature senescing *Arabidopsis* overexpressing *At*ACBP3. Such accumulation of PA and arabidopsides resulting from lipid peroxidation in overexpressing *At*ACBP3 plants likely promoted leaf senescence. The N-terminal signal sequence/transmembrane domain in *At*ACBP3 was shown to be essential in *At*ACBP3-green fluorescent protein targeting and in promoting senescence. Observations that

recombinant *At*ACBP3 binds PC, PE, and unsaturated acyl-CoAs *in vitro* and that *At*ACBP3 overexpression enhances degradation of the autophagy (ATG)-related protein ATG8 and disrupts autophagosome formation suggest a role for *At*ACBP3 as a phospholipid binding protein involved in the regulation of leaf senescence, perhaps by modulating membrane phospholipid metabolism and ATG8 stability in *Arabidopsis*. Accelerated senescence in plants overexpressing *At*ACBP3 is dependent on salicylic acid but not jasmonic acid signaling (Chye, et. al., 2010).

The binding of arachidonyl-CoA is very interesting because this molecule is not known to be synthesized by *Arabidopsis* or by several other plants. A possible explanation for this involves *At*ACBP3 in lipid-mediated signaling during a fungal infection. The expression of 3-hydroxy-3-methylglutaryl CoA reductase is induced by arachidonic acid in the lipids of plant pathogenic fungi during a fungal invasion in potato (Choi, et al, 1994). Since *At*ACBP3 is localized at the periphery of tobacco BY-2 cells and onion epidermal cells (extracellular localization), it could be in a prime location to interact in the invasion of fungus and trigger the defense responses against the potential pathogen (Chye, et. al., 2005).

Recently, it was observed that tung trees were stricken with an unknown fungus (Figure 1-3) (Yicun Chen, Institute of Subtropical Forestry, Fuyang, China, personal communication). Since ACBP3 of *Arabidopsis* was found to be involved in binding arachidonyl-CoA as described above, it is possible that there may be a role for tung ACBP3a and ACBP3b in defense from fungal infections of the tung tree. A good indicator of this would be to compare *Vf*ACBP3a and *Vf*ACBP3b gene expression levels in healthy and infected tree tissues. Mutational and overexpression experiments determining the threshold defense of tung involving the two known *Vf*ACBP3 isoforms could provide insight into the potential defense roles these *Vf*ACBPs may play.

In a 2004 study by Walz, et. al., a network of defense proteins in *Cucurbita maxima* was revealed. Many different proteins can be separated from the sap of mature sieve tubes of various plant species. Only a small number of those have been identified. Due to sieve tubes' inability to perform transcription and translation, the proteins are possibly synthesized in the tightly connected companion cells. They are then transported into sieve elements through plasmodesmata. The protein composition of phloem sap suggests a role of these proteins not only for sieve tube maintenance, but also for plant physiology and development (Walz et. al., 2004).

Over 300 partial sequences generated by hybrid mass spectrometry were used to identify 45 different proteins from the phloem exudates of cucumber (*Cucumis sativus* L. cv. Hoffmanns Giganta) and pumpkin (*Cucurbita maxima* Duch. cv. Gelber Zentner) plants. In addition to previously described phloem proteins, it was possible to localize proteins with high similarity to an acyl-CoA binding protein, a glyoxalase, a malate dehydrogenase, a rhodanese-like protein, a drought-induced protein, and a ß-glucosidase. It was found that the majority of the identified proteins are involved in stress and defense reactions (Walz, et. al., 2004).

Figure 1-3. Digital pictures of a tung tree infected with an unknown fungus, Guangxi Autonomous Region, China, September 2010. *At*ACBP3 preferentially binds to arachidonyl-CoA that may allow for defense against fungal infections.

Figures 1-4, 1-5, and 1-6 show the transmembrane domain analyses of *Vf*ACBP3a, *Vf*ACBP3b, and *At*ACBP3 as determined by the TMHMM server that predicts transmembrane helices in proteins (http://www.cbs.dtu.dk/services/TMHMM/). Protein sequences of interest were entered into a text box provided on the website for transmembrane prediction calculations. *Vf*ACBP3a has its domain located at residue positions 5-27, *Vf*ACBP3b has its domain located at

positions 7-28 while *At*ACBP3 has its domain located at residue positions 7-26. It is important to note the location of the binding domains is in the N-terminal portion of both of these *Vf*ACBPs, which is well before the acyl-CoA binding domain that is located at residues 170-257 in *vf*ACBP3a and residues 187-274 in *Vf*ACBP3b. The term transmembrane domain (TMD) may characterize a single transmembrane alpha helix of a transmembrane protein. An alpha-helix in a membrane can be folded independently apart from the rest of the protein, much like the domains of water-soluble proteins. More generally, a TMD represents a three-dimensional protein structure that is thermodynamically stable within a membrane. It would be interesting to analyze the TMDs of *Vf*ACBP3a and *Vf*ACBP3b to see if there is any targeting of the proteins to extracellular spaces to perform their duties. An N-terminal secretory signaling peptide (amino acids 1-26) was found to overlap the TMD (amino acids 7-26) in *At*ACBP3 (Chye 2009) and targets *At*ACBP3 to extracellular spaces. This part of the protein is necessary for targeting GFP fusion protein, and for the overexpressed gene to impart its role in age-dependent leaf senescence mentioned earlier (Chye, et. al., 2010).

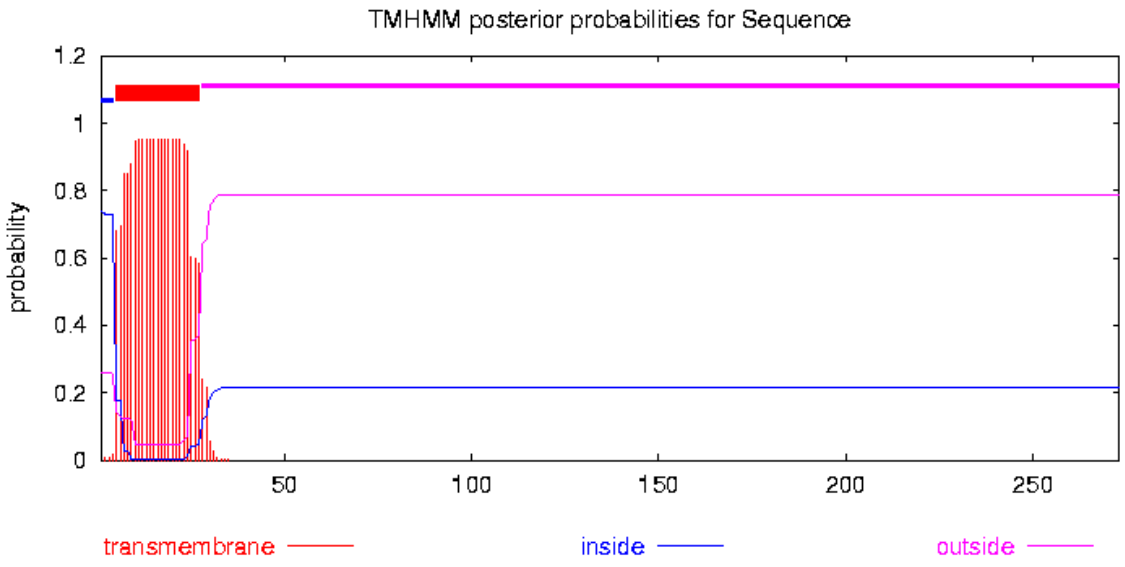

Figure 1-4. *Vf*ACBP3a hydropathy plot illustrating the potential transmembrane domain (TMD) location. *Vf*ACBP3a has a TMD located in the N-terminal portion at amino acids 5-27.

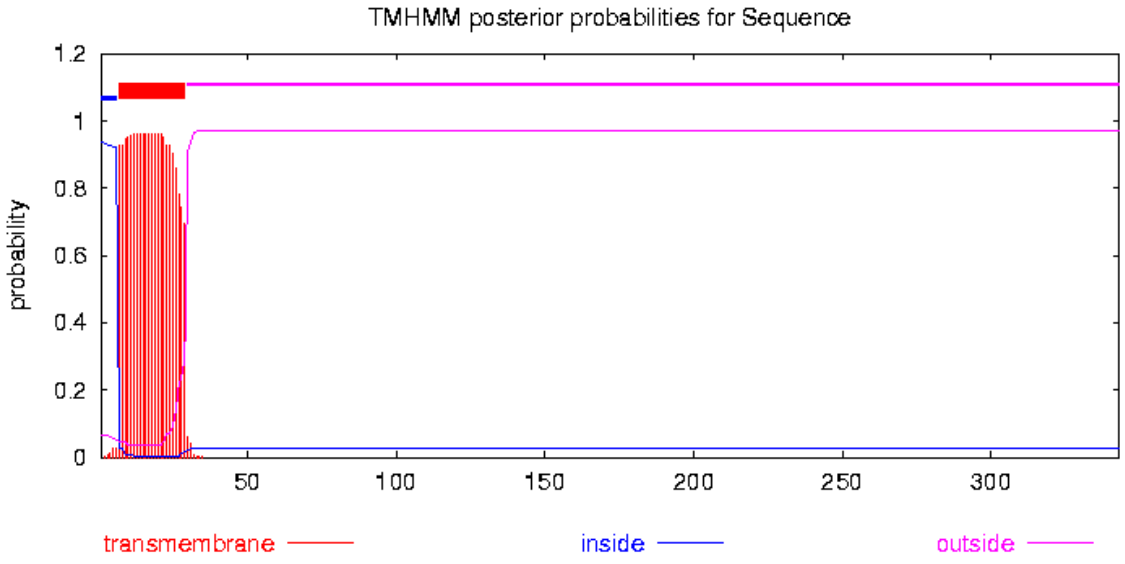

Figure 1-5. *Vf*ACBP3b hydropathy plot illustrating the potential transmembrane domain (TMD) location. *Vf*ACBP3a has a TMD located in the N-terminal portion at amino acids 7-28.

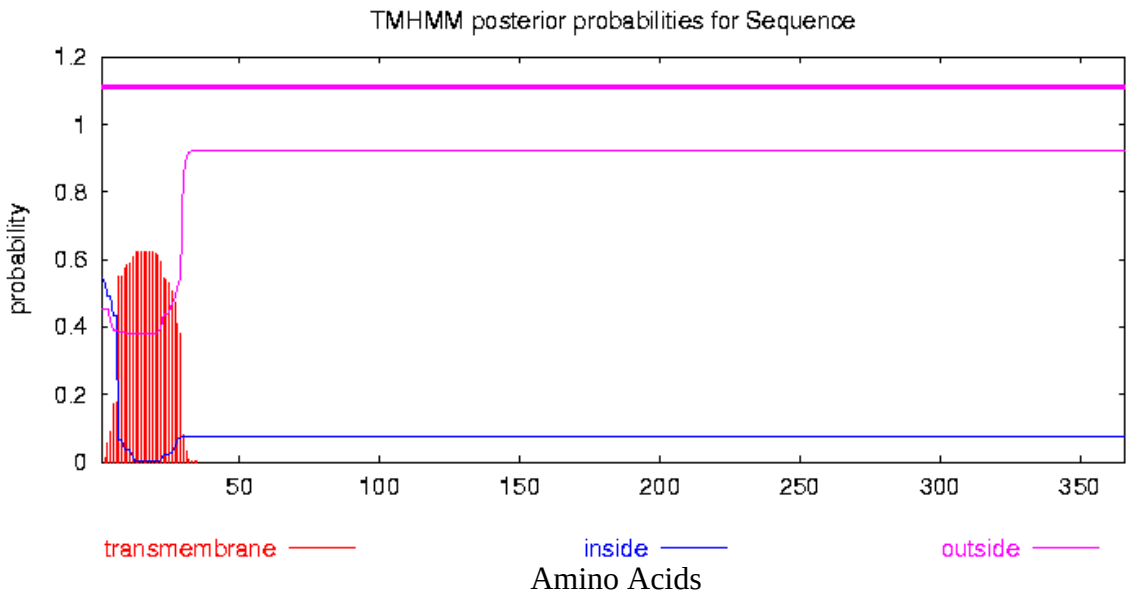

Figure 1-6. *At*ACBP3 hydropathy plot illustrating the potential transmembrane domain (TMD) location. *At*ACBP3 has a TMD located in the N-terminal portion at amino acids 7-26.

*At*ACBP4 and *At*ACBP5, comprised of 668 amino acids and 648 amino acids with molecular weights of 73.1 and 71.0 kDa respectively, are localized to the cytoplasm and in the case of *At*ACBP5, to both the cytosol and the peroxisome. Both proteins were found to bind oleoyl-CoA with great affinity. Analysis of lipid profiles illustrated that an *acbp4* knockout mutant contained less membrane lipids, such as digalactosyldiacylglycerol, monogalactosyldiacylglycerol, phosphatidylcholine, phosphatidylethanolamine and phosphatidylinositol, as opposed to *acbp4*-complemented lines that achieved levels similar to wild type, suggesting that ACBP4 may play a role in membrane lipid biosynthesis (Chye, et. al., 2008). The role of *At*ACBP5 has yet to be determined.

*Vf*ACBP4 has only been worked on for a short time before this publication, therefore, it is still a work in progress. Its full-length ORF has yet to be completely determined. Expression patterns in various tissues of tung will be discussed later, using a partial sequence of *Vf*ACBP4. *Vf*ACBP5 has not been cloned.

*At*ACBP6 is a 92 amino acid, 10.4 kDa protein, that is localized to the cytoplasm (Chye, et. al., 2008). It preferentially binds oleoyl-CoA and palmitoyl-CoA. This ACBP is highly conserved throughout eukaryotes, as figure 1-7 depicts. It is essentially a binding domain for fatty acyl-CoA esters with very little extra sequence added onto the N- or C-terminal end. It has no structural additions that are present in several other *Arabidopsis* ACBPs (Chye, et. al., 2008).

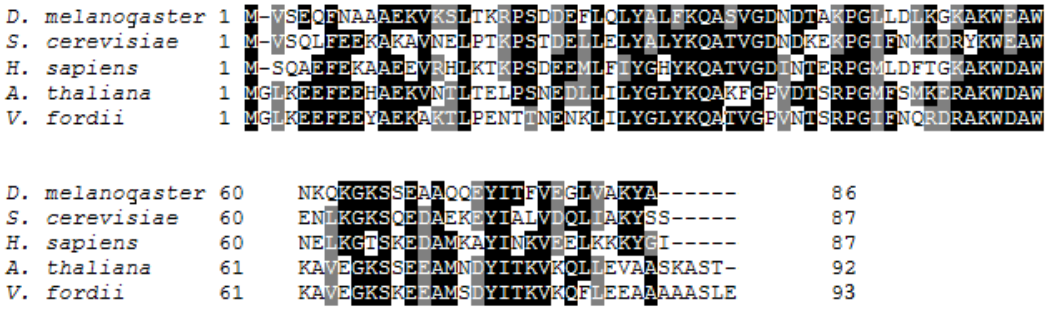

Figure 1-7. A collection of various eukaryotic soluble ACBPs illustrating the high conservation of sequences.

This high conservation in the sequences across organisms hints at the functions it can provide, such as in acyl-CoA pool maintenance and transportation functions in the cytoplasm, that it performs in many organisms (Chye, et. al., 2008). More specifically, overexpression of ACBP6 in *Arabidopsis* can enhance freeze tolerance (Chye, et. al., 2008). Filter binding assays, performed *in vitro,* indicated that histidine-tagged *At*ACBP6 binds phosphatidylcholine, but not phosphatidic acid or lysophosphatidylcholine, implying a role for *At*ACBP6 in phospholipid metabolism in *Arabidopsis,* including the possibility of *At*ACBP6 in the cytosolic trafficking of phosphatidylcholine (Chye, et. al., 2008). In humans, ACBP has shown to perform a variety of functions, including regulation of rate-limiting enzymes in cholesterol and fatty acid metabolism (Vock, 2010). In yeast, there are two homologs of ACBP and they have an influence on intracellular acyl-CoA pool size (Fedderson, et. al., 2007). So, pinpointing the function(s) of tung ACBP6 may be difficult, but as shown later, it exhibits a very general expression in tung tissues and this could be attributed to general role(s). Given the universal nature of ACBP6-like proteins

across nature, and the variety of roles these proteins play, it is likely that tung ACBP6 also fulfills many important roles. These roles may include transporting newly synthesized acyl-CoAs away from plastids (Johnson, et. al., 2000, Johnson, et. al., 2002) and/or facilitating lipid remodeling in phospholipid pathways (Yurchenko, et. al., 2009). This fits in with eleostearic acid biosynthesis, the removal from phospholipids, and the channeling into triacylglycerols. It may have no specific pathway involvement but provide with multiple utility-like duties in the cytoplasm, as seen throughout various eukaryotes.

Research focus

As previously mentioned, on a very broad scope, this study attempts to ascertain any functionalities or impacts ACBPs may have on tung. On a more specific scale, ACBPs in other organisms have been shown to provide transportation functions in biosynthetic pathways (Burton, et. al., 2005), potential defense mechanisms (Leung, et. al., 2006), and many other abilities. The results here will further the knowledge base of ACBPs.

Research objective

Identification of the sequences of *Vernicia fordii* ACBPs and analysis of expression patterns and protein:protein interactions provide insight to the potential role(s) of ACBPs in tung lipid metabolic pathways.

Obtaining the full-length sequences of *Vf*ACBPs allows for phylogenetic comparisons between ACBPs from tung and to other organisms' ACBPs. Some eukaryotic organisms have had more extensive studies to date on their functions and some of them show sequence similarity to tung ACBPs, thus allowing for potential connections to be made on their functions. Of course, not all proteins act the same in every organism, but a basic foundation for the path of research provides a large advantage. The tung tree produces its oil in the summer. Quantifying the

expression of *Vf*ACBP and comparing it to this crucial time frame in biosynthesis is key in attempting to shed light on potential *Vf*ACBP function. In addition, many protein-protein interactions occur en route to the production, modification, and storage of fatty acids in triacylglycerols in oil bodies in seeds. Some proteins are directly involved in the tung lipid biosynthetic processes. Thus, it was crucial to observe their potential interactions(s) with *Vf*ACBPs.

Protein targeting may also play an important role in regulating lipid biosynthesis and many of the enzymes involved in storage oil biosynthesis in developing seeds are also involved in production of lipids destined for normal cell membranes. Because of this, *Vf*ACBPs' presumed role in binding acyl-CoA and interacting with other proteins via protein-protein interactions, and the observations in other eukaryotic organisms of *Vf*ACBPs' general roles and transportation, results from this study may provide additional insight into the interplay of proteins in the tung biosynthetic system and if *Vf*ACBP is involved.

Even if ACBPs do not play a specific role in tung lipid biosynthesis, storage, and/or accumulation processes, *Vf*ACBPs may allow for defense mechanisms for tung. Other ACBPs, such as *At*ACBP6, provide freezing tolerance, which is important for growth in wintry seasons. The goals of the research involved in this study allow for a broad perspective on the prospective roles of ACBPS in tung lipid metabolism, pathogen defense mechanisms, or any other processes in tung trees.

Materials and Methods

Expressed Sequence Tag (EST)

Expressed Sequence Tag services for tung sequences, including *Vf*ACBPs, were conducted by the Agricultural Research Service Mid South Area Genomics Facility in Stoneville, MS. Expressed Sequence Tag (EST) sequences were generated from randomly selected cDNA from a developing tung seed cDNA library. This was performed from an arrayed library and annotated by the staff at the Agricultural Research Service Mid South Area Genomics Facility in Stoneville, MS. Homology-based comparisons using the Basic Local Alignment Search Tool (BLAST, http://blast.ncbi.nlm.nih.gov/Blast.cgi), to publicly available databases, namely, GenBank (http://www.ncbi.nlm.nih.gov/genbank/), were used to identify these clones. In this manner, ACBP6 and ACBP3a were identified in the library along with several other clones in the tung biosynthetic pathway.

Pyrosequencing

Pyrosequencing services for tung sequences, including *Vf*ACBPs, were performed by the Agricultural Research Service Mid South Area Genomics Facility in Stoneville, MS. In the same manner as EST, homology-based comparisons using the Basic Local Alignment Search Tool (BLAST, http://blast.ncbi.nlm.nih.gov/Blast.cgi), to publicly available databases, namely, GenBank (http://www.ncbi.nlm.nih.gov/genbank/), were used to identify the clones for *Vf*ACBPs. Through the efforts of this process, ACBP3b and ACBP4 were determined. Along with EST data, pyrosequencing allowed for the template for genome walking to determine the remainder of the sequences of each *Vf*ACBP.

Genome walking

Two gene-specific primers were designed. One was for the primary PCR reaction (GSP1) and one for the secondary PCR reaction (GSP2) for each ACBP. Primers are listed in figure 2-1. In general, the gene-specific primers were derived from sequences as close to the end of the known sequence as possible. For walking upstream from cDNA sequence, the primer was as close to the 5' end as possible. Gene-specific primers were chosen to be 25–28 nucleotides in length with a GC-content of 40–60% to ensure that the primers effectively anneal to the template at the recommended annealing and extension temperature of 67°C. Another constraint was that there be no more than three G's and C's in the last six positions at the 3' end of the primer. Five restriction sites were incorporated into the Genome Walker Adaptor, including Sal I (cohesive ends), Mlu I (cohesive ends), and overlapping Srf I (cohesive ends), Sma I (blunt ends), and Xma I (cohesive ends) sites.

The primary PCR master mix was prepared by combining the following reagents in a 0.5 mL tube: 40µL H_2O, 5µL 10X PCR Buffer, 1µL dNTP mix, 1µL anchored primer 1 (Invitrogen) (10 µM), 1µL GSP1 (10 µM), and 1µL BD Advantage 2 Polymerase mix (50X) (Invitrogen). These components were vortexed and briefly spun in a microcentrifuge. Forty-nine µL of the primary PCR master mix was added to the appropriately labeled tubes. One µL of each DNA library (EcoR V, DraI, Pvu II, and SspI) was added to the appropriately labeled tubes.

The following two-step cycle parameters were used in PCR: 7 cycles: 94°C for 25 seconds and 72°C for 4 minutes, then 32 cycles: 94°C for 25 seconds, 67°C for 4 minutes, and 67°C for an additional 4 min after the final cycle. Five µL of the primary PCR products were analyzed on a 1.5% agarose/2% EtBr gel, along with DNA size markers (BioRad). PCR products were analyzed by agarose gel electrophoresis and imaged on a GE Healthcare Fujifilm LAS-

3000 image analyzer. One µl of each primary PCR product was diluted into 49 µl of sterile H2O. A secondary PCR master mix was prepared by combining the following reagents in an 0.5-ml tube:

40 µL H_2O, 5µL 10X PCR Buffer, 1µL dNTP (10 mM each), 1µL anchored primer 2 (Invitrogen) (10 µM), 1µL GSP2 (10 µM), and 1µL BD Advantage 2 Polymerase Mix (50X). The components were vortexed and briefly spun in a microcentrifuge. Forty-nine µL of the secondary PCR master mix was added to the appropriately labeled tubes. One µL of each diluted primary PCR product was added to the appropriate tube. The following two-step cycle parameters for secondary PCR were used: 5 cycles: 94°C for 25 seconds and 72°C for 4 minutes, then 18–22 cycles: 94°C for 25 seconds, 67°C for 4 minutes, and 67°C for an additional 4 minutes after the final cycle. Five µL of the secondary PCR products was analyzed on a 1.2% agarose/EtBr gel, along with DNA size markers such as a 1 kb DNA ladder. Fragments of interest were cloned and analyzed using the pCR®2.1-TOPO® procedure outlined in the cloning section.

*Vf*ACBP3b	*Vf*ACBP4
5’-CGACGAAATTCATCGACCATTTCCGCAAC-3’	5’-GGGGAGCTGCAAAGTTGCAAGCACTGGC-3’
5’-GACGCTCTAGAATACCAACCTGGAT-3’	5’-TGATTCATTTGCATGTCTACAACAG-3’

Figure 2-1. Genome walking primers for *Vf*ACBP3b and *Vf*ACBP4.

Rapid Amplification of cDNA Ends (RACE)

EST and pyrosequencing allow for determination of partial cDNA sequences for some of the *ACBP* genes. Full-length sequences were obtained by Rapid Amplification of cDNA Ends (RACE). The full-length of *Vf*ACBP3a and *Vf*ACBP6 was obtained from the library annotation EST. Portions of the sequences for *Vf*ACBP3b and *Vf*ACBP4 were obtained via EST and pyrosequencing thereafter the 5’ ends up until the start codon and the 3’ ends until the stop

codon were determined by 5' and 3'RACE. These procedures used the Invitrogen (Invitrogen Corporation (Headquarters), 5791 Van Allen Way PO Box 6482 Carlsbad, California 92008) protocols with slight modifications. In order to obtain the first strand of cDNA synthesis in 5'RACE, the Invitrogen method for 3'RACE was used in addition to using the reverse transcriptase III enzyme provided by the 3'RACE kit along with sequencing parameters and other components of the protocol for 3'RACE. Components of the reaction included: 20 mM Tris-HCI (pH 8.4 at 22°C), 50 mM KCI, 2.5 mM $MgCI_2$, 10 mM DTT, 500 nM anchored primer (Invitrogen), 500 µM each dATP, dCTP, dGTP, dTTP, and 1 µg (≤50 ng/µl) of RNA. One µg of a previously isolated pooled RNA template, representative of all time points in seed development ranging from June 23 until September 1st was used AS a template. The reaction was mixed and equilibrated at 42°C for 5 minutes and 1 µL of SuperscriptIII RT was added followed by incubation at 42°C for 50 minutes. The reaction was terminated at 70°C and µL RNase H was added followed by incubation at 37°C for 20 minutes.

Following this, the typical 5'RACE protocol presented by Invitrogen was employed. A column purification procedure was used, involving the addition of 120 µL of 6 M NaI to the cDNA obtained from first strand synthesis followed by centrifugation at 13,000 x g. Preheated distilled water was used to elute the cDNA.

This was followed by a homopolymeric Terminal deoxynucleotidyl transferase (TdT)-tailing reaction of the cDNA. Components of the reaction include: 10 mM Tris-HCl (pH 8.4), 25 mM KCl, 1.5 mM $MgCl_2$, 200 µM dCTP, and cDNA. This reaction was incubated at 94°C for 2 minutes followed by addition of TdT and an incubation for 10 minutes at 37°C. The TdT was heat inactivated for 10 minutes at 65°C.

Lastly, amplification of the cDNA was performed using gradient PCR parameters. Components of the PCR include: 20 mM Tris-HCl (pH 8.4), 50 mM KCl, 1.5 mM $MgCl_2$, 400 nM GSP, 400 nM Abridged Anchor Primer (Invitrogen), 200 μM each dATP, dCTP, dGTP, dTTP, tailed cDNA, and 2.5 units Taq DNA polymerase. PCR protocol was as follows: 30 to 35 cycles, 94°C for 1-2 min, 94°C for 0.5-1 min, (gradient): 55°C to 70°C for 0.5-1 min, 72°C for 1-2 min, followed by: 72°C, 5-7 min, and an indefinite hold: 5°C, until the samples were removed.

cDNA was amplified by PCR using gene-specific nested reverse oligonucleotide primers (GSP) listed in Table 2-2, along with the Abridged Anchor Primer (AAP), 5'-GGCCACGCGTCGACTAGTACGGGIIGGGIIGGGIIG-3', provided by Invitrogen. 5-20 μl of 5' RACE products were analyzed by agarose gel electrophoresis according to standard protocols, using appropriate size standards followed by ultraviolet (UV) visualization of ethidium bromide-stained products. If samples' bands were not clear enough, an additional gradient PCR reaction was performed using another GSP, listed in table 2-3, along with an Abridged Universal Amplification Primer (AUAP), 5'-GGCCACGCGTCGACTAGTAC-3', instead of the AAP.

*Vf*ACBP3b GSP	*Vf*ACBP4 GSP
5'-ATACTGCTCCATAGCCACTTCTGGATTC-3'	5'-GGATCCAGCAAGCCAACCCCACACA-3'

Figure 2-2. 5'RACE Gene Specific Primers (GSP) for *Vf*ACBP3b and *Vf*ACBP4

*Vf*ACBP3b Nested GSP	*Vf*ACBP4 Nested GSP
5'-GTTTCCAAGCCTTTGCCAAGCATTCCAC-3'	5'-CACCACCAGAGCCCTGCCTCTGTTTTG-3'

Figure 2-3. 5'RACE Nested Gene Specific Primers (GSP) for *Vf*ACBP3b and *Vf*ACBP4.

Much like the 5'RACE protocol detailed above, the Invitrogen method for 3'RACE was used with the reverse transcriptase III enzyme along with sequencing parameters and other components from the 3'RACE kit. Components of the reaction included: 20 mM Tris-HCI (pH 8.4 at 22°C), 50 mM KCI, 2.5 mM $MgCI_2$, 10 mM DTT, 500 nM AP, 500 μM each dATP,

dCTP, dGTP, dTTP, and 1 μg (≤50 ng/μl) of RNA. One μg of a previously isolated pooled RNA template, representative of all time points in seed development ranging from June 23 until September 1st was used here. The reaction was mixed and equilibrated at 42°C for 5 minutes and 1 μL of SuperscriptIII RT was added followed by incubation at 42°C for 50 minutes. The reaction was terminated at 70°C and μL RNase H was added followed by incubation at 37°C for 20 minutes.

The components of the reaction employed in amplifying the cDNA were as follows: 20 mM Tris-HCl (pH 8.4), 50 mM KCl, 1.5 mM $MgCl_2$, 200 nM GSP, 200 nM Abridged Universal Amplification Primer (AUAP) or Universal Amplification Primer (UAP) (Invitrogen), 200 μM each dATP, dCTP, dGTP, dTTP, and 0.1 unit/μL Taq DNA polymerase. Two μL from the cDNA synthesis reaction was added to a PCR tube. The reaction was then centrifugated. The reaction was incubated at 94°C for 3 min. Gradient PCR was performed at 35 cycles. PCR protocol was as follows: 30 to 35 cycles, 94°C for 1-2 min, 94°C for 0.5-1 min, (gradient): 55°C to 70°C for 0.5-1 min, 72°C for 1-2 min, followed by: 72°C, 5-7 min, and an indefinite hold at 5°C, until the samples were removed. Following amplification, 10 to 20 μL of the amplified sample was analyzed using agarose gel electrophoresis and ethidium bromide staining, and the appropriate molecular size standards. The optimal products of the PCR were chosen in a secondary gradient PCR reaction, using another GSP, listed in figure 2-5, along with an Abridged Universal Amplification Primer (AUAP), 5'-GGCCACGCGTCGACTAGTAC-3'.

*Vf*ACBP3b GSP	*Vf*ACBP4 GSP
5’-GGTTCATCGCGGTTAACCGATTTCTCAG-3’	5’-GCATCAATTTCATCCCAAGTCATGTTCTCG-3’

Figure 2-4. 3’RACE Gene Specific Primers (GSP) for *Vf*ACBP3b and *Vf*ACBP4

*Vf*ACBP3b Nested GSP	*Vf*ACBP4 Nested GSP
5’-CTGGTTCGTCGACGAAATTCATCGACCA-3’	5’-GTGTAACAGATTGACCCCCAGGTGGAGAC-3’

Figure 2-5. 3’RACE Nested Gene Specific Primers (GSP) for *Vf*ACBP3b and *Vf*ACBP4.

The amplification products were cloned into the pCR®2.1-TOPO® vector provided by Invitrogen, as described in the bacterial transformation section. DNA was extracted from two individual transformants and sequenced.

Polymerase Chain Reaction (PCR) to amplify full-length open reading frames

The full-length open reading frames of three of the *Vf*ACBPs were amplified with the respective primers in figure 2-6.

***Vf*ACBP3a Sense Primer**	***Vf*ACBP3a Antisense Primer**
5’-GGATCCATGGCCATGGAGCTTTTCTTTGAATTGG-3’	5’-ATGGGTCGACTTAGGCGTGCAACTTTCTCACTTGG-3’
***Vf*ACBP3b Sense Primer**	***Vf*ACBP3b Antisense Primer**
5’-CTATAGGATCCGAGCTGCTTCAAGAGCTCTTTGTC-3’	5’-ACTTAGTCGACTCATTCTGTAGCCCTGTTCTCCAA-3’
***Vf*ACBP6 Sense Primer**	***Vf*ACBP6 Antisense Primer**
5’-GGATCCATGGGTTTGAAGGAGGAATTTGAGGAGT-3’	5’-ATCAGTCGACCTAAGAAGCAGCAGCAGCAGCTTC-3’

Figure 2-6. PCR Primers for *Vf*ACBP3a, *Vf*ACBP3b, and *Vf*ACBP6 to amplify the full-length ORFs.

One µg of a pooled cDNA template, representative of all time points in seed development (henceforth termed as weeks after fluorescence, WAF) ranging from June 23 until September 1st was used for amplification of each the ACBPs along with the Platinum® Pfx enzyme and accompanying manufacturer’s protocol (Invitrogen). Components of the reaction include: 10X Pfx Amplification Buffer at 5 µl, 10 mM dNTP mixture at 1.5 µl, 50 mM $MgSO_4$ at 1 µl, primer mix (10 µM each) at 1.5 µl, template DNA (10 pg - 200 ng) ≥1 µl, Platinum® Pfx DNA polymerase at 0.4-1 µl, autoclaved, distilled water to 50 µl. The PCR cycling parameters used in

the amplifications of the full-length ORFs for *Vf*ACBP3a and *Vf*ACBP3b were initial denaturation at 94°C for 30 seconds followed by 30 cycles of 94°C for 1 minute and 60°C for 1 minute, and a final extension at 72°C for 3 minutes. For *Vf*ACBP6, the cycling parameters were the same except the 60°C step was for 20 seconds. PCR products were analyzed by agarose gel electrophoresis and imaged on a GE Healthcare Fujifilm LAS-3000 image analyzer. Samples were cleaned and concentrated in Zymo columns (Zymo Research Corporation, 625 W. Katella Ave., Suite #30, Orange, CA 92867 U.S.A.) and resulting DNA was used to transform bacteria (see bacterial transformation protocol).

The amplification products were cloned into the pB50 vector, as described in the bacterial transformation section. DNA was extracted from two individual transformants and sequenced.

Bacterial transformation

Four µL of fresh PCR product was added to 1 µL salt solution (TOPO®) and 1 µL TOPO® vector and incubated at room temperature for 30 minutes. This reaction mix was added to TOP10 competent cells on ice and incubated for 15 minutes. It was heat-shocked in a 42°C water bath and chilled on ice for 2 minutes. 250 µL super optimal broth with catabolite repression (SOC) was added and incubated at 37°C for one hour. 100µL aliquots were plated and incubated at 37°C overnight on 2XYT with kanamycin antibiotic plates. Bacterial colonies were subject to PCR screening using the M13 forward and reverse sequencing primers, GTAAAACGACGGCCAGT and AACAGCTATGACCATG respectively, provided by the TOPO® kit. Two bacterial colonies were picked with a sterile spreading stick and the stick was used to inoculate an 8 mL 2XYT plus kanamycin culture (100 micrograms per mL kanamycin). Cultures were shaken at 250 RPM at 37°C overnight. Cells were centrifuged at 10,000 x g for 10 minutes and DNA was extracted from the pellet using Wizard Plus Mini-preps (Promega

Corporation, 2800 Woods Hollow Road Madison, WI 53711 USA), and eluted with 50 µL Tris-EDTA.

Sequencing

All of the DNA constructs generated were sequenced utilizing the DTCS Quickstart kit 1 (Beckman Coulter, Fullerton, CA) and analyzed with a Beckman Coulter 8800 Genetic Analysis System equipped with the CEQ8000 software suite. The sequences were manipulated and analyzed using VectorNTI Advance 10.0 and 11.0 software (InforMax, Invitrogen Life Science, Frederick, MD), and compared to other sequences employing World Wide Web based BLAST algorithm programs. Phylogenetic comparisons were performed by the generation of multiple sequence alignments using the CLUSTALX program, with default settings.

Reverse transcription polymerase chain reaction (RT-PCR)

Reverse transcription (RT) reactions were carried out using the BioRad (Life Science Research 2000 Alfred Nobel Drive Hercules, CA 94547 USA) iScript™ cDNA Synthesis Kit as per manufacturer's protocol. Components of the reaction included: 5x iScript reaction mix 4 at µL, iScript reverse transcriptase at 1 µL, nuclease-free water to 20 µl, and RNA template at 1 µg (total RNA). The reaction protocol of this mixture, in PCR microtubes, was as follows: 5 minutes at 25ºC, 30 minutes at 42ºC, 5 minutes at 85ºC, followed by 4ºC. As mentioned earlier, the templates used in this reaction were the RNAs ranging from (weekly) June 23rd until September 1st (11 individual samples) along with leaf and flower RNA with the exception that these were not pooled. A non-reverse transcriptase template was used as a negative control. Following RT-PCR, the nucleic acid concentration of each sample (13 total) was quantified on a Nanodrop ND-1000 spectrophotometer and diluted to 1 µg/µL.

Quantitative Real-time Polymerase Chain Reaction (qPCR)

Real-time PCR was performed with a BioRad C1000 core unit PCR thermocycler with a BioRad CFX96 head unit for qPCR. The PCR reaction was carried out in a final volume of 25 µL, which included 2 µL cDNA, 10 µL SYBR Green master mix, 2.5 µL of 5 µM sense and antisense primers, and H_2O. The PCR conditions consisted of 40 cycles at 95 °C for 30 s, 60 °C for 30 s, and 72°C for 1 60 s. The reference gene included with each run was tung ubiquitin ligase. Samples were assayed in triplicate. Means and standard deviations were calculated from the data obtained. For each sample, at least three assays were performed. The data was normalized using BioRad software (BioRad CFX Manager version 1.5). Each baseline was adjusted based upon a value that was found from taking the average of all the combined runs per *Vf*ACBP. This average baseline value was subsequently applied to each run. In addition, any c(t) value that deviated by more than 0.5 from the average c(t) value of a specific time point in all runs for one *Vf*ACBP, was not taken into consideration. The c(t) value, which is the threshold crossing cycle, was calculated as the mean of three different assays.

Split-ubiquitin-based membrane yeast two-hybrid analysis

Protein:protein interactions between different tung ACBP proteins and other proteins expressed in developing seeds were assayed using the Dualsystems Biotech (San Pedro, CA) DUAL-membrane split-ubiquitin system. The yeast strain NMY51, genotype: *MATa his3delta200 trp1-901 leu2-3,112 ade2 LYS2::(lexAop)4-HIS3 ura3::(lexAop)8-lacZ (lexAop)8-ADE2 GAL4),* was used to perform this procedure. NMY51 has a ura3 genotype. Two different growth markers and a lacZ reporter ensure the highest possible stringency in a library screen, resulting in fewer false positives. This yeast strain was transformed with different combinations of bait and prey plasmids. Yeast containing bait and prey plasmids were cultured overnight in a

medium consisting of 8 mL synthetic dextrose (SD) (2% [w/v] dextrose, 0.67% [w/v] yeast nitrogen base without amino acids, 2 g L^{-1} synthetic mix of amino acid supplements, minus leucine and tryptophan; SD-LT) (Bufferad, IL) in an orbital incubator at 30ºC and 250 RPM. Then, ~500 µL of cell culture was transferred to 10 mL of fresh SD-LT medium and the cells were cultured again for another 4-6 hours. Cells were pelleted by centrifugation, washed with water, and then resuspended in 1 mL of water. The activation of the histidine and adenine reporter genes was tested by performing a serial dilution assay where the first cell suspension had an OD_{600} value of 0.5, and 6 subsequent samples were prepared via 1:5 serial dilutions. Cells from each dilution were plated on SD-LT and SD-LTHA plates (SD-LT also lacking histidine and adenine) and were incubated for 3 days at 30ºC. Plates were observed after 24 hours, 42 hours, and 72 hours respectively in order to monitor cell growth on a GE Healthcare Fujifilm LAS-3000 image analyzer using the digital white-light setting.

The lacZ reporter activation was observed by β-galactosidase activity for quantitative analysis using the β-galactosidase assay kit from Pierce Protein Research Products (Thermo Scientific, Rockford, IL). Cultures were grown exactly as described above in SD-LT liquid media. After back-dilution, cultures were spun down for 10 minutes at 3500 rpm. Supernatant was poured off and pellets were resuspended in the remaining volume of SD-LT media and centrifuged at 14,500 RPm for 1 minute. Supernatant was removed and pellet was washed once with water and resuspended in 1 mL water. The OD_{600} of the culture was measured and the volume of cells needed to make 350 µL of 1 OD concentration was calculated. A working solution (350 µL) contained within the kit was added and the mixture was incubated at 37°C at 300 RPM until a yellow color change was observed (minutes for strong interactors and up to 24 hours for weak ones). A stop solution (300µL) provided with the kit was added once yellow

color was observed and the elapsed time was recorded. Cell debris was removed by centrifugation at 14,500 rpm for 30 seconds followed by transferring 900 µL of the supernatant to a fresh tube and stored at 4°C until absorbance measurements were taken. The absorbance was measured in triplicate at 420 nm using a Nanodrop ND-1000 spectrophotometer against a blank containing sterile water with working solution and stop solution. Enzyme activity was calculated in Miller units (Miller 1972), using the equation:

β-galactosidase activity = $(1000 \cdot A_{420}) \div (t \cdot V \cdot OD_{600})$, where, t = time (minutes) of incubation, V = volume of cells (mL) used in the assay.

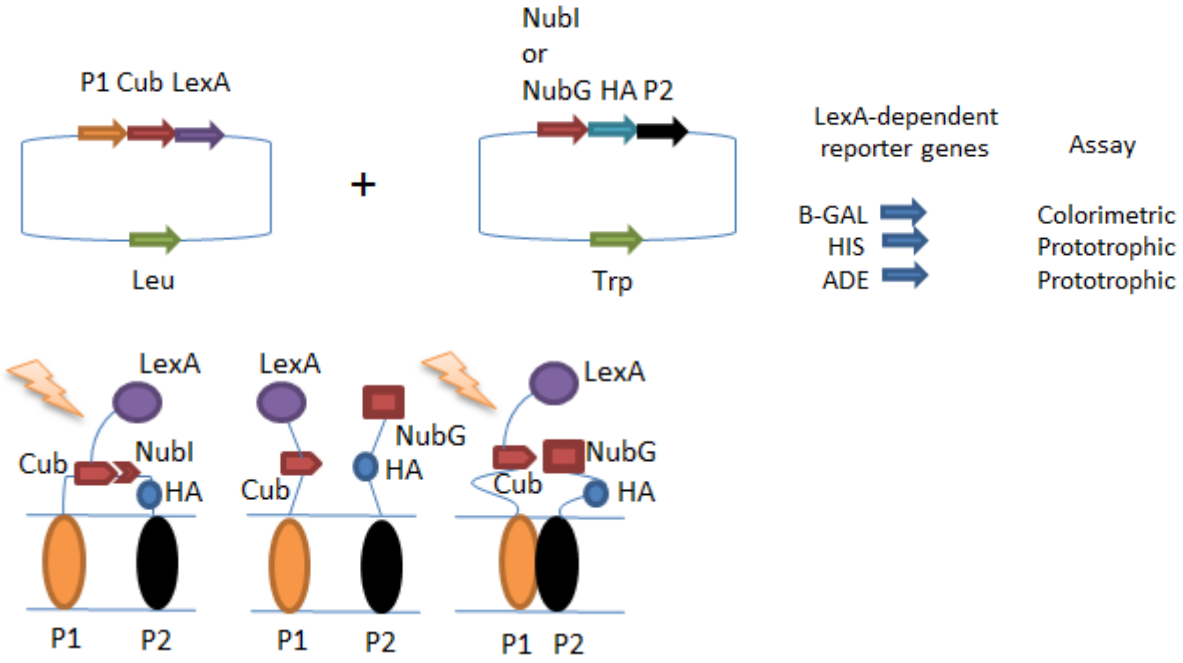

Figure 2-7. Illustration of the split ubiquitin system. Two proteins of interest, P1 and P2, produce a whole ubiquitin moiety due to the NubI half having a high affinity for the Cub half of the split ubiquitin, despite the proteins not being in close proximity. The LexA reporter gene is cleaved and is later transcribed. Mutated Nub, NubG, will only produce a whole ubiquitin moiety with Cub when the two proteins of interest are in close enough proximity to bring the two halves of ubiquitin together.

Ubiquitin-specific proteases (UBPs) recognize and cleave the fusions of ubiquitin and a target protein immediately after a double glycine motif (Gly-Gly-X) that is located at the C-terminus of ubiquitin (http://www.dualsystems.com/technologies/protein-interaction-

screening/split-ubiquitin-system.html). UBPs recognize the folded ubiquitin as opposed to a specific sequence of a polypeptide chain as in other proteases (http://www.dualsystems.com/technologies/protein-interaction-screening/split-ubiquitin-system.html). The expression of ubiquitin in yeast can occur as an N-terminal half (Nub) in addition to a C-terminal half (Cub). The affinity the halves have for each other remains unchanged, and they can spontaneously reassemble to form a split-ubiquitin. Nub and Cub moieties are co-expressed within a single cell, and a reporter protein that is fused to the C-terminus of ubiquitin will be cleaved off upon re-assembly of the Nub and Cub moieties into split-ubiquitin (http://www.dualsystems.com/technologies/protein-interaction-screening/split-ubiquitin-system.html). To facilitate use of split ubiquitin as a sensor of protein:protein interaction strength, a point mutation was introduced into the N-terminal half of ubiquitin to produce NubG. This mutation completely eliminates the affinity of the two halves for one another. Separate NubG and Cub portions are not recognized by UBPs, and thus no cleavage of the reporter gene occurs. In this system, a prey protein is fused to NubG while the bait is fused to Cub followed by a reporter gene (http://www.dualsystems.com/technologies/protein-interaction-screening/split-ubiquitin-system.html). Upon interaction of the bait and prey, NubG and Cub are brought close enough together to reconstitute split-ubiquitin. This results in the release of the reporter protein through the action of the UBPs (http://www.dualsystems.com/technologies/protein-interaction-screening/split-ubiquitin-system.html).

Binary vector plasmid construction for *in planta* applications

Two constructs were created and used for different purposes. The first construct consisted of a plasmid vector used for the expression of *Vf*FADX driven by the β-conglycinin promoter in

conjunction with either *Vf*ACBP3a or *Vf*ACBP6 to analyze eleostearic acid content in seeds of transformed *Arabidopsis thaliana*. The second construct consisted of *Vf*ACBPs (Figures 2-8 through 2-10) placed into a plasmid allowing for the expression of DsRed fluorescence (Figure 2-12) to analyze total fatty acid changes in wild type *Arabidopsis thaliana* upon the introduction of *Vf*ACBP3a (Figure 2-9) or *Vf*ACBP6 (Figure 2-10). The protocol used to transform the vectors is similar in approach to the TOPO® protocol, with a key exception. Both *Vf*ACBPs were placed into the pB50 vectors mentioned earlier, and were cut with the restriction enzyme, AscI. AscI cut out the promoter-gene-terminator cassette, which was ligated into either the AscI site (for pB110 the DsRed vector) or the MluI site of pE29 (which contains *Vf*FADX, see Figure 2-11). Components of the restriction digest included: 5 µL NE buffer (New England Biolabs (NEB) 240 County Road Ipswich, MA 01938-2723 USA), 0.5 µL 100x BSA, 5 µg plasmid DNA, 1.5 µL each restriction enzyme (NEB), water to 50 µL. Transformation procedures occurred as described earlier. Samples were cleaned and concentrated in Zymo columns. These samples were then transformed into either the plasmid expressing *Vf*FADX or the pB110 plasmid (Figure 2-12) allowing for the expression of DsRed fluorescence.

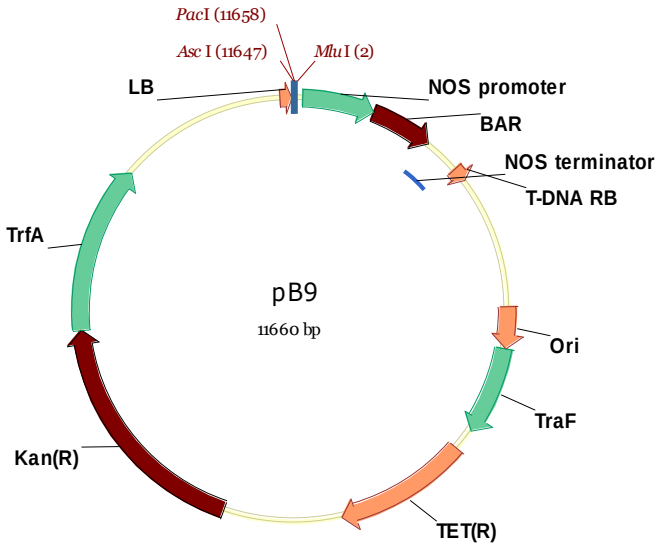

Figure 2-8. Vector pB9 pBAR with the NOS promoter and terminator sequences.

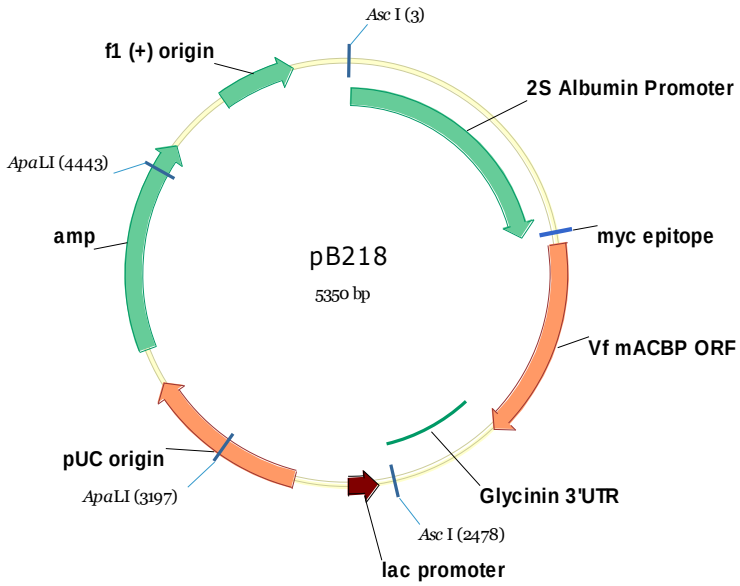

Figure 2-9. Vector pEB218 which contains *Vf*ACBP3a (seen here as *Vf*mACBP) in pB50.

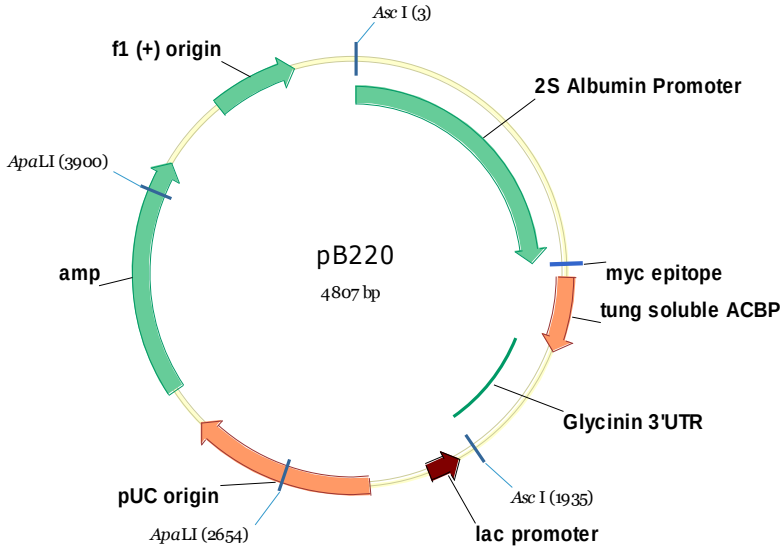

Figure 2-10. Vector pEB220 which contains *Vf*ACBP6 (seen here as tung soluble ACBP) in pB50.

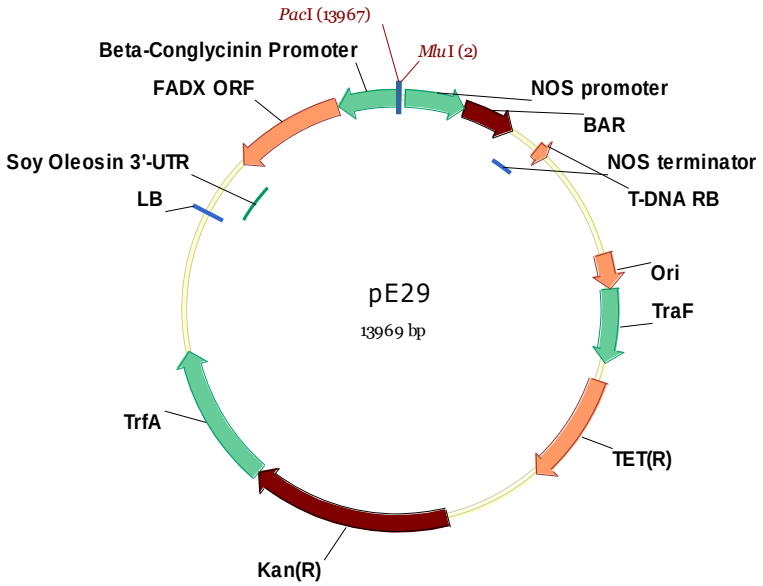

Figure 2-11. Vector pE29 which contains *Vf*FADX.

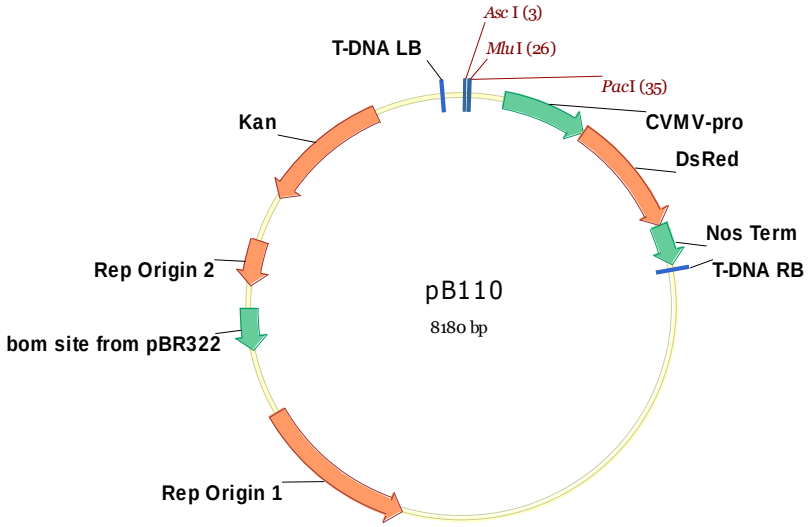

Figure 2-12. Vector pB110 which contains DsRed.

Floral dip method for *in planta* transformations

Work involving *in planta* transformations included a floral dip method first adapted by Clough and Bent, 1998. *Arabidopsis* plants were grown in pots until flowering. First bolts were clipped to encourage proliferation of many secondary bolts and the plants were ready roughly 4-6 days after clipping. A strain of *Agrobacterium tumefaciens* (C58) was prepared to carry the

gene of interest, either ACBP3a or ACBP6, in a binary vector. A large liquid culture (600 mL) was grown at 28°C in 2XYT broth with antibiotics to select for the binary plasmid. *Agrobacterium* cells were pelleted by centrifugation and resuspended in 300 mL of 5% sucrose solution, containing 0.01-0.02% Silwet L-77. The above-ground parts of plants were dipped in *Agrobacterium* solution for 10 seconds, with gentle agitation. The dipped plants were placed under a dome or cover for 16 to 24 hours to maintain high humidity (plants can be laid on their side if necessary), without exposure to excessive sunlight. The plants were then watered and grown to maturity. Dry seeds were harvested afterward as will be described. Transformants were selected using a glufosinate herbicide resistance selectable marker, or a DsRed (red fluorescence protein) marker. Putative transformants were transplanted to soil and grown.

Transformed *Arabidopsis* lines followed a specific generational naming convention. Dipped parental plants: $T_{0;}$ seeds that come off of those: $T_{1;}$ seeds from T_1: T_2, and seeds from T_2: T_3. Stated differently, the T_1 generation breeds T_2 seeds, and the T_2 generation breeds T_3 seeds.

Fatty Acid Methyl Ester (FAME) Analysis

Plant tissues or dirt were separated using a 30 mesh size separating filter and seeds were placed in appropriately labeled 1.5 mL Eppendorf tubes. Approximately 30 mg of seeds were placed into 1.5 mL Eppendorf tubes along with 500 µL of hexane and steel beads and were pulverized in a bead beater for 5 minutes followed by centrifugation (13000xg/2min). 300 µL of extract was transferred to 13x100 Corning culture tubes. Seven hundred µL hexane and 400 µL sodium methoxide in methanol solution was added and the reaction incubated at room temperature for 10 minutes. Two mL hexane and 2 mL saturated NaCl solution was added and

then the tubes were centrifuged for 5 minutes in a tabletop swinging bucket centrifuge. Two mL of the top layer was transferred to 2 mL vials for gas chromatography analysis or stored at -20°C.

Gas chromatography

An Agilent Technologies (5301 Stevens Creek Blvd Santa Clara CA 95051 United States) gas chromatographer containing an autosampler along with Agilent Chemstation software was used to analyze the fatty acid methyl ester content of the aforementioned extracts. The gas chromatographer contains a Supelco SP-2380 column with helium as the carrier gas at a flow rate of 36 cm/second. The initial oven temperature is 160°C with no hold, followed by a ramp up of 4°C/minute up to 200°C and followed by a 5 minute hold. Vials were placed on the autosampler and analyzed one at a time.

Statistical analysis

Student's t-tests were used for comparison of the fatty acid content elicited gas chromatography results (calculated using Microsoft Excel, 2007). Differences at $P < 0.05$ were accepted as significant. Statistical analysis of the comparison between the various plant constructs was performed using the unpaired, two-tailed t test.

Results

The elucidation of *Vernicia fordii* Acyl-CoA Binding Proteins (ACBPs)

Previously, many of the other biosynthetic enzymes of the tung lipid biosynthetic pathway were identified, cloned, and analyzed for their potential roles in the production of α-eleostearic acid in the oil bodies in seeds of the tung tree (Shockey, et al., 2006). In order to identify tung ACBPs for analysis of their roles in the tung biosynthetic pathway, it was required to obtain their full-length cDNAs as an initial step. Expressed Sequence Tag (EST) sequencing allowed for a short, transcribed cDNA sequence. Approximately 5000 randomly selected clones were chosen and utilizing homology-based comparisons, such as BLAST, (http://blast.ncbi.nlm.nih.gov/Blast.cgi). These were compared to a publicly available database, GenBank (http://www.ncbi.nlm.nih.gov/genbank/), to identify two of the *Vf*ACBPs; *Vf*ACBP3a and *Vf*ACBP6. Both of the *Vf*ACBP ESTs contained entire open reading frames. The *Vf*ACBP3a open reading frame, from start codon until the stop codon, is 822 base pairs (274 amino acids) in size. *Vf*ACBP6, similar to other eukaryotic small, soluble ACBPs, has an open reading frame of 279 base pairs (93 amino acids).

The other two *Vf*ACBPs, *Vf*ACBP3b and *Vf*ACBP4, were obtained through a more contemporary technique, as compared to EST, called pyrosequencing. Pyrosequencing is a method of DNA sequencing that is based upon a principle called sequencing by synthesis (Weber, et al., 2007). It is reliant upon detection of pyrophosphate release when nucleotides are incorporated (Weber et. al., 2007).

Unlike the EST sequencing results for *Vf*ACBP3a and *Vf*ACBP6, the contigs from pyrosequencing for both *Vf*ACBP3b and *Vf*ACBP4 covered only a portion of the 3' ends of the respective ORFs. Full-length cDNA clones for these genes were obtained by genome walking

and Rapid Amplification of cDNA Ends (RACE). Of these, only *Vf*ACBP4 has not been completely sequenced at this time. The pyrosequencing sequences yielded a 683 base pair (227 amino acids) sequence for *Vf*ACBP3b, including 341 base pairs (113 amino acids) of the 3' UTR and 342 base pairs (114 amino acids) of coding sequence, meaning that 784 base pairs (261 amino acids) were required to reach the start methionine codon. Pyrosequencing yielded a 397 base pair (132 amino acids) sequence for *Vf*ACBP4, including 103 base pairs (34 amino acids) of coding sequence, the stop codon, and 291 base pairs (97 amino acids) of 3' UTR, meaning that roughly 1905 base pairs (635 amino acids) will be required to reach the start codon.

Genome walking and RACE to obtain full length open reading frames

It was difficult to ascertain full-length cDNAs for longer open reading frames, such as the case with *Vf*ACBP3b and especially *Vf*ACBP4, due to limitations in the cDNA library synthesis of pyrosequencing. Thus, the use of the genome walking and RACE techniques were needed to produce full-length clones. As was mentioned previously, the ACBPs that were identified by EST and pyrosequencing, the genome walking and RACE products, and the full-length ORFs, were compared to a publicly available database, GenBank to identify any sequence similarity to other plant ACBPs.

*Vf*ACBP3b required to two rounds of genome walking in addition to one round of RACE in order to reach the start methionine, due to the genome walking products generating only part of the 5' sequence up to the start methionine. *Vf*ACBP4 also required RACE after genome walking, but the remaining 5' portion of the sequence is not completed at this time. Despite this, the partial sequence was used to perform phylogenetic analysis and to design real-time quantitative PCR primers.

After a full-length cDNA sequence was obtained from RACE PCR and genome walking for *Vf*ACBP3b, specific PCR primers (listed in Materials and Methods) were designed to obtain a full-length cDNA based on classic 3-step PCR parameters.

Confirming the identity of 4 unique *Vernicia fordii* ACBPs

The sequences for many of the proteins of the tung lipid pathway from the EST and pyrosequencing data were compared to online databases (GenBank, http://www.ncbi.nlm.nih.gov/genbank/) to confirm their identities. As was the case with the *Vf*ACBPs, a homology-based method from the *Arabidopsis* genome website (TAIR, http://www.arabidopsis.org/Blast/index.jsp) was used to compare the sequences borne out of the initial EST and pyrosequencing data. These cDNA sequences were compared to the TAIR10 protein database to see if any of these proteins were similar to proteins from other organisms. *Vf*ACBP6 was most similar to *Arabidopsis thaliana* ACBP6, (Representative Gene Model Number: AT1G31812.1, 1e-42, 69% identity, and 73% positives) through using the nucleotide database, TAIR10. *Vf*ACBP3a, using the TAIR10 protein database, was found to be most similar to *Arabidopsis thaliana* ACBP3 (AT4G24230.6, 1e-41, 73% identity, and 74 %positives). Interestingly, *Vf*ACBP3b, using the TAIR10 amino acid database, was most similar to a *Ricinus communis* ACBP (8e-37, 73% identity, and 79% positives). *Vf*ACBP4 was most similar to *Arabidopsis thaliana* ACBP4 (AT3G05420.2).

*Vf*ACBP3a and *Vf*ACBP3b are similar to one another in sequence and to the *Arabidopsis thaliana* ACBP3. As can be seen in figure 3-1, BLAST results yielded differing best matches for either ACBP3a and ACBP3b. ACBP3a had the greatest sequential similarity with *Arabidopsis* ACBP3. ACBP3b compared most similarly to sequences of *Ricinus communis* (*E*-value of $9e^{-37}$) and *Populus trichocarpa* (*E*-values of $1e^{-31}$ and $1e^{-30}$) ACBPs. *Arabidopsis* ACBP3 was the fifth-

most similar sequence, yielding an *E*-value of $1e^{-19}$. These results indicate that these two tung ACBP3 sequences are isoforms and they are not the same protein.

Both the EST and pyrosequencing techniques provide cDNA contig sequences, and it was initially believed that *Vf*ACBP3a and *Vf*ACBP3b could actually be one protein and not two isoforms. Both of the *Vf*ACBPs are different in size, *Vf*ACBP3a being 819 base pairs while *Vf*ACBP3b is 1125 base pairs in their respective ORF lengths. They are very similar to *Arabidopsis* ACBP3 but to differing extents. As figure 3-2 shows, *Vf*ACBP3b is related to *At*ACBP3 but is more related to other ACBPs (Parts A and B). *Vf*ACBP3b was found to be more similar to a *Ricinus communis* and a *Populous trichocarpa* ACBP (Part B) than *At*ACBP3 (Part A). The two ACBP3s from tung are not even that similar in sequence. Figure 3-1, Parts A-D, illustrates several parts of the nucleotide sequences (Parts A and B) and proteins (Parts C and D) of both *Vf*ACBPs upon comparison. Comparing these two gives very little similarity even with the shortest word length, 16, that is possible in the BLAST program.

(A)

```
Score = 71.3 bits (38),  Expect = 3e-16
 Identities = 68/81 (84%), Gaps = 7/81 (8%)
 Strand=Plus/Plus

Query  667  AAGTTCTCTGCTCGCT-CAAAGTGGAATGCATGGCAACA-ACTTGGGAACATGAGTCCAG
724
            |||||  ||||||| | | |||||||||||| |||||| |  ||||| ||||||| |||||
Sbjct  821  AAGTT-GCTGCTCG-TGCCAAGTGGAATGCTTGGCAA-AGGCTTGGAAACATGAATCCAG
877

Query  725  -AGATGGCTATGGAGCAGTAT  744
             || ||||||||||||||||
Sbjct  878  AAG-TGGCTATGGAGCAGTAT  897
```

(B)

```
 Score = 51.0 bits (27),  Expect = 4e-10
 Identities = 35/39 (90%), Gaps = 0/39 (0%)
 Strand=Plus/Plus

Query  475  GAGGATGATTGGGAAGGAATAGAAAGGAGTGAGTTGGAG  513
            |||||||||||||||| || || ||||||||| ||||||
Sbjct  631  GAGGATGATTGGGAAGGGATTGAGAGGAGTGAATTGGAG  669
```

(C)

```
Score = 36.6 bits (83),  Expect = 8e-07, Method: Compositional matrix
adjust.
 Identities = 26/71 (37%), Positives = 38/71 (54%), Gaps = 9/71 (12%)

Query  3   MELFFELVLTLVVSFFCSFILAKLISLA---NDHDFENKTTHYHNF-QPECKD-----YW
53
           MEL  EL +T V +  CSF++AKL+S+A    D   +++ +   N  Q   +D     Y+
Sbjct  1   MELLQELFVTAVFAVVCSFLIAKLVSMAMAGADSSHDSQFSKSQNVDQKITRDDDDLQYF
60

Query  54  ETGKKFGFVSE  64
           E  K  GF SE
Sbjct  61  EKLKVEGFKSE  71
```

(D)

```
Score =  137 bits (345),  Expect = 3e-37, Method: Compositional matrix
adjust.
 Identities = 63/109 (58%), Positives = 81/109 (75%), Gaps = 1/109 (0%)

Query  158  EEDDWEGIERSELEKRFGAAVAYVGSIDNANKLSSTLSNGLKLQLYGLHQVAIEGPCHLP
217
            +EDDWEGIERSELE+ F  A  +V S D    L+S  S+ ++++LYGLH+VA EGPC
Sbjct  210  DEDDWEGIERSELEQIFAKAAKFVESGDKDEGLTSVGSD-VQMELYGLHKVATEGPCREQ
268

Query  218  QPMPLKFSARSKWNAWQQLGNMSPEMAMEQYINLVSTSIPEWMKDAFGD  266
             PM LK +AR+KWNAWQ+LGNM+PE+AMEQY+ LVS  +P WM+D   D
Sbjct  269  PPMALKVAARAKWNAWQRLGNMNPEVAMEQYVALVSDKVPGWMEDKSTD  317
```

Figure 3-1. BLAST comparisons of *Vf*ACBP3a and *Vf*ACBP3b. Parts A and B: BLASTn results of *Vf*ACBP3a (Query) against *Vf*ACBP3n (Subject) illustrate that these two *Vf*ACBPs are not very similar in their nucleotide sequences. Parts C and D: BLASTp results of *Vf*ACBP3a (Query) against *Vf*ACBP3b (Subject) illustrate that these two *Vf*ACBPs are not very similar in their protein sequences.

So, not only are the two proteins different lengths, but they do not share very much identity. These data illustrate that there are two isoforms of *Vf*ACBP3; *Vf*ACBP3a and *Vf*ACBP3b. This discovery of *Vf*ACBP3b is interesting because of both an absence of an ortholog in *Arabidopsis thaliana* and its presence as an ortholog in *Ricinus communis* and *Populous trichocarpa.* This presence in *Ricinus communis* shows the shared *Euphorbiaceae* lineage of tung and castor.

(A)

```
Query: 682 EGPCREQPPMALKVAARAKWNAWQRLGNMNPEVAMEQYVALVSDKVPGWMEDKSTDNGKP 503
           EG CRE  PMA+ ++ARAKWNAWQ+LGNM+ E AMEQY+ALVS ++PG  +   T  GK
Sbjct: 268 EGSCREAQPMAVMISARAKWNAWQKLGNMSQEEAMEQYLALVSKEIPGLTKAGHT-VGKM 326

Query: 502 GSTEAA-----NHGAL--PSDLSTS----SSHHPYITEER 416
              E +     N G+L  P++L T+    SS +  ++ ER
Sbjct: 327 SEMETSVGLPPNSGSLEDPTNLVTTGVDESSKNEIVSGER 366
```

(B)

```
BLAST AGAINST ALL TAIR PLANT PROTEINS
>ref|XP_002510117.1| acyl-CoA-binding protein, acbp, putative [Ricinus commu
          Length = 343

 Score =  153 bits (386), Expect = 8e-37,   Method: Composition-based stats.
 Identities = 82/111 (73%), Positives = 88/111 (79%), Gaps = 5/111 (4%)

Query: 1   EGPCREQPPMALKVAARAKWNAWQRLGNMNPEVAMEQYVALVSDKVPGWMEDKSTDNGKP 60
           EGPC EQPPMALK+AARAKWNAWQRLGNMNPEVAMEQY+ALVSDKVPGWMED ST NGKP
Sbjct: 231 EGPCHEQPPMALKLAARAKWNAWQRLGNMNPEVAMEQYIALVSDKVPGWMEDTSTGNGKP 290

Query: 61  GSTEAANHGALPSDLSTSSSHHPYITEERNPEVAPGTEKNDLTGGLILENR 111
           GS E  N G L SDL+T +     I EERNPE    TEKNDLTG   +E+R
Sbjct: 291 GSAEEVNPGGLASDLTTKN-----IAEERNPEATTDTEKNDLTGVSNMESR 336
```

Figure 3-2. BLAST analyses of *Vf*ACBP3a and *Vf*ACBP3b. Part A represents *Vf*ACBP3b compared to *At*ACBP3 illustrating the similarities between the two proteins. Part B shows the first hit from *Vf*ACBP3b compared to a TAIR10 database of all green plant proteins. *Vf*ACBP3b is most similar to *Ricinus communis* ACBP despite its vast similarity to *At*ACBP3, thus illustrating its uniqueness compared to *Vf*ACBP3a.

The *At*ACBPs have highly conserved binding domain residues (Xiao and Chye, 2009). Perhaps the most important property of ACBPs is their specific binding to acyl-CoA and as such, it is critical that they contain certain residues that constitute a binding domain (Xiao and Chye,

2009). There are 8 critical binding domain amino acid residues in the acyl-CoA binding domain of *Arabidopsis thaliana* ACBP6: F5, K35, D40, F47, K54, W58, A69, and Y73. Figure 3-3, part A illustrates the critical residues of tung ACBP3a as compared to *At*ACBP6. *Vf*ACBP3a has a match of 7 of the 8 critical residues for acyl-CoA binding, while *Vf*ACBP3b (not pictured) also matched 7 of the residues, but the difference was that the 4th critical residue, P (proline), was different (proline in *Arabidopsis* changed to serine in tung), while the difference for *Vf*ACBP3a was at the second residue, K (lysine) changed to a Q (glutamine) in tung. Interestingly, proline being changed to serine is a nonpolar to polar uncharged change. Lysine to glutamine is a basic polar to polar uncharged change. The implications of these changes are unknown. Tung ACBP6, on the other hand, matched 6 of these 8 residues (figure 3-3, part B). This illustrates the conservation of critical binding domain residues.

(A)

```
Query  170  LEKRFGAAVAYVGSIDNANKLSSTLSNGLKLQLYGLHQVAIEGPCHLPQPMPLKFSARSK  229
            LEK F AAV  +     A ++ +      K++L+GLH++A EG C   QPM +  SAR+K
Sbjct  1    LEKAFAAAVNLLEESGKAEEIGAEA----KMELFGLHKIATEGSCREAQPMAVMISARAK  56

Query  230  WNAWQQLGNMSPEMAMEQYINLVSTSIP  257
            WNAWQ+LGNMS E AMEQY+ LVS  IP
Sbjct  57   WNAWQKLGNMSQEEAMEQYLALVSKEIP  84
```

(B)

```
Query  3    LKEEFEEYAEKAKTLPENTTNENKLILYGLYKQATVGPVNTSRPGIFNQRDRAKWDAWKA  62
            LKEEFEE+AEK  TL E  +NE+ LILYGLYKQA  GPV+TSRPG+F+ ++RAKWDAWKA
Sbjct  1    LKEEFEEHAEKVNTLTELPSNEDLLILYGLYKQAKFGPVDTSRPGMFSMKERAKWDAWKA  60

Query  63   VEGKSKEEAMSDYITKVKQFLEEAA  87
            VEGKS EEAM+DYITKVKQ LE AA
Sbjct  61   VEGKSSEEAMNDYITKVKQLLEVAA  85
```

Figure 3-3. Tung ACBP6 and ACBP3a critical binding residues in the acyl-CoA binding domain. Red arrows represent amino acid changes while black represent no changes. Part A: Seven of the eight resiudes believed to be critical in the binding of acyl-CoA are direct matches in *Vf*ACBP3a (query) of tung as compared to *At*ACBP3 (subject). Part B: Six of the eight residues believed to be critical in the binding of acyl-CoA are direct matches in *Vf*ACBP6 (query) as compared to *At*ACBP6 (subject).

The structure of the highly conserved, soluble bovine ACBP

Through NMR studies, the three-dimensional structure of bovine ACBP has been determined (Andersen, et. al., 1991). This ACBP is similar to all other ~10 kDa ACBPs found throughout many eukaryotes, including *Arabidopsis* and *Vernicia fordii* ACBP6. Through these studies, and since there is a high amount of conservation between these ACBPs, it is possible to observe some of the features that may be present in these ACBPs, and is thus relevant to tung ACBP6. The bovine ACBP has been shown to be an up-down-down-up four-K-helix bundle (A1 through A4) with an overhand loop connecting two helices (Andersen, et. al., 1991). This bundled arrangement of ACBP is unique amongst other known four-helix folds (Andersen, et. al., 1991). The arrangement is skewed, since one of the helices is disjointed from two other helices, which results in only four helix-helix interfaces, as opposed to the typical six interfaces as seen in the well-known four-helix bundles (Andersen, et. al., 1991). All of the interaction angles between helices in the bovine ACBP were calculated using the program, PRONTO (Andersen, et. al., 1991). The residues at the nearest contact in the four helix interfaces are Ala9 and Tyr31, within helices A1-A2, Phe5 and Ile74, in helices A1-A4, Ala34 and Ala69, in helices A2-A4, and Ser29 and Trp58, in helices A2-A3 (Andersen, et. al., 1991). All of the central residues of bovine ACBP were determined from calculations using a set of structures of ACBP using the program XPLOR (Andersen, et. al., 1991). All of the central residues, aside from Ser29, are highly conserved in the sequences of ACBP (Andersen, et. al., 1991). It is also apparent that many of the residues that make up the interfaces are conserved throughout evolution (Andersen, et. al., 1991). The most conserved interface is between helices A1 and A4, and the least conserved between helices A2 and A4 (Andersen, et. al., 1991). The edges of the interfaces are where the most dramatic differences in structure are located, which are possibly

compensated for by similar changes or by an increased dynamic structure (Andersen, et. al., 1991). Therefore, it is of a high probability that the four-helix bundle architecture is conserved throughout many different species, including *Arabidopsis* and tung ACBP6 (Andersen, et. al., 1991).

Quantitative Real-Time Polymerase Chain Reaction (qPCR) revealed dynamic expression patterns for *Vf*ACBPs

After each of the *Vf*ACBPs was cloned and analyzed, the testing and analysis of their expression patterns was performed. Ultimately, qPCR was used to determine and analyze tissue specific expression patterns of the tung ACBPs and compare these results with enzymes that have known functions in tung. This was done to determine if there is any function(s) the *Vf*ACBPs may have in tung. Quantitative real time PCR (qPCR) was used to amplify and quantify targeted DNA molecules. The principal difference between classic PCR and real time PCR is that the reaction is observed in real time as opposed to the detection of a product at the end of the amplification process.

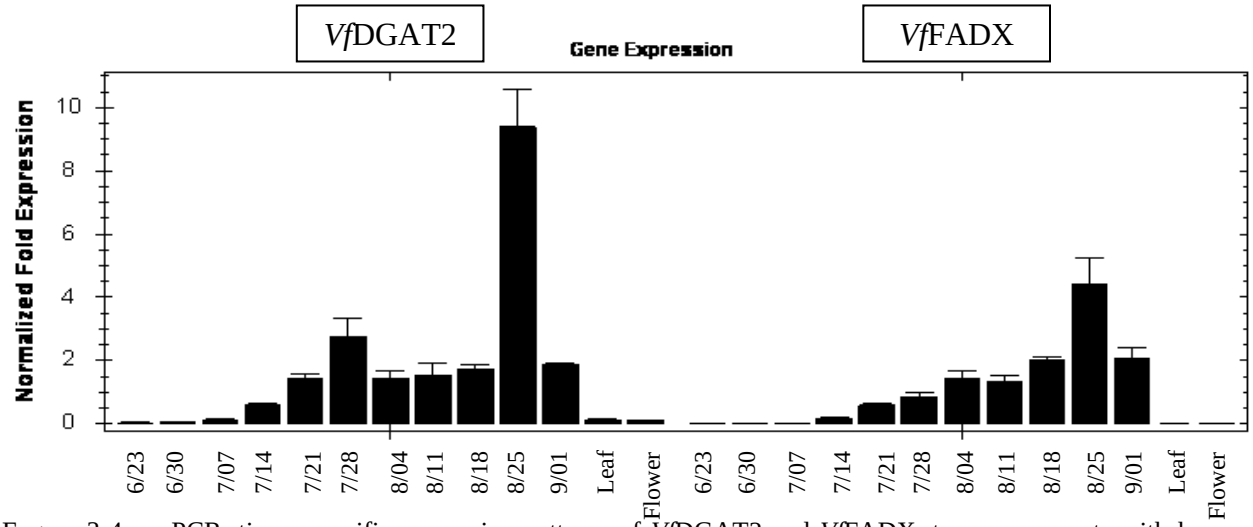

Fugure 3-4. qPCR: tissue-specific expression patterns of *Vf*DGAT2 and *Vf*FADX, two components with known roles of the tung lipid biosynthetic pathway.

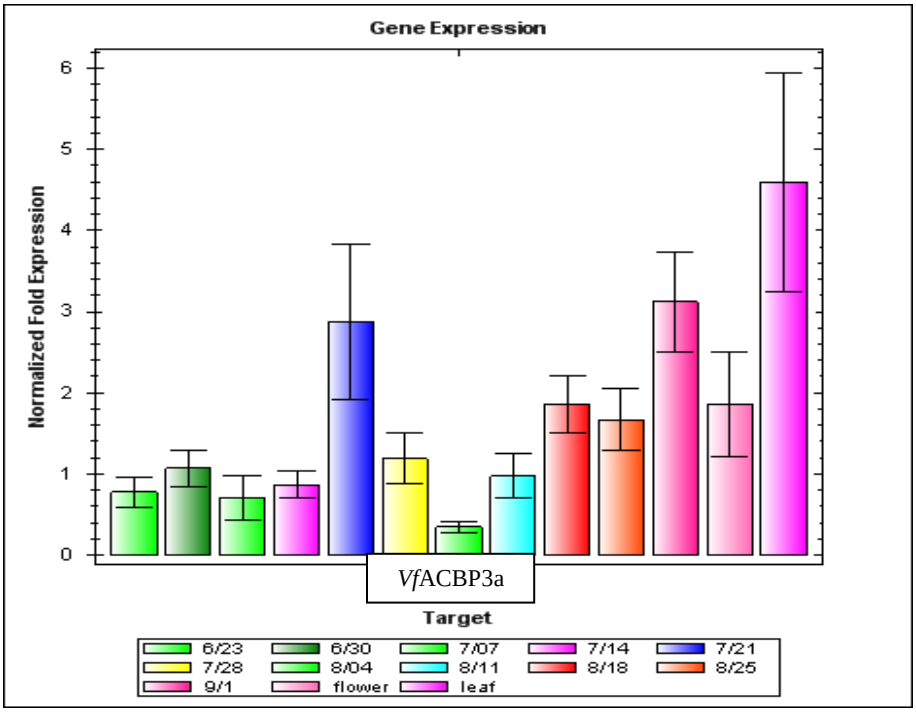

Figure 3-5. qPCR: tissue-specific expression patterns of *Vf*ACB3a.

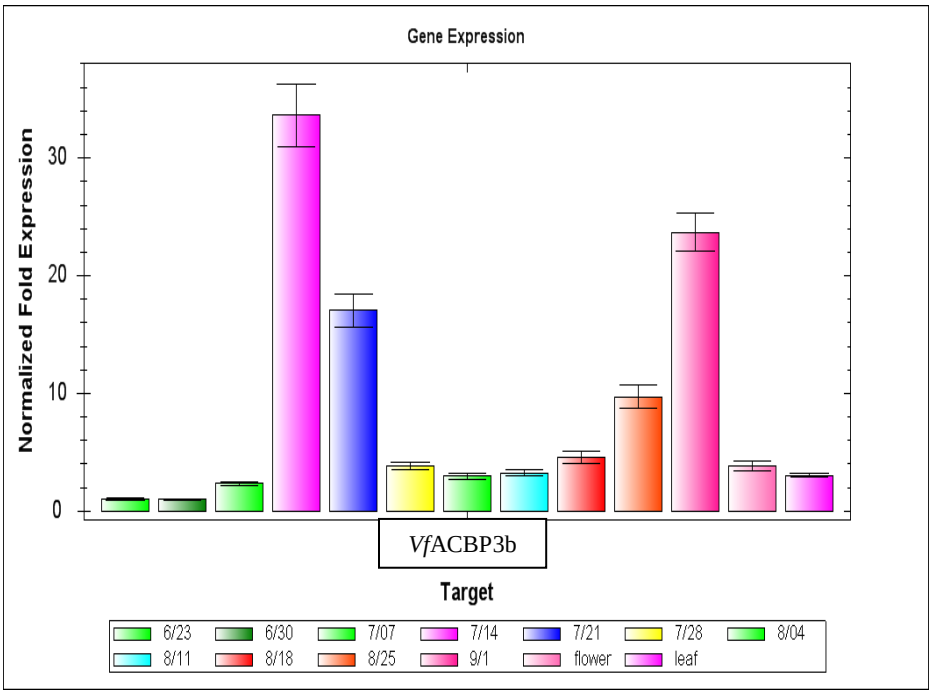

Figure 3-6. qPCR: tissue-specific expression patterns of *Vf*ACB3b.

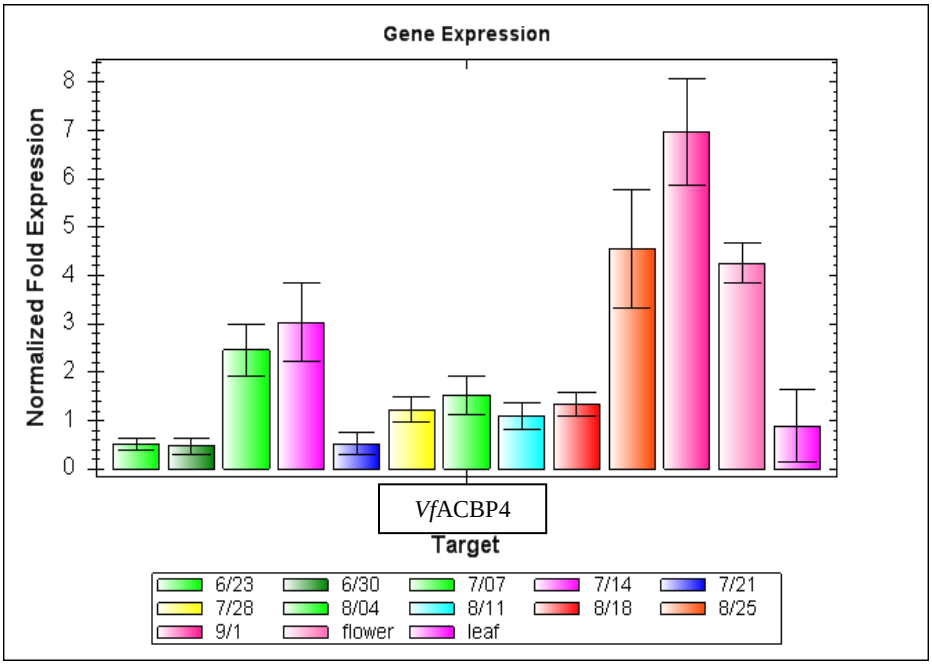

Figure 3-7. qPCR: tissue-specific expression patterns of *Vf*ACB4.

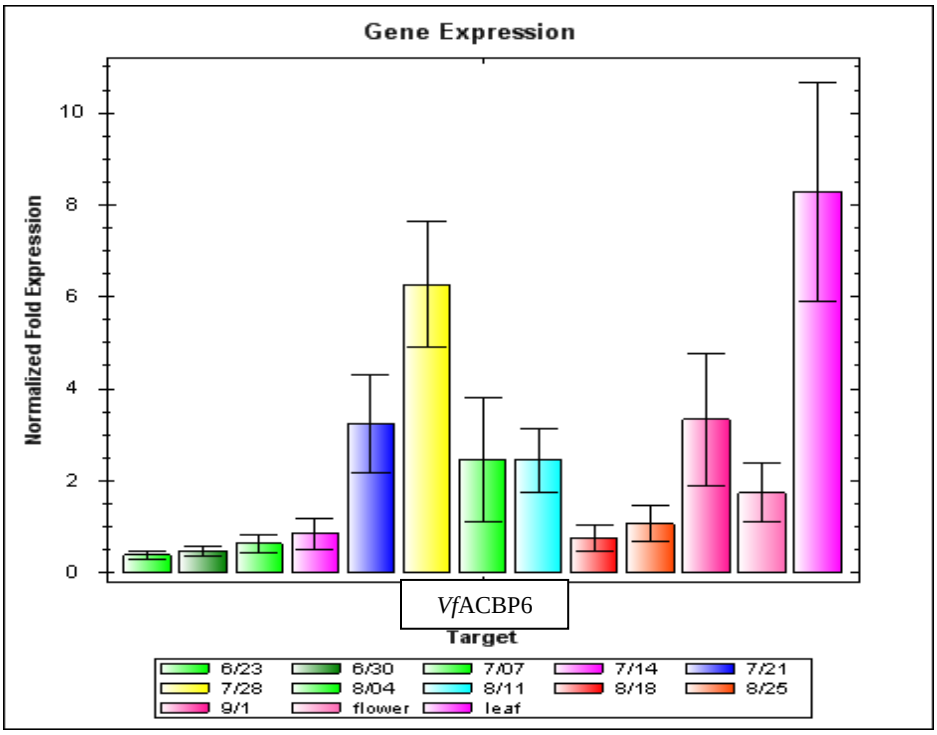

Figure 3-8. qPCR: tissue-specific expression patterns of *Vf*ACBP6.

Each of the dates shown in figures 3-4 through 3-8 are representative of the weeks after flowering. June 23rd is the date in seeds that is 8 weeks after flowering (WAF) with each subsequent date being one week after that. The range shown here is from 8 to 18 WAF.

Referring to figure 3-4, the expressions of both DGAT2 and FADX had a very distinct pattern. Tung express these enzymes, along with several others, at a greater rate when the production of α-eleostearic acid in seed oil bodies stored in triacylglycerols (TAGs) was increased. This corresponds to mid to late summer, with little expression in leaf and flower tissues. Both *Vf*DGAT2 and *Vf*FADX exhibit a bimodal expression pattern, with an increase in expression in mid-summer, followed by a subsequent decrease, and then another increase. Neither expressed highly, or at all, in leaves and flowers.

All 4 *Vf*ACBPs had expression levels that correlated with *Vf*DGAT2 and *Vf*FADX expression levels except that there was higher expression in leaf and flower tissues by the *Vf*ACBPs. Each of the *Vf*ACBPs had an expression pattern that was low at the early weeks after fluorescing (WAFs), rose in mid-summer, lowered again, then rose closer to the fall. In contrast to *Vf*DGAT2 and *Vf*FADX, the *Vf*ACBPs expressed at higher levels in leaf and flower tissues. Despite the common bimodal expression pattern, the levels of expression of each *Vf*ACBP were very different from one another and *Vf*DGAT2 and *Vf*FADX. *Vf*ACBP3b expressed at the highest levels as compared to every other protein. There was a dramatic difference between the very high levels of expression of 7/14, 7/21, and 9/1 for *Vf*ACBP3b compared to the other *Vf*ACBPs and *Vf*DGAT2 and *Vf*FADX. Clearly, *Vf*ACBP3b was expressed much higher at WAFs in the seeds of tung. In addition, compared to itself, it expressed in low amounts in leaf and flower tissues; however, these amounts are comparable to the other *Vf*ACBPs but in greater amount than *Vf*DGAT2 and *Vf*FADX, which showed very little expression. Like *Vf*ACBP6,

*Vf*ACBP3a exhibited its highest expression in leaf tissues. *Vf*ACBP3a also appeared to have less difference in expression between each of the WAFs where it was expressed in leaf and flower. *Vf*ACBP4 expressed at its highest at 9/1 and like the pattern exhibited by *Vf*ACBP3b, it had a low level of expression in leaf tissues. *Vf*ACBP6 was very similar in overall expression as *Vf*ACBP3a, except its initial rise in expression occured later (peaks at 7/28 as opposed to 7/21 in *Vf*ACBP3a).

	6/23	**6/30**	**7/7**	**7/14**	**7/21**	**7/28**	**8/4**	**8/11**	**8/18**	**8/25**	**9/1**	**Flower**	**Leaf**
***Vf*ACBP3a**	0.8	1.0	0.7	0.8	2.8	1.2	0.4	0.9	1.8	1.6	3.2	1.8	4.5
***Vf*ACBP3b**	1.0	1.0	2.0	34.0	17.0	4.0	3.0	4.0	5.0	8.0	24.0	4.0	3.0
***Vf*ACBP4**	0.5	0.4	2.4	3.0	0.4	1.2	1.4	1.2	1.3	4.4	6.8	4.2	0.6
***Vf*ACBP6**	0.4	0.5	0.6	0.8	3.3	6.2	2.5	2.5	0.7	0.9	3.3	1.8	8.2
***Vf*DGAT2**	0.0	0.0	0.1	0.5	1.5	2.9	1.5	1.6	1.7	9.5	1.8	0.1	0.1
***Vf*FADX**	0.0	0.0	0.0	0.1	0.5	0.7	1.5	1.3	1.8	4.3	1.9	0.0	0.0

Figure 3-9. Normalized fold expression data of the *Vf*ACBPs and *Vf*DGAT2 and *Vf*FADX. Each value is normalized to the reference gene, tung ubiquiting ligase.

Previously, tung DGAT2 and FADX, two components with known roles in the tung metabolic pathway, were analyzed by qPCR (figure 3-4). The expressions of these were shown to coincide with the peak of TAG accumulation (Shockey, et. al., 2006). Each *Vf*ACBP also exhibited unique patterns and levels of expression, as seen in Figure 3-9. One aspect of their expression that is commonly seen amongst each of them, however, is that they generally have increased expression in mid-summer months, first in July and then later in late August. Essentially, in a sequential manner, each of the *Vf*ACBPs are expressed at low levels in the earliest days of summer then, expression rises in mid-summer, lowers again, and rises closer to the fall. These results show that the *Vf*ACBPs are specifically expressed at certain times, and this expression can be lowered or raised. What this means for the potential roles of each *Vf*ACBP is

unknown, but the relevance of the expression pattern is consistent with peak TAG accumulation. One interesting result is the expression patterns of each *Vf*ACBP in the leaf and flower tissues. Both *Vf*DGAT2 and *Vf*FADX are not expressed in these tissues. Thus, these data show a unique expression pattern for *Vf*ACBPs.

Overall, this data shows unique expression patterns of the *Vf*ACBPs. They express differently, not only amongst themselves, but when compared to *Vf*DGAT2 and *Vf*FADX. The general levels of expression are also markedly different between each *Vf*ACBP and *Vf*DGAT2 and *Vf*FADX. These data show that each *Vf*ACBP is expressed at differing levels but have specific WAFs in seeds that they are expressed high or low. Likewise, each exhibits unique levels of expression in leaves and flowers perhaps suggesting that each may have a unique biological function.

Split-Ubiquitin Yeast Two-Hybrid Analysis: qualitative plate assays

Each of the *Vf*ACBPs was expressed in all tissues, including seeds, and with some interesting differences and some interesting similarities. If they are expressed in seeds, they may participate in complex lipid synthesis. So, split ubiquitin yeast two-hybrid analysis was performed using the *Vf*DGATs. Previous studies in our lab showed that each *Vf*DGAT, *Vf*DGAT1 and *Vf*DGAT2, is targeted to different subdomains of the ER membrane (Shockey, et. al., 2006). They have different affinities for eleostearic acid containing substrates when expressed in yeast, and are therefore expected to perform different biological roles *in planta*. In each of those different subdomains, there might be different complexes of protein isoforms to carry out those specific tasks. It is possible that some of the *Vf*ACBPs could be a part of one or both protein complexes, and this can be tested through protein:protein interactions by split ubiquitin. In addition, since the *Vf*ACBPs are expressed in seeds (just not seed specific), and

interact with the *Vf*DGATs, they were expressed in the seeds of transgenic plants to study the effects of *vf*ACBP expression on seed lipid fatty acid content.

A split-ubiquitin-based membrane yeast two-hybrid assay was performed in order to examine the interactions of the three of the tung ACBPs with themselves, one another, and two enzymes known to be involved in tung lipid biosynthesis, DGAT1, and DGAT2. This assay is similar in principle to the classic two-hybrid assay in yeast cells, with the exception that the protein-protein interactions can take place anywhere in the yeast cell, including in cellular membranes, as opposed to the nucleus only, a situation that may greatly improve the fidelity of measuring protein-protein interactions of membrane-bound proteins (Snider et al., 2010).

Despite the potential to fuse the ACBPs with either NubG to the N terminus and Cub-LexA to the C terminus or NubG to the C terminus and Cub-LexA to the N terminus, it was observed that fusing ACBPs with NubG to the N terminus and Cub-LexA to the C terminus was needed to avoid false negative results (Dyer, personal communication).

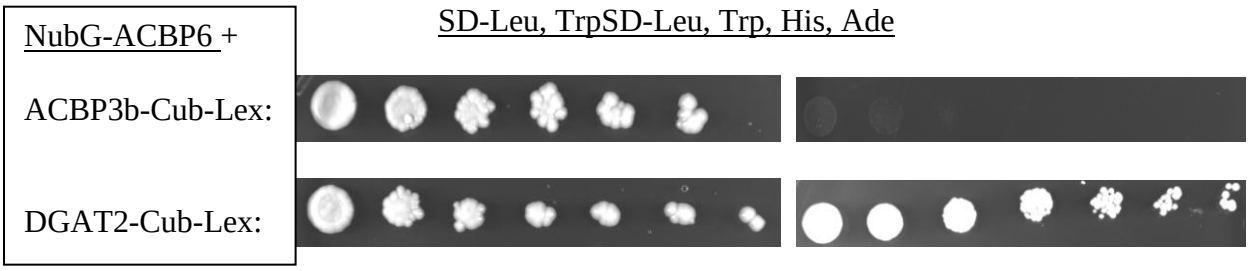

Figure 3-10. Example of two split-ubiquitin SD-LT and SD-LTHA plate results. Dilutions are increased from left to right. The left-most parts of figure 3-7 represent SD-LT plates, which serve as positive controls for growth. The right-most parts of figure 3-7 show SD-LTHA plates, which select for interactions. *Vf*ACBP6 does not interact with *Vf*ACBP3a but does interact with *Vf*DGAT2.

(A)

Bait	Prey	Interactivity
Cub-LexA	NubG-ACBP3a	No Interaction Observed
pCCW-Alg5-Cub-LexA	NubG-ACBP3a	**Interaction Observed**
ACBP3a-Cub-LexA	NubG-ACBP3a	No Interaction Observed
ACBP3b-Cub-LexA	NubG-ACBP3a	No Interaction Observed
ACBP4-Cub-LexA	NubG-ACBP3a	No Interaction Observed
ACBP6-Cub-LexA	NubG-ACBP3a	No Interaction Observed
DGAT1-Cub-LexA	NubG-ACBP3a	**Interaction Observed**
DGAT2-Cub-LexA	NubG-ACBP3a	**Interaction Observed**

(B)

Bait	Prey	Interactivity
Cub-LexA	NubG-ACBP3b	No Interaction Observed
pCCW-Alg5-Cub-LexA	NubG-ACBP3b	**Interaction Observed**
ACBP3a-Cub-LexA	NubG-ACBP3b	No Interaction Observed
ACBP3b-Cub-LexA	NubG-ACBP3b	No Interaction Observed
ACBP4-Cub-LexA	NubG-ACBP3b	No Interaction Observed
ACBP6-Cub-LexA	NubG-ACBP3b	No Interaction Observed
DGAT1-Cub-LexA	NubG-ACBP3b	**Interaction Observed**
DGAT2-Cub-LexA	NubG-ACBP3b	**Interaction Observed**

(C)

Bait	Prey	Interactivity
Cub-LexA	NubG-ACBP4	No Interaction Observed
pCCW-Alg5-Cub-LexA	NubG-ACBP4	**Interaction Observed**
ACBP3a-Cub-LexA	NubG-AC4P4	No Interaction Observed
ACBP3b-Cub-LexA	NubG-ACBP4	No Interaction Observed
ACBP4-Cub-LexA	NubG-ACBP4	No Interaction Observed
ACBP6-Cub-LexA	NubG-ACBP4	No Interaction Observed
DGAT1-Cub-LexA	NubG-ACBP4	**Interaction Observed**
DGAT2-Cub-LexA	NubG-ACBP4	**Interaction Observed**

(D)

Bait	Prey	Interactivity
Cub-LexA	NubG-ACBP6	No Interaction Observed
pCCW-Alg5-Cub-LexA	NubG-ACBP6	**Interaction Observed**
ACBP3a-Cub-LexA	NubG-ACBP6	No Interaction Observed
ACBP3b-Cub-LexA	NubG-ACBP6	No Interaction Observed
ACBP4-Cub-LexA	NubG-ACBP6	No Interaction Observed
ACBP6-Cub-LexA	NubG-ACBP6	No Interaction Observed
DGAT1-Cub-LexA	NubG-ACBP6	**Interaction Observed**
DGAT2-Cub-LexA	NubG-ACBP6	**Interaction Observed**

Figure 3-11. Split ubiquitin interactions of the *Vf*ACBPs. All of the *Vf*ACBPs interact with *Vf*DGAT1, *Vf*DGAT2, and the positive control bait (pCCW-Alg5-Cub-LexA) but not with other *Vf*ACBPs or themselves. This positive interaction only occurs if NubG is attached to the N-terminus of *Vf*ACBPs. *Vf*ACBPs with Cub-LexA fused to its C-terminus (results not shown), *Vf*ACBPs with Cub-LexA fused to its N-terminus (results not shown), or *Vf*ACBPs

with NubG fused to its C-terminus (results not shown), did not show interactivity with any preys or baits respectively, including positive controls.

Because each of the ACBPs interacted with both *Vf*DGAT1 and *Vf*DGAT2, two enzymes with known functionality in the tung lipid biosynthetic pathway, ACBPs may provide a role in the incorporation of eleostearic acid into complex lipids such as triacylglycerols. Due to the transient nature of the protein fusions as discussed above, it was difficult to discern if there would be any significant interaction between any of the ACBPs with one another. As it stands, it would be difficult to determine what role this would even provide. The aim of this study is to identify any influences tung ACBPs have, or what general roles they play, not just those involved in eleostearic acid channeling and accumulation. Clearly, these results show that *Vf*ACBPs interact with *Vf*DGAT1 and *Vf*DGAT2 in a qualitative manner. Beta-galactosidase assay were performed to quantitatively determine the interactivities seen here.

Split-Ubiquitin Yeast Two-Hybrid Analysis: quantitative beta-galactosidase assays

More specifically, β-galactosidase assays were performed to confirm and quantify the results attained from the serial plate dilution assays. Indeed, the β-galactosidase correlated very well with those of the plate dilution assays.

The enzyme β-galactosidase cleaved lactose to glucose and galactose for the usage as a carbon or energy source. The result was the production of a yellow color in solution, which can be used to determine enzyme concentration. Afterward, spectrophotometric measurements were made to determine optical densities of the solution. These OD readings were used in a formula to calculate enzyme activity, expressed in Miller units.

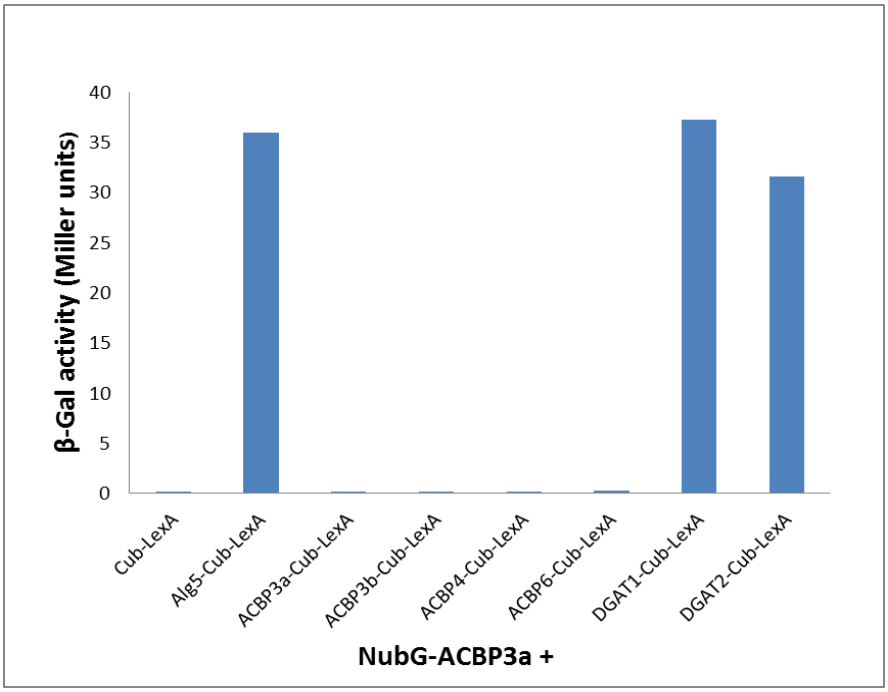
β-Gal activity (Miller units)
40
35
30
25
20
15
10
5
0
Cub-LexA
Alg5-Cub-LexA
ACBP3a-Cub-LexA
ACBP3b-Cub-LexA
ACBP4-Cub-LexA
ACBP6-Cub-LexA
DGAT1-Cub-LexA
DGAT2-Cub-LexA
NubG-ACBP3a +

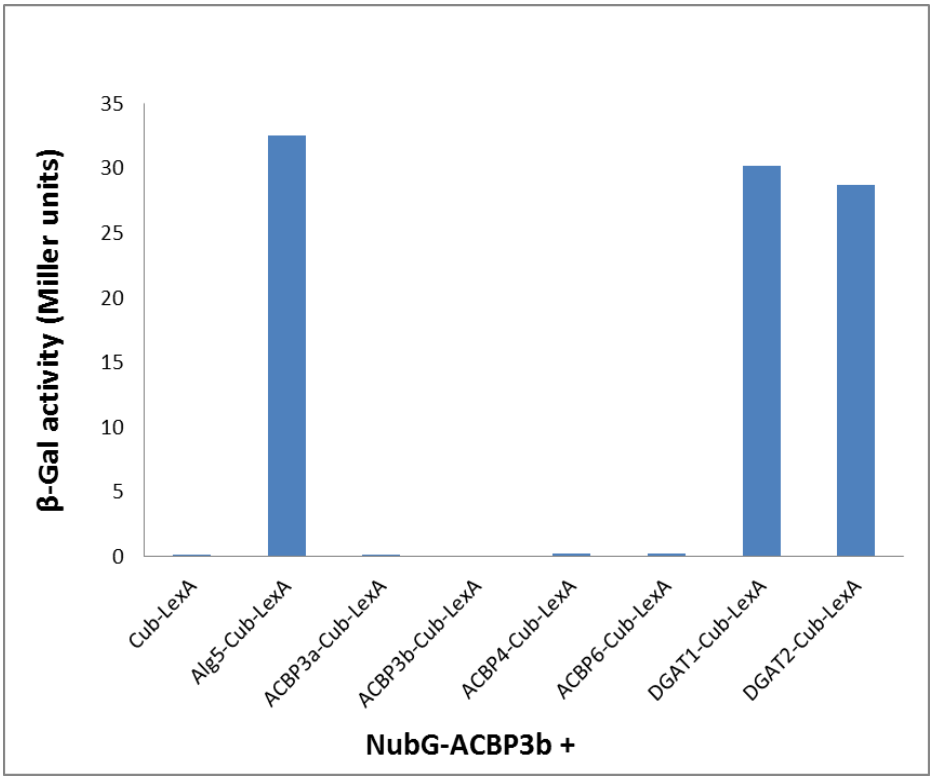
β-Gal activity (Miller units)
35
30
25
20
15
10
5
0
Cub-LexA
Alg5-Cub-LexA
ACBP3a-Cub-LexA
ACBP3b-Cub-LexA
ACBP4-Cub-LexA
ACBP6-Cub-LexA
DGAT1-Cub-LexA
DGAT2-Cub-LexA
NubG-ACBP3b +

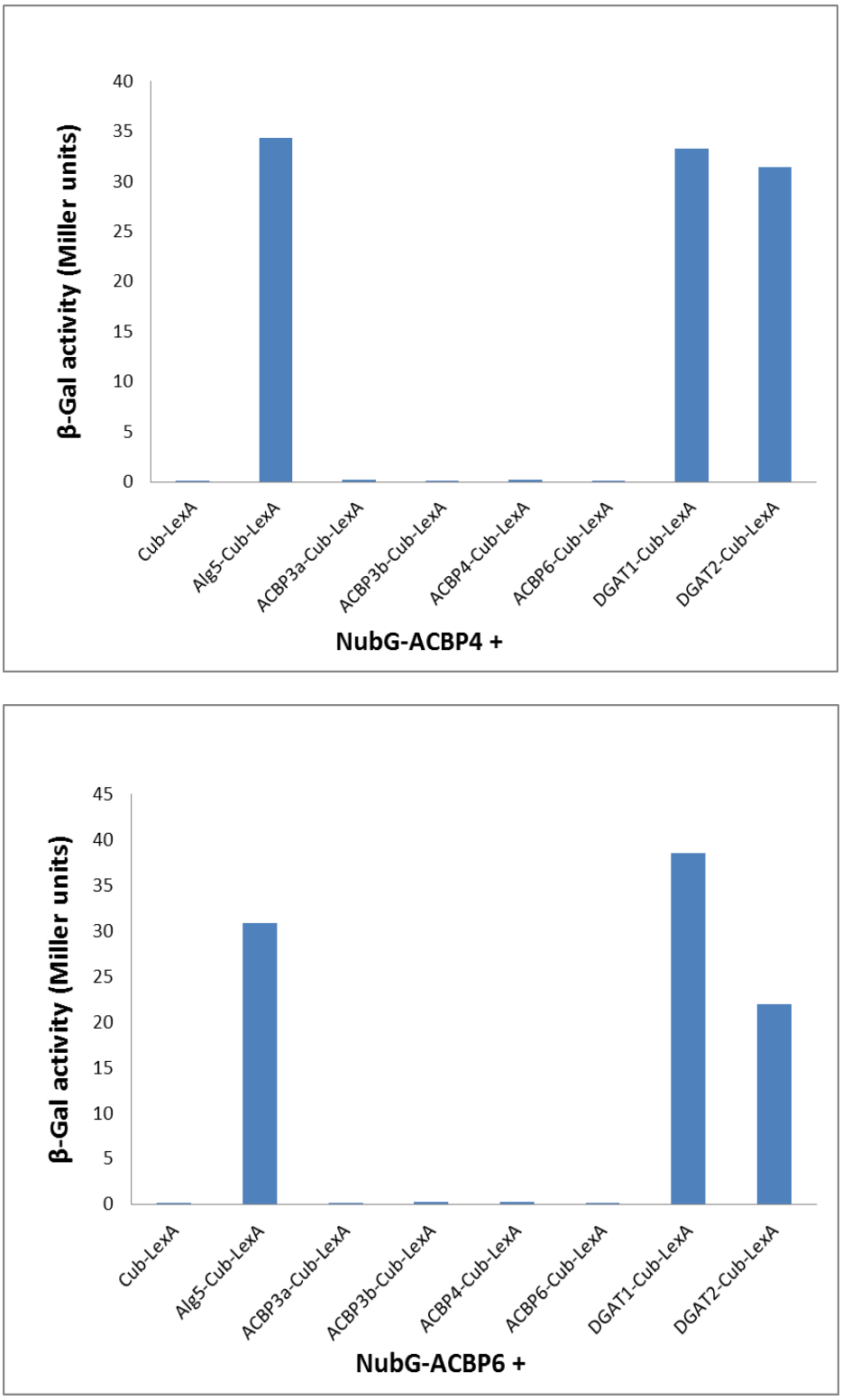

Figure 3-12. β-Galactosidase Assay results for the *Vf*ACBPs and their respective interacting Baits.

The results presented in the above figures confirm what was summarized previously in the plate dilution assay results section. It illustrates the strong interactivity of the *Vf*ACBPs with *Vf*DGAT1 and *Vf*DGAT2, along with the positive control, Alg5-Cub-LexA. The interaction of the *Vf*ACBPs with themselves is as weak as the negative control, Cub-LexA. This suggests that the *Vf*ACBPs do not form dimers or any other form of homopolymers. It does not, however, eliminate the possibility of self-interaction. Thus far, the tung ACBPs appear to perform their functions independently of one another.

The interactions were very similar in strength across all *Vf*ACBPs, with the exception of the *Vf*ACBP6 and its interaction with *Vf*DGAT2. Interestingly, *Vf*ACBP6 has a weaker interaction with *Vf*DGAT2 as compared to all of the other *Vf*ACBPs.

Fatty Acid Methyl Ester (FAME) Analysis and Gas Chromatography (GC) does not reveal any seed specific biosynthetic functions of ACBPs

Since qPCR showed that each *Vf*ACBP is expressed in seeds, and split ubiquitin analysis demonstrated that they interact with the *Vf*DGATs, the *Vf*ACBPs were expressed in the seeds of transgenic plants to study the effects of *Vf*ACBP expression on seed lipid fatty acid content.

One of the primary goals of this project and the culmination of other projects on the tung pathway is to produce α-eleostearic acid in high amounts in a transgenic system. “High amounts” is defined as a sizeable percentage of α-eleostearic acid versus all other fatty acids produced. As mentioned earlier, the oil of tung consists of approximately 80% eleostearic acid (wt/wt total fatty acids). Genes involved in the production of this fatty acid were placed into transgenic plants due to its useful drying properties and industrial applications. Fatty acid methyl esters (FAME) were created by alkali catalyzed reactions between fatty acids and methanol through transesterification. The fatty acid content in the seeds of transgenic *Arabidopsis* lines was

analyzed. Essentially, there were two main approaches to expressing tung ACBPs in transgenic *Arabidopsis*. The first was to analyze the potential role of *Vf*ACBPs, when co-expressed with *Vf*FADX in *fad3/fae1*, to determine whether these proteins increased the eleostearic acid content in seed lipids compared to the expression of *Vf*FADX alone.

These constructs contained the *fad3/fae1* double mutant which completely diverts the tung biosynthetic pathway toward α-eleostearic acid production via a diverged desaturase, FADX. Otherwise, linolenic acid would be produced if FAD3 were available for use. FAD3 would act as a competitor for linoleic acid substrate of FADX (Dyer, et. al., 2002) and the product of FAD3, linoleic acid, is toxic when produced in the same tissues as eleostearic acid. FAE1 is an elongase; thus deleting it is expected to prevent production of very long-chain fatty acids. Also, this absence of the enzyme reduces the use of oleic acid, which could be in turn be used FAD2 to make more linoleic acid.

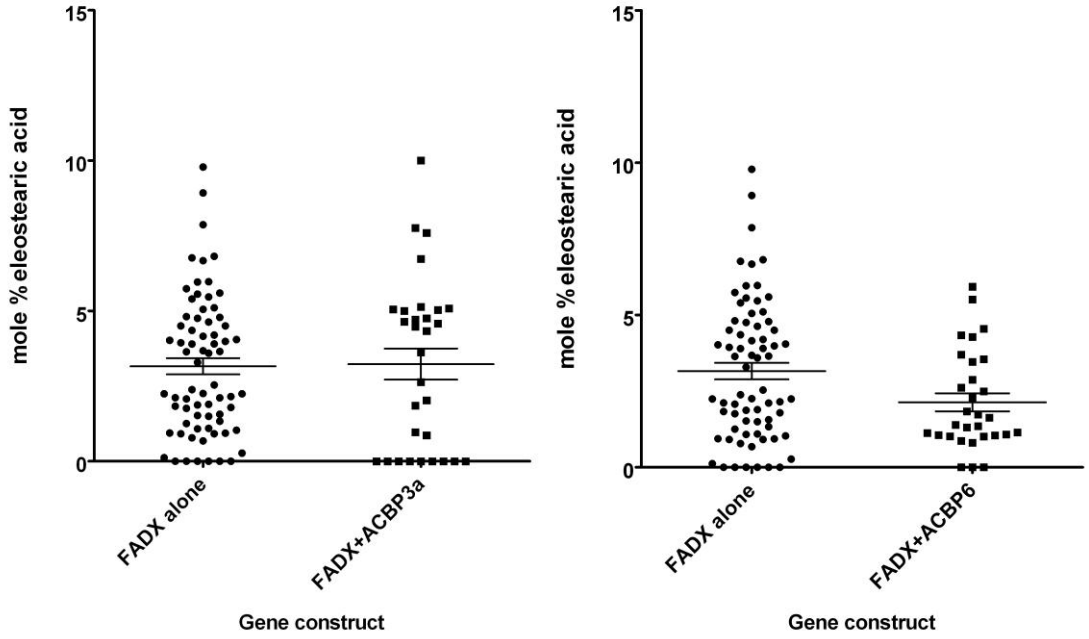

Figure 3-13. Bulk T_2 generation scatter plots of *Vf*ACBP3a and *Vf*ACBP6.

Figure 3-13 illustrates T_2 generation scatter plots of both *Vf*ACBP3a and *Vf*ACBP6 co-expressed with *Vf*FADX in *fad3/fae1*versus plants expressing *Vf*FADX alone. As the data shows,

there are no real "boosters" of eleostearic acid content when the *Vf*ACBP are introduced. So, it was imperative to investigate the effects of *Vf*ACBP co-expression on any other fatty acids in seeds.

(A)

Construct	16:0	18:0	Eleostearic acid
*Vf*FADX T_2 #53:	6.406	3.09	5.464
*Vf*FADX T_2 #60:	6.698	3.278	5.106
*Vf*FADX T_2 #63:	6.54	3.143	4.754
*Vf*FADX T_2 #68:	6.33	3.05	4.787
Avg.	6.4935	3.14025	5.02775
Std. Dev.	0.161628	0.09942	0.331329
versus			
*Vf*FADX + *Vf*ACBP6 T_2 #2	7.231	2.621	5.932
*Vf*FADX + *Vf*ACBP6 T_2 #19	7.615	2.911	4.547
*Vf*FADX + *Vf*ACBP6 T_2 #24	7.312	2.789	5.511
*Vf*FADX + *Vf*ACBP6 T_2 #3	7	2.863	4.339
*Vf*FADX + *Vf*ACBP6 T_2 #4	6.965	2.783	4.28
Avg.	7.2246	2.7934	4.9218
Std. Dev.	0.263595	0.11014	0.751615

(B)

Student's T-test	16:0	18:0	Eleostearic acid
P-values	0.001588257	0.001759445	0.787320396
	Significantly Different	Significantly Different	Not Significantly Different

Figure 3-14. Transformed lines with binary plasmid carrying *Vf*FADX (driven by the seed-specific beta-conglycinin promoter) as compared to *Vf*ACBP6 co-expressing *Vf*FADX T_2 plants with similar eleostearic acid values. Part A: Analysis of the average 16:0 and 18:0 values as compared to constructs lacking *Vf*ACBP6 to see if there was a significant difference. Individually and on average, these *Vf*ACBP6 constructs have lower 18:0 percentage values while higher 16:0 percentage values as compared to plant lines lacking *Vf*ACBP6. Part B: Student's t-test to examine the significance of the average 16:0 and 18:0 values of *Vf*ACBP6 plants co-expressing *vf*FADX as compared to *Vf*FADX lines lacking *Vf*ACBP6.

(A)

Construct	16:0	18:0	Eleostearic acid
*Vf*FADX T_2 #33	6.166	3.673	6.815
*Vf*FADX T_2 #43	6.019	3.613	9.785
*Vf*FADX T_2 #65	6.277	3.238	8.927
Avg.	6.154	3.508	8.509
Std. Dev.	0.129418	0.235744	1.528486
versus			
*Vf*FADX + *Vf*ACBP3a T_2 #12	6.861	2.782	7.768
*Vf*FADX + *Vf*ACBP3a T_2 #14	7.542	2.891	10.01
*Vf*FADX + *Vf*ACBP3a T_2 #19	7.161	2.781	7.594
*Vf*FADX+ *Vf*ACBP3a T_2 #30	7.789	2.937	6.731
Avg.	7.33825	2.84775	8.02575
Std. Dev.	0.409827	0.078771	1.398388

(B)

Student's T-test	16:0	18:0	Eleostearic acid
P-values	0.006699341	0.031673901	0.688888577
	Significantly Different	Slightly Significantly Different	Not Significantly Different

Figure 3-15. Transformed lines with binary plasmid carrying *Vf*FADX (driven by the seed-specific beta-conglycinin promoter) as compared to *Vf*ACBP3a co-expressing *Vf*FADX T_2 plants with similar eleostearic acid values. Part A: Analysis of the average 16:0 and 18:0 values as compared to constructs lacking *Vf*ACBP3a to see if there was a significant difference. Individually and on average, these *Vf*ACBP3a constructs have lower 18:0 percentage values while higher 16:0 percentage values as compared to plant lines lacking *Vf*ACBP3a. Part B: Student's t-test to examine the significance of the average 16:0 and 18:0 values of *Vf*ACBP3a plants co-expressing *Vf*FADX as compared to *Vf*FADX lines lacking *Vf*ACBP3a.

Student's t-tests were performed in order to observe any statistical significance of the results from the transgenic *Arabidopsis* lines that were produced. The results from both Figures 3-14 and 3-15 illustrate the differences in the 16:0 and 18:0 saturated fatty acid content of seed oil from transformed *Arabidopsis Vf*FADX lines containing tung *Vf*ACBP6 and *Vf*ACBP3a co-expressing *Vf*FADX as compared to *Vf*FADX lines without *Vf*ACBP with similar eleostearic acid

values. All of the 16:0 fatty acid percentages were higher individually and collectively on average for both *Vf*ACBP6 and *Vf*ACBP3a versus FADX lines without *Vf*ACBPs. All of the 18:0 fatty acid percentages were lower individually and collectively on average for both ACBP6 and ACBP3a as compared to *Vf*FADX plants not co-expressed with *Vf*ACBP. There was a statistically significant difference in the 16:0 and 18:0 content ($P < 0.05$) despite the lack of significant difference in eleostearic acid content in both contsructs. Clearly, these two *Vf*ACBPs affect the 16:0 and 18:0 fatty acid content in seeds. So, these two *Vf*ACBPs have an effect on the fatty acids in tung.

Of important note is that these lines are selected by Basta herbicide resistance, and therefore it is not so simple to sort out homozygous T_3 lines. Unfortunately, there is such a small sample size produced form these lines that it is difficult to ascertain any specific information with regard to the influence of *Vf*ACBPs on eloestearic acid content in seeds. However, acyl-CoA is used in a very large number of reactions in the cell and not just in lipid synthesis. For example, they are involved directly in the Kennedy Pathway (GPAT, LPAT, and DGAT), and indirectly as in LPCAT (Yurchenko, et. al., 2009). So, it is difficult to predict based on this preliminary analysis what its role may be in lipid metabolism in tung seeds. But, there are some statistically significant differences with 16:0 and 18:0, so it seems to be altering the size and content of at least one pool of acyl-CoAs in the seeds.

The second approach to expressing tung ACBPs in transgenic *Arabidopsis* involved analyzing the effects of *Vf*ACBP expression on entire normal metabolism of seed FAs in general. This was accomplished by expression in wild type *Arabidopsis thaliana* (ecotype *Columbia*) which makes a number of fatty acids that are not seen in *fad3/fae1* constructs. Plants were grown with either *Vf*ACBP6 or *Vf*ACBP3a expressed. Since wild type *Arabidopsis* does not produce

eleostearic acid, the analysis of the seed oils in these plants was used to monitor comprehensive fatty acid profile changes and composition when expressing a tung ACBP. In direct opposition to the Basta screening in the *Vf*FADX expressing lines, these lines used *Ds*Red screening used for selection, making the identification of homozygous T_3 lines much easier. Essentially, all seeds chosen in the identification of homozygous lines were visualized as bright red fluorescing seeds. This is a clear-cut method that is much easier than the Basta selection method.

In figures 3-16 and 3-17, those lines that are highlighted, ACBP3a + DsRed T_2 #1 and ACBP6 + DsRed T_2 #2, were chosen to produce T_3 lines, since their seeds were brightly red fluorescing. Seeds that were obviously fluorescent were chosen over seeds that were not as brightly red fluorescing. Figures 3-16 and 3-17 illustrate the effects of inserting *Vf*ACBP3a and *Vf*ACBP6 into wild type *Arabidopsis* plants. Looking at each line, there are several differences in the individual fatty acid contents and overall composition of *Vf*ACBP3a and *Vf*ACBP6 as compared to the averages of wild type plants. These differences clearly illustrate that introducing *Vf*ACBP3a and *Vf*ACBP6 has an effect on comprehensive fatty acid profiles.

Wild type *Columbia*	**16-0**	**18-0**	**18-1**	**18-2**	**18-3**	**20-1**	**20-2**
Averages	7.304	3.044	12.533	28.504	16.877	19.722	2.389
Std. Dev.	±0.095	±0.089	±0.511	±0.306	±0.392	±0.327	±0.127

Construct							
ACBP3a + DsRed T_2 #1	6.686 ˅	2.987 ˅	14.137 ^	28.003 ˅	17.253 ^	20.043 ^	1.832 ˅
ACBP3a + DsRed T_2 #2	6.829 ˅	2.913 ˅	13.205 ^	27.972 ˅	17.850 ^	19.892 ^	1.987 ˅
ACBP3a + DsRed T_2 #6	8.362 ^	3.399 ^	11.773 ˅	30.017 ^	15.847 ˅	17.170 ˅	2.497 ^
ACBP3a + DsRed T_2 #9	8.385 ^	3.106 ^	14.578 ^	31.332^	13.371 ˅	16.707 ˅	2.441 ^
ACBP3a + DsRed T_2 #10	8.889 ^	3.167 ^	12.563 ^	32.213^	14.254 ˅	15.360 ˅	2.858 ^
ACBP3a + DsRed T_2 #12	6.874 ˅	2.977 ˅	14.170 ^	29.076^	16.531 ˅	20.122 ^	1.639 ˅
ACBP3a + DsRed T_2 #13	8.125 ^	3.479 ^	11.843 ˅	29.450^	16.148 ˅	17.517 ˅	2.467 ^
ACBP3a + DsRed T_2 #17	8.036 ^	3.231 ^	13.011 ^	30.283^	15.012 ˅	17.506 ˅	2.467 ^
ACBP3a + DsRed T_2 #18	8.226 ^	2.959 ˅	13.151 ^	30.707^	15.495 ˅	17.128 ˅	2.542 ^
ACBP3a + DsRed T_3 #1-18	6.673 ˅	2.619 ˅	13.583 ^	29.246 ^	16.775 ˅	20.662 ^	1.994 ˅
ACBP3a + DsRed T_3 #1-19	6.618 ˅	2.609 ˅	13.436 ^	27.800 ˅	18.168 ^	20.848 ^	1.980 ˅
ACBP3a + DsRed T_3 #1-23	6.532 ˅	2.664 ˅	13.138 ^	27.858 ˅	17.869 ^	20.952 ^	2.144 ˅
ACBP3a + DsRed T_3 #1-24	6.650 ˅	2.687 ˅	13.672 ^	29.411^	16.538 ˅	20.861 ^	1.861 ˅
ACBP3a + DsRed T_3 #1-25	6.673 ˅	2.692 ˅	13.045 ^	27.989 ˅	17.918 ^	21.081 ^	1.972 ˅
ACBP3a + DsRed T_3 #1-26	7.711 ^	3.536 ^	12.569 ^	28.976 ^	15.989 ˅	19.111 ˅	2.384 ˅

Figure 3-16. Wild type *Columbia Arabidopsis thaliana* plant lines expressing *Vf*ACBP3a, in the T_2 and T_3 generations, as compared to plant lines lacking *Vf*ACBP3a. Each plant line shown above is representative of lines that differ markedly in fatty acid content from plant lines lacking *Vf*ACBP3a. This difference is determined by comparing the individual 16-0, 18-0, 18-1, 18-2, 18-3, 20-1, and 20-2 values of each T_2 and T_3 plant line to the individual average values of the plant lines lacking *Vf*ACBP3a.

Wild type *Columbia*	**16-0**	**18-0**	**18-1**	**18-2**	**18-3**	**20-1**	**20-2**
Averages	7.304	3.044	12.533	28.504	16.877	19.722	2.389
Std. Dev.	± 0.095	±0.089	±0.511	±0.306	±0.392	±0.327	±0.127

Construct							
ACBP6 + DsRed T_2 #1	7.700 ^	3.154 ^	13.400 ^	29.064 ^	16.028 ˅	18.527 ˅	2.451 ^
ACBP6 + DsRed T_2 #2	7.360 ^	2.921 ˅	11.843 ˅	28.272 ˅	17.269 ^	19.789 ^	2.628 ^
ACBP6 + DsRed T_2 #3	7.429 ^	2.619 ˅	11.337 ˅	28.774 ^	17.670 ^	20.302 ^	2.637 ^
ACBP6 + DsRed T_2 #4	6.777 ˅	2.878 ˅	12.417 ˅	27.242 ˅	17.417 ^	21.608 ^	2.408 ^
ACBP6 + DsRed T_2 #5	7.135 ˅	3.119 ^	12.597 ^	27.065 ˅	16.963 ^	21.353 ^	2.583 ^
ACBP6 + DsRed T_2 #6	7.046 ˅	3.142 ^	12.871 ^	27.300 ˅	16.756 ˅	21.388 ^	2.494 ^
ACBP6 + DsRed T_2 #7	6.546 ˅	2.616 ˅	18.064 ^	26.735 ˅	14.322 ˅	17.952 ˅	1.898 ˅
ACBP6 + DsRed T_2 #8	7.280 ˅	3.180 ^	12.650 ^	27.407 ˅	16.986 ^	20.624 ^	2.531 ^
ACBP6 + DsRed T_2 #9	7.281 ˅	3.138 ^	13.106 ^	27.622 ˅	16.988 ^	21.120 ^	2.465 ^
ACBP6 + DsRed T_3 #2-16.713	˅	2.839 ˅	13.809 ^	27.272 ˅	18.428 ^	20.820 ^	1.629 ˅
ACBP6 + DsRed T_3 #2-26.738	˅	2.819 ˅	14.565 ^	27.786 ˅	17.757 ^	20.128 ^	1.839 ˅
ACBP6 + DsRed T_3 #2-47.139	˅	2.808 ˅	12.664 ^	27.720 ˅	17.918 ^	21.260 ^	2.197 ˅
ACBP6 + DsRed T_3 #2-76.767	˅	2.889 ˅	13.553 ^	27.375 ˅	18.613 ^	20.807 ^	1.499 ˅
ACBP6 + DsRed T_3 #2-96.692	˅	2.797 ˅	14.281 ^	27.823 ˅	18.191 ^	20.130 ^	1.893 ˅
ACBP6 + DsRed T_3 #2-106.843	˅	2.681 ˅	13.831 ^	26.809 ˅	19.683 ^	20.100 ^	1.782 ˅
ACBP6 + DsRed T_3 #2-116.649	˅	2.812 ˅	13.754 ^	27.500 ˅	18.347 ^	20.475 ^	2.021 ˅
ACBP6 + DsRed T_3 #2-156.324	˅	2.401 ˅	13.793 ^	27.026 ˅	19.532 ^	20.612 ^	1.899 ˅

Figure 3-17. Wild type *Columbia Arabidopsis thaliana* plant lines expressing *Vf*ACBP6, in the T_2 and T_3 generations, as compared to plant lines lacking *Vf*ACBP3a. Each plant line shown above is representative of lines that differ markedly in fatty acid content from plant lines lacking *Vf*ACBP6. This difference is determined by comparing the individual 16-0, 18-0, 18-1, 18-2, 18-3, 20-1, and 20-2 values of each T_2 and T_3 plant line to the individual average values of the plant lines lacking *Vf*ACBP6.

Figures 3-16 and 3-17 contain small arrows illustrating the changes in individual saturated or unsaturated fatty acid contents in each construct. This helps to display, in more detail, the effects that *Vf*ACBP3a and *Vf*ACBP6 have on the comprehensive fatty acid profiles upon their expression in wild type *Arabidopsis* plants.

The *Vf*ACBP3a T_2 constructs in figure 3-15 appear to vary considerably; however, 18:2 fatty acid content seems to increase with the introduction of *Vf*ACBP3a, with the exception of two constructs. The T_3 plants, with the exception of 18:2 and 18:3 fatty acids content, exhibit uniform changes. There is a decrease in 16:0, 18:0, and 20:2 content with an increase in 18:1 and 20:1 fatty acids as compared to the wild type plants lacking *Vf*ACBP3a. The introduction of

*Vf*ACBP3a shifts 16:0, 18:0, and 20:2 production to the production of 18:1 and 20:1 fatty acids in the T_3 generation.

In the case of *Vf*ACBP6 T_3 constructs, there is a uniform change in each construct from the wild type plants not containing *Vf*ACBP6. All *Vf*ACBP6 constructs' 16:0, 18:0, 18:2, and 20:2 content decreased from the wild types not containing *Vf*ACBP6, while the 18:1, 18:3, and 20:1 content increased. Introducing *Vf*ACBP6 appears to shift the production of 16:0. 18:0, 18:2, and 20:2 to the production of 18:1, 18:3, and 20:1 in the T_3 generation. The T_2 constructs vary considerably in 18:0, 18:3, 20:1, and 20:2, while 16:0, 18:1, and 18:2 content shows the same change as the T_3 plants (decrease, increase, and decrease).

Comparing the results of *Vf*ACBP3a and *Vf*ACBP6, with the exception of 18:3 in the constructs for *Vf*ACBP3a, either *Vf*ACBP appeared to shift the production of fatty acids toward the 18:1 and 20:1 unsaturated fatty acids. Both *Vf*ACBP3a and *Vf*ACBP6 shifted saturated fatty acid production to produce certain unsaturated fatty acids. This clearly shows the shift toward the production of certain unsaturated fatty acids as compared to the wild types not expressing *Vf*ACBPs. Since tung produces α-eleostearic acid (18:3), the shift upon the introduction of *Vf*ACBP6 was especially intriguing.

Wild Type *Columbia*	**16-0**	**18-0**	**18-1**	**18-2**	**18-3**	**20-1**	**20-2**
Averages:	7.303875	3.044125	12.53263	28.50388	16.8768	19.7221	2.38863
***Vf*ACBP3a T_2**	**16-0**	**18-0**	**18-1**	**18-2**	**18-3**	**20-1**	**20-2**
Averages:	7.7085	3.05925	13.862	30.156	15.35225	18.058	2.1925
	^	^	^	^	v	v	v
VfACBP3a T_3	**16-0**	**18-0**	**18-1**	**18-2**	**18-3**	**20-1**	**20-2**
Averages:	7.292857	2.910571	12.32057	28.75329	16.97529	20.33871	2.316857
	v	v	v	^	^	^	v
VfACBP6 T_2	**16-0**	**18-0**	**18-1**	**18-2**	**18-3**	**20-1**	**20-2**
Averages:	6.894333	2.805	14.108	27.41633	16.336	19.783	2.311333
	v	v	^	v	v	^	v
VfACBP6 T_3	**16-0**	**18-0**	**18-1**	**18-2**	**18-3**	**20-1**	**20-2**
Averages:	6.889727	2.921364	13.70145	27.55573	18.13664	20.32445	1.883182
	v	v	^	v	^	^	v

Figure 3-18. Average values of *Vf*ACBP3a and *Vf*ACBP6 T_2 and T_3 lines expressed in wild type *Columbia* plants as compared to wild type *Columbia* plants lacking *Vf*ACBP3a and *Vf*ACBP6.

Additionally, on average (Figure 3-18), T_2 plants showed an increase in 18:1 and 20:1 with a decrease in 16:0, 18:0, 18:2, 18:3, and 20:2 content. The T_3 plants showed an increase in 18:1, 18:3, and 20:1, with a subsequent decrease in 16:0, 18:0, 18:2, and 20:2. Again, the T_3 plants showed similar changes as illustrated in the individual statistical measurements (Figure 3-17), that being a shift to one very long chain monounsaturated fatty acid and two long chain unsaturated fatty acids.

Another interesting test involved the analysis of the amounts of red seeds produced in the T_2 and T_3 generations of the wild type *Arabidopsis* constructs expressing *Vf*ACBP3a and *Vf*ACBP6. In figure 3-19, *Vf*ACBP6 had a total of 64 brown seeds seen in a pool of 270 seeds total (24%). A single transgene insertion should result in T_2 seed pools with 75% red seed, and 25% brown. Two copies would be seen at 94% (15/16) red, and 6% brown. This is consistent with a single transgene insertion of *Vf*ACBP6. Figure 3-20, on the other hand, illustrates *Vf*ACBP3a as having 70 brown seeds out of a pool of 180 seeds (39%). This is a very large

amount of brown seeds seen in the T_2 generation. This anomaly was probably due to subjectivity of the perceived lack of sensitivity of the light source and filter combination that was used in the procedure. A new type of green light flashlight and red filter goggles that is much more powerful has recently been purchased and these results will be re-evaluated.

	Brown/Total		Homozygous (100% Red Seeds)	Notes
***Vf*ACBP6** T_2 #2	64/270 (24%)	**T_3 2-1**	**Y**	
		T_3 2-2	N	
		T_3 2-3	**Y**	
		T_3 2-4	**Y**	
		T_3 2-5	**Y**	
		T_3 2-6	**Y**	
		T_3 2-7	**Y**	
	***Vf*ACBP6**	T_3 2-8	N	
		T_3 2-9	**Y**	
		T_3 2-10	N	**Mostly brown**
		T_3 2-11	**Y**	
		T_3 2-12	N	
		T_3 2-13	**Y**	
		T_3 2-14	**Y**	
		T_3 2-15	**Y**	
		100% Red/Total	11/15 (73%)	

Figure 3-19. Brown and red seeds observed in T_2 and T_3 seeds of *Vf*ACBP6.

	Brown/Total		Homozygous (100% Red Seeds)	Notes
***Vf*ACBP3a**	70/180			
T_2 # 1	(39%)	T_3 1-1	N	
		T_3 1-2	**Y**	
		T_3 1-3	N	
		T_3 1-4	N	
		T_3 1-5	N	
		T_3 1-6	**Y**	
		T_3 1-7	N	**Mostly brown**
		T_3 1-8	N	**Mostly brown**
		T_3 1-9	N	
		T_3 1-10	**Y**	
		T_3 1-11	N	
		T_3 1-12	N	
		T_3 1-13	N	
		T_3 1-14	**Y**	
	VfACBP3a	T_3 1-15	N	
		T_3 1-16	N	
		T_3 1-17	N	
		T_3 1-18	**Y**	
		T_3 1-19	N	
		T_3 1-20	**Y**	
		T_3 1-21	N	
		T_3 1-22	N	
		T_3 1-23	N	
		T_3 1-24	N	
		T_3 1-25	N	
		T_3 1-26	**Y**	
		T_3 1-27	N	
		T_3 1-28	N	
		T_3 1-29	N	**Mostly brown**
		100% Red/Total	7/29 (24%)	

Figure 3-20. Brown and red seeds observed in T_2 and T_3 seeds of *Vf*ACBP3a.

It would be expected for all of the T_3 seeds to be 100% red homozygous if a T_2 line is chosen that has been shown to contain (statistically) a single insertion. Each T_3 line was measured in the same way as the singular T_2 line that was chosen to plant the T_3 generation. A pool of seeds was analyzed for red seeds versus brown ones. These pools of seeds were analyzed to see if every seed in the pool was bright red fluorescent with no brown seeds present. So, any row labeled with a Y (for yes) represents a pool of seeds that is 100% red. Unfortunately, based

on the results shown in both figures 3-17 and 3-18, the production of completely red homozygous seeds from the chosen T_2 lines did not produce 100% homozygous seeds. The T_3 generation of seeds in *Vf*ACBP6 chosen from the second line of T_2 seeds, shows 73% homozygous red seeds, and a set of seeds (2-10) were seen as containing mostly brown seeds. Likewise, only 24% *Vf*ACBP3a constructs contained 100% red seeds. Again, re-evaluation using a more sensitive light source and filter is necessary in the near future. In addition, Southern blots may be performed to confirm or deny the possibility of the single insertion events that were statistically shown here in the T_2 seed pools.

Discussion

Overview

Acyl-CoA Binding Proteins (ACBPs) have been analyzed in many eukaryotic systems for approximately 25 years and have been shown to play a variety of roles as described above. These analytical processes reveal that an analysis of components with the presumed abilities of ACBP should be sought after in the tung lipid metabolic pathway. Many other components within this pathway have been investigated (Shockey, et. al., 2006). Coenzyme A has an established role in the synthesis and oxidation of fatty acids and other lipids; thus, a protein capable of binding long chain acyl coenzyme A esters is relevant to analyze since it may participate in several aspects of seed lipid metabolism.

Regardless of the category of biological study, whether it includes cell biology, biochemistry, or molecular biology, there have been major advances that have come from extensive studies of biological membranes. These membranes not only create a barrier to the outside of the cell, but also delimit the various subcellular organelles contained within the cell. The fractionation of subcellular organelles along with the investigations of biochemical compartmentalization of enzymatic functions (deDuve, et al., 1965) along with the propagation of the fluid mosaic model (Singer and Nicholson, 1972) have illustrated the importance of proteins in membranes.

In one classic example, the enzyme ATPase, which catalyzes the decomposition of adenosine triphosphate (ATP) into adenosine diphosphate (ADP) and a free phosphate ion. It requires a lipid bilayer environment for its activity. It has now become apparent through several recent studies that many other enzymes demand the proper lipid environment to provide their function(s) (Ohlrogge and Browse, 1995). For example, *E. coli* glycerol-3-phosphate

acyltransferase is inactive in a homogeneous state, but re-attained its activity upon the addition of *E. coli* phospholipids, mixtures of phospholipids, or pure phospholipids (Scheideler and Bell, 1989).

Due to their increasing role as a major raw resource for the production of food and non-food products, vegetable oils have become one of the more industrially important resources in the chemical industry (FAOSTAT, 2007). Some of the more prominent sources of vegetable oils for industrial applications include sunflower, rape, soybean, and oil palm. Moreover, the lipids that compose their seeds constitute ≥40% of the dry weight of the seeds (FAOSTAT, 2007, Biermann et. al., 2000). More than 500 fatty acids, combined into an untold number of natural triglycerides have been identified in plant species (Aitzetmüller, et. al., 2003). These findings, along with the highly utilized sources of plant lipids, make it evident that there is a great importance in the genetic engineering of plant lipids. Unfortunately, one of the major obstacles in putting the information on genetic engineering of plant lipids into practical application is the understanding of the biochemical pathways involved in the production of the lipids, and in the temporal and tissue specific expression of the genes. Finally, the enzymes in the pathways must also channel fatty acids into their necessary destination(s).

Little information is available regarding the structures of many of the enzymes involved in complex lipid biosynthesis in part due to the problems encountered in purifying membrane-bound enzymes (Browse and Sommerville, 1991). One of the approaches involved in countering this, however, is generating mutants of lipid metabolism (Browse and Sommerville, 1991). For example, mutants with alterations in membrane lipid composition have been used to study the structural and adaptive roles of lipids (Browse and Sommerville, 1991). In addition, gene probes that are derived from soluble proteins can be used to clone membrane-bound counterparts of

fatty acid synthesis, since the crucial reactions of fatty acid synthesis are conserved (Heinz, 1993). Thus, it stands to reason that certain requirements of fatty acids in the biosynthetic process can be tested through mutational and/or transformational studies. An example of this comes from an experiment performed for trans Δ3-hexadecanoic acid, through the determination of a mutation at a single locus, *fadA.* The carriers of this mutation lack trans-16:1 (Hugly, et. al., 1991). This is an acyl chain that performs a role in an aspect of photosynthesis; however, its loss did not appear to have an effect on the function of chloroplasts.

Transformational and mutational studies can also be extended to examine the functional importance of particular lipid classes. Also, the transcriptional regulation of genes involved in the lipid classes can be studied due to the availability of cDNAs and clones for fatty acid synthase components of plants. Unfortunately, there are many complications at the biochemical level, such as the interactions of fatty acid synthase components *in vivo* (if there are even any), the nature of substrate entering and the product produced from the plastid, and several other unresolved issues (Browse and Sommerville, 1991). It is imperative that the major unanswered questions be addressed so genetic engineering of lipids, including those processes involved in the storage of lipids, like the tung biosynthetic pathway, can provide important applications in industry.

An in-depth look at acyl-CoA binding proteins and their potential influence(s) in tung

The most predominant form of acyl-CoA binding protein (ACBP) as has been observed in various eukaryotes, is a highly conserved, approximately 10 kDa cytosolic protein (Chye, 1998, Gersuk, et al., 1995, McDonough, et. al., 1992, Mogensen, et. al., 1987). It was initially identified and analyzed in mammals as a neuropeptide that is capable of inhibiting diazepam, a drug that is used for treating a variety of ailments, including insomnia and anxiety, by binding to

the GABA (γ -aminobutyric acid) receptor (Gersuk, et. al., 1995). Following this observation, many subsequent studies have identified ACBP as binding to long-chain acyl-CoA esters, those of length from 12 to 22 carbons, with both high specificity and affinity (Ivell, et. al., 2000, Kragelund, et. al., 1993). A wide array of evidence has indicated that ACBP performs as an intracellular acyl-CoA transporter and an acyl-CoA pool former (Faergeman, et. al., 2007). Yeast ACBP has been identified, and is essential for the elongation of fatty acids, synthesis of sphingolipids, sorting of proteins, and vesicular trafficking (Schjerling, et. al., 1996). The evidence provided by these studies in addition to many others demonstrate a crucial role for ACBP in binding and transporting acyl-CoA (Faergeman, et. al., 2007).

Previously, it was determined that bovine ACBP's structure, as examined by NMR, was a four α-helix bundle protein (Kragelund et. al., 1993, Faergeman, et. al., 1996, Andersen et. al., 1991). Several chordate ACBP proteins have been analyzed to reveal a substantial number of conserved residues that are either hydrophobic or are found to be involved in binding of an acyl-CoA ester within its binding site (Faergeman, et. al., 1996, Andersen et. al., 1991). A majority of the conserved hydrophobic residues engage in the propagation of three mini-cores within the structure of the ACBP, producing a network of interactions between the helixes of the ACBP (Andersen et. al., 1991). Whether this structure shares any similarity to tung ACBP6 has yet to be determined, but it provides a basic framework from which to work, especially when deciphering the binding preferences, and how or if these preferences influence the role(s) of tung ACBP6.

The presence of large gene families within a single species encoding different functional paralogs of ACBP has been noted. In mammals, in addition to the protein initially identified as ACBP, which was initially identified in the human liver (L-ACBP), homologous unique ACBP-

like cDNAs have been characterized in the testes (T-ACBP) and brain (B-ACBP) (Taskinen, et. al., 2007. Two unique ACBP-like genes have been determined specifically in *Digitalis lanata* (Metzner, et. al., 2000), and six in *Arabidopsis* (Chye, 1998). Also, multiple inactive ACBP pseudogenes have been characterized in various genomes of mammals, including those in rat and human (Taskinen, et. al., 2007).

In addition to ACBP occurring as an independent protein, many ACBP-like domains have been characterized in several large, multifunctional proteins found in various eukaryotic species. These proteins include large membrane-associated proteins with N-terminal ACBP domains, multifaceted enzymes containing both ACBP and peroxisomal enoyl-CoA and 2-enoyl-CoA isomerase domains, and proteins containing an ACBP domain along with ankyrin repeats (Taskinen, et. al., 2007, Burton, et. al., 2005, Chye, et. al., 2008).

In humans, long chain acyl-CoAs (LCACoA) were initially considered to be an intermediate in lipid metabolism; however, recent studies have indicated that LCACoA have become increasingly recognized as modulators of a large range of functions in cells. The properties involved in regulation necessitate a strict control of the concentration of intracellular LCACoA in a manner that simultaneously allows much variation in the lipogenesis rate and β-oxidation and a sufficient supply of LCACoA for specific purposes such as the acylation of proteins. Despite many intracellular proteins having been reported to bind LCACoA, including liver fatty acid binding protein (L-FABP) and sterol carrier protein 2 (SCP2), currently, ACBP is characterized as the primary intracellular acyl-CoA binding protein (Taskinen, et. al., 2007). Since many of the ACBPs found in eukaryotic systems provide various functions to their specific organisms, it is reasonable to hypothesize that ACBPs may also have some influence on not just seed specific lipid metabolism in tung, but other functions as well. ACBPs can be hypothesized

to play a role in the regulation, bindings, and transportation involved throughout cellular metabolism. The information provided here provides strong reasons to pursue the study of ACBPs in tung.

Much of molecular biology involves comparing sequences, structures, and functions of genes and the proteins they encode. This information is then used to compare genes and proteins from one organism to another. Many of the lipid metabolic functions of ACBPs are conserved in other organisms, such as in *Arabidopsis* thaliana (Chye, et. al., 1998). These functions may or may not be similar in tung, but it would be reasonable to investigate any potential functions given the importance of ACBPs in other organisms' lipid metabolic pathways. Although, not every ACBP will perform the same function(s) in one organism as it does another, the structures and functions of previously characterized ACBPs are still relevant. At the very least, tung ACBPs can be experimented upon in similar manners to other ACBPs to observe if the results attained are in any way similar.

Identification of Acyl-CoA binding proteins in *Vernicia fordii*

Scientists around the globe are working diligently to sequence and assemble the genomes of a multitude of organisms, for a variety of crucial reasons. Obtaining a sequence of a genome and identifying a complete set of genes are often two necessary goals of sequencing projects; however, the most crucial set of information revolves around an understanding of gene expression. The understanding of when a gene is expressed allows for the examination of its expression under both normal and altered conditions.

An Expressed Sequence Tag (EST) is representative of a portion of a complete cDNA which can be utilized to aid in the identification of unknown genes and in the mapping of their positions in a genome (Mount, 2004). As EST technology continues to improve, the time

necessary to locate and describe a gene in great detail quickly declines. ESTs allow researchers a relatively cheap and fast path to the discovery of unique genes. With this discovery comes the information provided to analyze gene expression and regulation, along with the construction of genomic maps.

The ease of access and use as a gene discovery tool produced by ESTs is due to the organization provided via a searchable database that can also provide access to certain genome data. This utility, along with the speed and cost of generating data, provides the generation of hundreds of thousands of ESTs available for public use. Upon the generation of an EST, researchers may submit their tags to a database called GenBank, which is the NIH sequence database in operation by NCBI.

As mentioned in the results section, two of the tung ACBPs were identified from EST sequencing project: *Vf*ACBP6 and *Vf*ACBP3a. Initially, these ACBPs were known as a soluble ACBP (*Vf*ACBP6) and simply a larger, possibly membrane-associated ACBP (*Vf*ACBP3a). The nomenclature provided by Chye and her colleagues, through various experiments on *Arabidopsis thaliana* ACBPs, has identified 6 unique ACBPs (Chye, 1998). The tung ACBPs were named using Chye's nomenclature.

As mentioned, the other two ACBPs from tung were identified from data analysis via pyrosequencing, a more contemporary counterpart to EST. Upon the completion of the process, the nucleotide sequence can be determined from a Pyrogram trace by visualizing signal peaks (Weber, et. al., 2007, Yang, et. al., 2010).

The data from these two processes, EST and pyrosequencing, was received in the form of a large Microsoft Word document. The data provided is used to search and compare the

sequences in this file to those in an online database, such as GenBank. In addition, the BLAST tool is used to compare sequences and make reasonable judgments of the sequences on-hand.

As was described on pages 68-71 and Figures 3-1 and 3-2 of the Results section, *Vf*ACBP3a and *Vf*ACBP3b are not very similar in their nucleotide or protein sequences. The two proteins are also of different lengths. They were both found to be sequentially similar to *At*ACBP3. *Vf*ACBP3b, however, was most similar to *Ricinus communis* (castor) ACBP, showing the shared Euphorbiaceae (spurge) lineage of tung and castor. This shows that orthologs of *Vf*ACBP3b do exist in other plants. This presence in castor but absence in *Arabidopsis thaliana* of an orthologous ACBP3b suggests that the gene duplication event that gave rise to ACBP3a and ACBP3b came about after the split of the forbearers of *Arabidopsis* and tung.

Rapid Amplification of cDNA Ends (RACE) and genome walking to obtain full length Open Reading Frames (ORFs) of *Vf*ACBPs

Part of the sequences of each *Vf*ACBP were found through EST and pyrosequencing. Genome walking and RACE techniques were used to provide the sequence of an RNA transcript from these known sequences to complete the ORFs. Using DNA of interest, genome walking constructs pools of uncloned, adaptor-ligated genomic DNA fragments, termed libraries. RACE, on the other hand, produces a cDNA copy of an RNA sequence of interest, via reverse transcription, followed by amplification of cDNA copies. These cDNA copies were sequenced afterward. If these sequences are long enough, they may map to a full-length mRNA that has been already described.

The initial step in 5'RACE was to use reverse transcription which generated a cDNA copy of a region of an RNA transcript. An unknown end portion, in this case the 5' end, of a transcript was copied utilizing a known sequence from within the transcript. The copied region

was bounded by the known sequence, at the 5' end. From this point, mRNA was used as a template in cDNA synthesis. The principal difference between 3'RACE and 5'RACE, aside from the 3'end of the sequence in question, is that 3'RACE takes advantage of the poly(A) tail of mRNA.

As was mentioned, 5'RACE was performed using 3'RACE parameters, including SuperScript™ III reverse transcriptase. Perhaps the higher rate of success using the SuperScript™ III reverse transcriptase as opposed to the SuperScript™ II reverse transcriptase lies in some of the principal performance differences provided by the different enzymes. Fidelity and processivity of the two enzymes were shown to be no different from one another, but the specific activity is 25% higher in SuperScript™ III reverse transcriptase, the half-life of SuperScript™ III reverse transcriptase is 35-fold longer, and SuperScript™ III reverse transcriptase produces very strong bands in similar reactions that SuperScript™ II reverse transcriptase has catalyzed that only produce faint bands (http://tools.invitrogen.com/content/sfs/productnotes/F_071215_Superscript%20III%20Enzyme%20RD-MKT-TL-HL.pdf). Thus, it stands to reason that the SuperScript™ III reverse transcriptase provided a much greater advantage in catalyzing the 5'RACE first strand synthesis reaction.

Both of the enzymes are a point mutant of Moloney murine leukemia virus RT (M-MLV RT). Much like M-MLV, they are DNA polymerases that synthesize complementary DNA strands from single stranded DNA, RNA, or RNA:DNA hybrids; however, compared with wild type RTs, the SuperScript RTs deliver higher yields of full-length cDNA. Both have been engineered to reduce RNase H activity and provide an increase in thermal stability. The enzymes are best used to synthesize cDNA at a temperature range of 42 to 55°C. Because they are not

significantly inhibited by ribosomal and transfer RNA, they produce first-strand cDNA from total RNA preparations (http://tools.invitrogen.com/content/sfs/productnotes/F_071215_Superscript%20III%20Enzyme%20RD-MKT-TL-HL.pdf).

Tissue specific expression of *Vf*ACBP through quantitative real-time PCR

Quantitative real-time polymerase chain reaction (qPCR) is a technique based on classic PCR, which amplifies and quantifies a DNA molecule of interest at the end of the reaction. qPCR allows for simultaneous detection and quantification (as the absolute number of copies or relative amount upon normalization to a DNA input or additional normalizing genes) of one or more target sequences in a DNA sample. There are two methods used in qPCR, but the method applied in this research was through the use of a fluorescent dye, SYBR Green, that intercalates with any double-stranded DNA (dsDNA).

In this study, qPCR was used to provide quantitative measurements of tung ACBP transcript abundance and to determine how the expression of these ACBPs change over time in seed development and other tissues. These data were used to compare the expression patterns of the *Vf*ACBPs to other known components of the tung lipid metabolic pathway that exhibit specific expression patterns. Comparing known components to the *Vf*ACBPs allows for an understanding of some of their functions.

Previously, tung DGAT2 and FADX, two components with known roles in the tung metabolic pathway, were analyzed by qPCR (figure 3-4). The expressions of these were shown to coincide with the peak of TAG accumulation (Shockey, et. al., 2006). Each *Vf*ACBP also exhibited unique patterns and levels of expression, as seen in Figure 3-9. One aspect of their expression that is commonly seen amongst each of them, however, is that they generally have

increased expression in mid-summer months, first in July and then later in late August. Essentially, in a sequential manner, each of the *Vf*ACBPs are expressed at low levels in the earliest days of summer then, expression rises in mid-summer, lowers again, and rises closer to the fall. These results show that the *Vf*ACBPs are specifically expressed at certain times, and this expression can be lowered or raised. What this means for the potential roles of each *Vf*ACBP is unknown, but the relevance of the expression pattern is consistent with peak TAG accumulation. One interesting result is the expression patterns of each *Vf*ACBP in the leaf and flower tissues. Both *Vf*DGAT2 and *Vf*FADX are not expressed in these tissues. Thus, these data show a unique expression pattern for *Vf*ACBPs.

In a 2002 study, a contrapuntal network of gene expression was observed during *Arabidopsis* seed filling. In this case, contrapuntal refers to two peaks of activity from different sets of proteins and enzymes during *Arabidopsis* seed development; one early and one late. cDNA microarrays were used to examine changes in gene expression during Arabidopsis seed development and to compare wild-type and mutant *wrinkled1 (wri1)* seeds that have an 80% reduction in oil. Between 5 and 13 days after flowering, a period preceding and including the major accumulation of storage oils and proteins, ~35% of the genes on the array changed at least twofold, but a larger fraction (~65%) showed little or no change in expression. Genes whose expression changed most tended to be expressed more in seeds than in other tissues. Genes related to the biosynthesis of storage components displayed unique temporal expression patterns. For example, a number of genes encoding core fatty acid synthesis enzymes showed a bell-shaped expression 5 and 13 days after flowering. In contrast, the expression of storage proteins, oleosins, and other known abscisic acid–regulated genes increased later and remained high. Genes for photosynthetic proteins followed a pattern very similar to that of fatty acid synthesis

proteins, implicating a role in CO_2 fixation and the supply of cofactors for oil synthesis. Expression profiles of key carbon transporters and glycolytic enzymes reflected shifts in flux from cytosolic to plastid metabolism. Despite major changes in metabolism between *wri1* and wild-type seeds, ~1% of gene expression levels differed by more than twofold, and most of these were involved in central lipid and carbohydrate metabolism. Thus, these data define in part the downstream responses to disruption of the WRI1 gene (Ruuska, et. al., 2002).

In summary, there were two peaks of activity from different sets of proteins and enzymes during *Arabidopsis* seed development; one early and one late. The tung ACBPs as shown here by qPCR have two peaks of expression during seed development. Perhaps, there is a contrapuntal gene expression pattern occuring and *Vf*ACBPs may be examples of genes that are expressed during both waves.

Looking at Figure 3-9, *Vf*ACBP3a is similar to *Vf*ACBP6 in that it is expressed at its highest in leaf and exhibits some expression in flower as well. Again, like all of the other proteins analyzed in figures 3-4 through 3-8, it exhibits a bimodal expression pattern, with a rise in expression around mid-July, with a subsequent decrease, followed by an increase near the fall. Also, like each *Vf*ACBP, it expresses in leaf and flower tissues, which is unique from *Vf*DGAT2 and *Vf*FADX.

Interestingly, *Vf*ACBP3b exhibits the greatest differences in expression levels as compared to every other protein analyzed via qPCR. In some cases, it expresses upwards of over 30 times as much as other *Vf*ACBPs. For example, at July 14th, July 21st, and September 1st, it is expressed at a higher level than any other *Vf*ACBP, *Vf*DGAT2, or *Vf*FADX at any point in time. This means that *Vf*ACBP3b can be the highest expressing *Vf*ACBP, and can also express much higher than *Vf*DGAT2 and *Vf*FADX. Despite this, it expresses at very low levels in other times,

especially at June 23th, June 30th, and July 7th. *Vf*ACBP3b is expressed anywhere from 16 to 30 times less at these points than July 14th, July 21st, and September 1st. Clearly, there is a need to increase the expression of *Vf*ACBP3b in a dramatic fashion and then decrease in a similar scale; however, the reason for this is unknown. It does not express very highly in leaf or flower tissues as compared to the times it is expressed highly. Again, there is a dramatic difference in expression levels. It is, however, expressed comparably in flower tissues to all of the other *Vf*CBPs. There is just a huge change in expression levels as compared to the other tissues its expressed in. It is similar to the expression in leaf and flower tissues as *Vf*DGAT2 and *Vf*FADX in that those tissues are among the lowest *Vf*ACBP3b is expressed.

*Vf*ACBP4 exhibits high expression in flower and low in leaf as compared to its own expression levels. It expresses at its highest in the late summer days, especially September 1st. Its initial rise in expression appears to come about a little earlier than the other *Vf*ACBPs, with its two highest points being at July 7th and July 14th. It is also expressed at low levels in leaf tissues.

*Vf*ACBP6 has a high expression, relative to its overall expression in other tissues, in leaf tissues. It is not expressed highly in flowers. Its initial onset of expression is the latest of the *Vf*ACBPs, with its highest expression at July 28th in the first "peak" of the bimodal pattern exhibited by all the *Vf*ACBPs and *Vf*DGAT2 and *Vf*FADX. *Vf*ACBP6, as presented in various other organisms, is known to play a variety of roles. Perhaps its versatility is exhibited in tung as well, but it is clear that its time of expression is specific. It is, like the other *Vf*ACBPs, expressed in leaves and flowers though, illustrating its general tissue expression pattern.

In summation, each of the *Vf*ACBPs is expressed at differing levels at specific times. They are all expressed, however, in leaves, flowers and seeds. Despite the lack of tissue

specificity, they are all expressed at different levels in these tissues, each displaying unique expression patterns.

Split ubiquitin as a sensor of protein interactions: qualitative plate assays

Split ubiquitin yeast two-hybrid analysis is a technique used to discover protein:protein interactions by testing for physical interactions between two proteins. These protein:protein interactions are used as a way of learning role(s) of one protein by observing if it rubs up against another protein with a known role.

Positive controls for these experiments were designed so that a protein is expressed as a fusion with the wild-type Nub sequence, NubI. NubI has a high affinity for Cub and the reconstitution of ubiquitin is not reliant upon the physical interaction of two fusion proteins being analyzed. On the other hand, fusion of a protein with the mutated version of Nub, NubG, resulted in a fusion protein that has a low affinity for Cub. The Cub and NubG domains stay separated unless they are brought in close proximity by two fusion proteins interacting. This allows for the interaction of Cub and NubG which reconstitutes ubiquitin thus allowing release of the reporter protein LexA for reporter gene activation.

The interactions shown in the results section indicate interactions between all tung ACBPs and the two isozymes of *Vf*DGAT: DGAT1 and DGAT2. Both *Vf*DGAT1 and *Vf*DGAT2 catalyze the formation of triglycerides from diacylglycerol and acyl-coA (Shockey, et. al., 2006). Even though both isozymes catalyze similar reactions, they have no sequence homology to one another (Shockey, et. al., 2006). These results show an interaction between *Vf*DGAT and the *Vf*ACBPs, but how the interaction occurs and in what orientation is not clear. It is unknown what role, if any, this interaction has in the plant. Normally, the quadruple knockout plates in the dilution assay are allowed to grow at 30°C for 72 hours and then the plates' pictures are taken

and recorded. Interestingly, the interactions between the *Vf*ACBPs and the *Vf*DGATs were so strong, that the plate dilution assays showed cell growth after only 24 hours on quadruple knockout plates and the spots of cell growth did not dramatically increase in diameter after that amount of time. All non-interacting combinations did not show any cell growth at all even after 72 hours. This strength and weakness of interactivity was also seen later in the β-galactosidase assays, through the rapid yellowing of the solution, which is representative of a positive interaction.

As seen in some of the *Arabidopsis* ACBPs, like ACBP4 and ACBP5 that contain kelch motifs allowing for protein-protein interactions, it is difficult to hypothesize how *Vf*ACBPs and *Vf*DGATs would interact based upon the different components comprising the different proteins. Both (His)6-*At*ACBP4 and (His)6-*At*ACBP5 bind [^{14}C]oleoyl-CoA with high affinity, [^{14}C]palmitoyl-CoA with lower affinity and do not bind [^{14}C]arachidonyl-CoA. Hence, these *At*ACBPs with kelch motifs have functional acyl-CoA-binding domains that bind oleoyl-CoA. Their predicted cytosol localization suggests that they could maintain an oleoyl-CoA pool in the cytosol or transport oleoyl-CoA from the plastids to the ER in plant lipid metabolism (Chye, et. al., 2004). Likewise, regarding the larger ACBPs from tung, there exists a possibility of an additional component that drives interactivity.

In addition, some DGATs have suspected acyl-CoA binding motifs (Weselake, et. al., 2000). In the 2000 study by Weselake, et. al., the fragment, *Bn*DGAT1$_{(1\text{-}116)}$His$_6$, interacted with [1-^{14}C]oleoyl-CoA, suggesting that the N-terminal region of *Bn*DGAT1 may have a role in binding cellular acyl-CoA. Also, some residues in *Saccharomyces cerevisiae* ACBP have been mapped to the area near the thioester bond (Knudsen, et. al., 1994). There is a possibility that these two areas, the N-terminal region that binds acyl-CoA on *Bn*DGAT and the residues near

the thioester bond in *Sc*ACBP, may interact. Future experiments would include making split ubiquitin constructs containing only these regions in *Vf*DGATs and *Vf*ACBPs. The process seen in the studies presented above could then be repeated, but with these new constructs to further identify binding capabilities of *Vf*DGATs and *Vf*ACBPs.

When paired with one another, the *Vf*ACBPs did not produce any cells on quadruple-knockout plates. This illustrates that dimerization or any other form of homopolymerization doesn't occur with these particular ACBP proteins. It does not, however, eliminate the possibility of self-interaction. Thus far, the tung ACBPs appear to perform their functions independently of one another.

It was consistently observed that fusion proteins containing Cub-LexA linked to the N-terminus of an ACBP protein yielded strong positive reporter gene activation when paired with the Alg5-NubI control protein. Fusion proteins containing Cub-LexA linked at the C-terminus of ACBP, however, produced a significant decrease, or complete absence, of reporter gene activation when paired with Alg5-NubI. The basis for this effect is currently unknown, but these results were consistently observed with many different Cub/Nub fusion proteins, and similar results have been reported in the literature (Deslandes et al., 2003; Obrdlik et al., 2004). As such, results were not included from reciprocal testing of NubG and Cub on both the N and C termini of ACBP proteins.

Split ubiquitin: β-galactosidase assays as a quantification tool for the interactions of *Vf*ACBPs

The lacZ gene of the lac operon in *E. coli* encodes the β-galactosidase enzyme, which is a roughly 120 kDa and 1000 amino acid tetrameric protein. The function provided by the enzyme is to cleave lactose to glucose and galactose so they may be utilized as energy sources. A yellow color is produced upon the recognition and cleavage of the artificial substrate o-nitrophenyl-β-D-galactoside (ONPG) yielding galactose and o-nitrophenol. The production of o-nitrophenol per

unit time is proportional to the concentration of β-galactosidase when ONPG is in excess over the enzyme in a reaction. Due to this, the enzyme concentration can be determined based on the production of yellow color (Gietz, 1997).

The β-galactosidase assays were performed to quantify and confirm the interactions that were observed in the serial dilution plate assays. For a detailed list of interactions between the tung ACBPs and other components, please see pages 73-76 in the Results section and Figures 3-11 and 3-12. Indeed, the results attained from β-galactosidase assays correlated well with the interaction strengths observed in the serial dilution plate assays. The Miller Units indicate strength of interaction, and as can be seen in Figure 3-12, and *Vf*ACBP3a, *Vf*ACBP3b, and *Vf*ACBP6 either interact strongly or not at all with other proteins. Due to the strength of interactivity and the strong results obtained from the positive and negative controls, *Vf*ACBP3a, *Vf*ACBP3b, and *Vf*ACBP6 interact with both *Vf*DGAT1 and *Vf*DGAT2. This was first observed in the plate dilution assays and correlated with β-galactosidase assays. Again, as stated with the plate dilution assays, there was an immediate response in the experiment, for the β-galactosidase assays, showing positive interactions between the *Vf*ACBPs and *Vf*DGATs. Normally, the component solutions involved in the process are incubated at 37°C for as long as it takes for the solution to turn yellow. The positive interaction combinations frequently started turning yellow even before they were placed in the incubator, usually within seconds of preparing the solution. This is an correlation with the fast growth on the quadruple knockout plates, illustrating the strength of the positive interactions. The two *Vf*DGAT proteins are involved in tung lipid metabolic processes, and if there is interaction between the them and the *Vf*ACBPs, perhaps there are some role(s) for *Vf*ACBPs in metabolic processes involving *Vf*DGAT1 and *Vf*DGAT2. These interactions would have to be qualified since the *Vf*ACBPs may have unique localizations and possible specific binding affinities to certain fatty acyl-CoAs. As alluded to earlier, both of the *Vf*DGATs use acyl-coA in their role for the production of TAG from DAG. If there is a

role for any of the *Vf*ACBPs in the production of TAGs in tung, perhaps one of the functions is involved at the step for providing the *Vf*DGATs with acyl-CoA.

Fatty Acid Methyl Ester (FAME) Analysis in the derivatization of tung seed oil for analysis by gas chromatography

One of the most vital methods for analyzing lipids involves the preparation of methyl esters of fatty acids for analysis by chromatographic means. The transesterification of fatty acids commonly involves two methods; one using an acidic reagent as a catalyst or another using a basic reagent as a catalyst, the latter being used in this research. The transesterification of triglycerides and phospholipids occurs rapidly in anhydrous methanol in the presence of a basic catalyst, such as sodium methoxide, which allows for the exchange between methanol and glycerol. The required methyl esters are shortly obtained in quantitative yield.

$$RCOOR' + CH_3OH \xrightarrow{^-OCH_3} RCOOCH_3 + R'OH$$

Sodium methoxide in methanol reacts very quickly with a glycerolipid. For example, the complete transesterification of triacylglycerols and phospholipids occurs in a few minutes at room temperature in a glass tube. Using these conditions, there is usually no isomerization of double bonds in polyunsaturated fatty acids, though it is possible that alterations to fatty acids can occur. For example, prolonged or careless use of the reagents involved in the procedure can lead to degradation. Using basic reagents, aldehydes are not liberated from the plasmalogen forms of phospholipids, as opposed to when acidic conditions are applied. This may provide an advantage in simplifying the interpretations of gas chromatography traces (Christie, 1993).

Interestingly, the use of sodium methoxide and its counterpart prepared with potassium are often used for catalyzing the large-scale production of biodiesel. Sodium methoxide initiates an anionic addition polymerization with ethylene oxide. This leads to the formation of a

polyether with a large molecular weight. Animal fats or vegetable oils (fatty acid triglycerides) are transesterified with methanol to produce fatty acid methyl esters (FAMEs) (Christie, 1993).

FAMEs were prepared from total lipid extracts of transgenic *Arabidopsis* seeds, followed by gas chromatography (GC) to analyze the fatty acid content. GC is a type of partition chromatography which employs a gas as the mobile phase and a liquid as the stationary phase. The identification of all of the methyl esters in the samples from the extracted oil of the transformed *Arabidopsis thaliana* plants was made by comparing the retention times, which is the interval between the instant of injection and the detection of the component, of standard fatty acid methyl esters.

Statistical analysis of the seed oil content as attained from transgenic *Arabidopsis thaliana* expressing tung ACBPs

In 2009, there was a study conducted on the overexpression of *Brassica napus* ACBP, which is similar to ACBP6 of tung and *Arabidopsis*, in developing seeds of *Arabidopsis thaliana*. It was revealed that there was a significant increase in the polyunsaturated fatty acids 18:2cis$\Delta^{9,12}$ and 18:3cis$\Delta^{9,12,15}$ at the expense of very long monounsaturated fatty acid 20:1cisΔ^{11} and saturated fatty acids in T_2 and T_3 generations of *A. thaliana* seeds. In addition, recombinant *B. napus* ACBP (rBnACBPP) increases formation of phosphatidylcholine (PC) in the absence of added lysophosphatidylcholine in microsomes from yeast expressing *A. thaliana* lysophosphatidylcholine acyltransferase cDNA or in microsomes from cultures of *B. napus* L. cv. Jet neuf. Also, either recombinant *Brassica napus* ACBP or bovine serum albumin were observed to be critical for *A. thaliana* lysophosphatidylcholine acyltransferase catalysis of the transfer of an acyl group from PC into acyl-coA. Taken together, this data implies that the *B. napus* ACBP affects the equilibrium between metabolically active acyl-coA and phospholipid

pools involved in modifications of fatty acids and triacylglycerol assembly. ACBP overexpression during seed development may provide a valuable biotechnological approach in the alteration of fatty acid composition in seed oils (Yurchenko, et. al., 2009).

The results attained by Yurchenko, et. al., provided inspiration to test *Vf*ACBP6 in a similar manner. As stated earlier, constructs were created to analyze the effects of *Vf*ACBP expression on the entire normal metabolism of seed FAs in general by their expression in wild type *Columbia* plants. DsRed screening used for selection, making identification of homozygous T3 lines much easier. The *Vf*ACBP6 construct is more directly comparable to the data presented above by Yurchenko, et. al. This is because *Vf*ACBP6 is an ortholog of *Bn*ACBP6 and there is no known orthologous *Vf*ACBP3a in *Brassica napus*. The increase in 18:2*cis*$\Delta^{9,12}$ and 18:3*cis*$\Delta^{9,12,15}$ in T_2 and T_3 lines transformed with *Bn*ACBP, coming at the expense of very long monounsaturated fatty acid 20:1cisΔ^{11} and saturated fatty acids, wasn't completely observed in any of the constructs listed in Figure 3-18 or Figure 3-17 for *Vf*ACBP6.

Individually (Figure 3-17), *Vf*ACBP6 T_2 constructs vary considerably in 18:0, 18:3, 20:1, and 20:2, while 16:0, 18:1, and 18:2 content shows the same change as the T_3 plants (decrease, increase, and decrease). These results do not compare to the *Bn*ACBP6 results. For the T_3 plants, introducing *Vf*ACBP6 appears to shift the production of 16:0, 18:0, 18:2, and 20:2 to the production of 18:1, 18:3, and 20:1. This is somewhat similar to the results attained for *Bn*ACBP6, except for the increased production in very long chain monounsaturated fatty acids (20:1). There is not a complete shift of production to long chain unsaturated fatty acids.

Additionally, on average (Figure 3-18), T_2 plants show and increase in 18:1 and 20:1 with a decrease in 16:0, 18:0, 18:2, 18:3, and 20:2 content. The T_3 plants showed an increase in 18:1, 18:3, and 20:1, with a subsequent decrease in 16:0, 18:0, 18:2, and 20:2. Again, the T_3

plants showed similar changes as illustrated in the individual statistical measurements (Figure 3-17), that being a shift to one very long chain monounsaturated fatty acid and two long chain unsaturated fatty acids. Both the T_2 and T_3 generations exhibit different changes in the fatty acid profile as compared to the results observed for *Bn*ACBP6.

Overall, while there appears to be some similarities, not every change is comparable. This is not too surprising as even though they are orthologous, *Bn*ACBP6 is different from *Vf*ACBP6, which might have different acyl-CoA or membrane phospholipid binding affinities. In addition, the constructs created for *Vf*ACBP6 include the presence of a *myc* tag, which will have to be removed in future experiments. Also, different promoters are used in the vector constructs for *Vf*ACBP6 from *Bn*ACBP6. It is interesting how introduction of *Vf*ACBP6 in both statistical measures showed an increase in very long chain monounsaturated fatty acids (20:1). There appears to be a channeling of the production of saturated fatty acids to specific long chain and very long chain fatty acids.

Individually, the T_2 plants of *Vf*ACBP3a, as seen in Figure 3-16, varied too much to surmise what effects *Vf*ACBP3a had on the changes to fatty acid content. The T_3 generation exhibited a decrease in 16:0, 18:0, and 20:2 content with an increase in 18:1 and 20:1 fatty acids as compared to the wild type plants lacking *Vf*ACBP3a. Again, as seen with *Vf*ACBP6, there appears to be a shift from saturated fatty acids to specific unsaturated fatty acids and interestingly, to a very long chain monounsaturated fatty acid.

Figure 3-18 illustrates the average changes in fatty acid content that *Vf*ACBP3a introduction produced. In the T_2 generation, there was an increase in 16:0, 18:0, 18:1, and 18:2, with a decrease in 18:3, 20:1, and 20:2. This is different from any result attained thus far, as there is an increase in saturated fatty acid content with a decrease in both very long chain fatty acids

and 18:3. The T_3 generation exhibited an increase in 18:2, 18:3, and 20:1, and decrease in 16:0, 18:0, 18:1, and 20:2. These results are not consistent from one generation to the next. T_3 plants showed a decrease in saturated fatty acids as compared to the wild type, which is also a decrease from the T_2 generation. Like *Vf*ACBP6 (T_3), on average, there was an increase in 18:3 and 20:1 fatty acids; however, 18:2 content increased in the T_3 generation of plants expressing *Vf*ACBP3a. *Vf*ACBP6 T_3 plants showed an increase in 18:1. Still, both constructs displayed an increase in specific long chain and very long chain unsaturated fatty acids at the expense of saturated fatty acids and other unsaturated fatty acids in the T_3 generation on average.

The over-expression of ACBPs in various animal systems and yeast has been shown to increase acyl-coA pool size, due to an increase in specific acyl-coA species, and the rates of glycerolipid synthesis (Mandrup et al., 1993; Huang et al., 2005). The information presented in these studies gives reason to hypothesize that manipulating *Vf*ACBP expression in *Arabidopsis* can influence size and composition of the cellular acyl-coA pool.

As stated on pages 76-80, the potential role of *Vf*ACBPs when co-expressed with *Vf*FADX in *fad3/fae1* was analyzed. They were compared to plants expressing *Vf*FADX alone, and as Figure 3-13 indicates, there was no significant increase in eleostearic acid content. Again, the effects of *Vf*ACBP co-expression on any other fatty acids in the seeds was analyzed (Figures 3-14 and 3-15), and 16:0 and 18:0 content, but not eleostearic acid content was changed. This clearly indicates that introducing *Vf*ACBP3a or *Vf*ACBP6 affects saturated fatty acid content in seeds.

The method of selection for determining which seeds will be planted in subsequent generations for transgenic *Arabidopsis* wild type *Columbia* lines was through the use of a modified form of *Discosoma sp.* red fluorescent protein (DsRed) (Cahoon, et. al., 2007). Use of

DsRed produces bright red fluorescent seeds representative of successful transformations, which, after harvesting, can be picked from brown seeds to be planted and produce future generations. Referring to Figures 3-19 and 3-20, the *fad3/fae1* double mutants expressing *Vf*ACBP3a in T_2 lines elicited 70 brown seeds out of 180 total seeds (~39% brown seeds). This is a high amount of brown seeds, but is more than likely a single insertion. The results will be re-evaluated upon the receipt of a more sensitive light source and filter used to screen for red seeds.

In addition, the generation of transgenic plants through *Agrobacterium*-mediated transformation can result in one or more inserts of the T-DNA. A common problem in the generation of transgenic plants is that *Agrobacterium* T-DNA-mediated transformation may result in the integration of more than one copy of foreign DNA, for instance as tandem or inverted repeats (Meza, et. al., 2002).

Using DsRed selection at times can be subjective due to the process of selecting red seeds. It is up to the viewer to determine which seeds to choose in order to plant the T_3 lines. Unfortunately, it is easy to accidentally pick a brown seed, whether it be attached to a red seed or even subjectively believed to be red when it is really brown, and plant future generations using that seeds. As stated, the red seeds are representative of successful transformations, and picking a brown seed would produce a plant that does not contain the transgene (*Vf*ACBPs). Also, the selection of red seeds is accomplished in the dark, so as to take advantage of a filter that removes extraneous low-levels of non-specific red emission background to determine fluorescence. Obviously, searching for red seeds in the absence of light creates a difficulty in selecting red seeds based on the individual performing the search. At this time, there is no specific plan to re-transform these lines, but in future, the issue has to be resolved. An approach to the resolution would be to perform a Southern blot to check if there is 1 or 2 loci in the genome.

In future experiments, the top two eleostearic acid producing lines coexpressing *Vf*FADX plus either *Vf*ACBP6 or *Vf*ACBP3a will be planted for the production of T_4 generation plants. One set of each of the constructs will be sprayed with a glufosinate-based herbicide to get an estimate of gene copy number. Another set of each construct will be grown out to maturity and seed fatty content will be analyzed by gas chromatography. In addition, plant lines expressing constructs containing *Vf*ACBP3b or *Vf*ACBP4, either alone or in conjunction with *Vf*FADX will be generated, but time constraints eliminated the possibility of these lines being produced in time for this publication.

Final Thoughts

This research primarily involved elucidating any functions of *Vf*ACBPs. The initial goal was to identify *Vf*ACBPs, clone, and sequence them. There has been extensive research on various ACBPs throughout many different organisms, many of which perform unique functions. This is especially true for the highly conserved ACBP, *Vf*ACBP6 as its counterpart, with homologues that were identified in all four eukaryotic kingdoms, Animalia, Plantae, Fungi and Protista, in addition to eleven species of eubacteria (Yurchenko, et. al., 2009, Xiao, et. al., 2009, Mogensen, et. al., 1987, Schjerling, et. al., 1996, Taskinen, et. al., 2007, Burton et. al., 2005). The *Vf*ACBPs, as a whole, were found to be orthologous to several ACBPs from many different organisms. There was, however, a unique ACBP, *Vf*ACBP3b, in that its best-matched orthologs were found in *Ricinus communis* and *Populus trichocarpa*, both members of the Spurge family (Euphorbiaceae), which is the same family as *Vernicia fordii*. Many of the orthologs for the *Vf*ACBPs were found in *Arabidopsis thaliana*, which is a member of the Brassicaceae family. So, this research provided a unique discovery through the elucidation of *Vf*ACBP3b.

In addition to the discovery of four *Vf*ACBPs, it is clear that *Vf*ACBP3a and *Vf*ACBP6 affect general fatty acid metabolic profiles, causing a shift in the production of specific fatty acids to the production of others. The *Vf*ACBPs are expressed at different times as well and may be contrapuntal in their gene expression patterns. They were also found to strongly interact with *Vf*DGAT1 and *Vf*DGAT2 both qualitatively and quantitatively.

These data provide a firm knowledge base for *Vf*ACBPs and allow for the creation of future experiments that will be completed in the coming months. The determination of acyl-CoA binding specificity is one such experiment. This will be performed through the use of a modified chromatographic procedure.

Yurchenko, et. al., also demonstrated through *in vitro* assays that recombinant *B. napus* ACBP strongly increases the formation of phosphatidylcholine in the absence of added lysophosphatidylcholine in microsomes from yeast expressing *A. thaliana* lysophosphatidylcholine acyltransferase (*At*LPCAT) cDNA or in microsomes from microspore-derived cell suspension cultures of *B. napus* L. cv. Jet Neuf. They also showed that *Bn*ACBP or bovine serum albumin (BSA) were crucial for *At*LPCAT to catalyze the transfer of an acyl group from PC into acyl-CoA *in vitro* (Yurchenko, et. al., 2009). *Vf*MBOAT1, likely a lysophosphatidylcholine acyltransferase, has recently been cloned into split ubiquitin vectors, much like the *Vf*ACBPs and *Vf*DGATs. *Vf*ACBP3a and *Vf*ACBP6 split ubiquitin constructs will be paired with these *Vf*MBOAT1 constructs. This will be a direct way to address the question of whether the LPCAT enhancement shown by Yurchenko, et. al., might also be occurring in tung seeds as well.

One possible source of concern is that the plant constructs created for *Vf*ACBP3a and *Vf*ACBP6 that were used for statistical analysis after FAME analysis, all have a *myc* tag. It is

possible that adding a *myc* tag could alter acyl-CoA binding or protein:protein interactions of either *Vf*ACBP3A or *Vf*ACBP6, and could affect (assumed) extracellular targeting of *Vf*ACBP3A. Some of the seed-specific expression work may be repeated using untagged protein constructs and in the case of expressing *Vf*ACBPs by themselves, will be expressed in whole plants using constitutive promoters like CaMV35S.

This research puts forth a better understanding of the current *Vf*ACBPs with many more experiments to come. ACBPs in general have been clearly shown to provide a variety of integral roles throughout various organisms. It is imperative that there be a continued effort in the analysis of these *Vf*ACBPs so as to enhance the knowledge of fatty acid metabolism. The furthering of the knowledge base of ACBPs can only help to enhance the studies for not just tung but other organisms as well.

References

Abbadi, A., Domergue, F., Meyer, A., Riedel, K., Sperling, P., Zank, T.K. and Heinz, E. (2001). Transgenic oilseeds as sustainable source of nutritionally relevant C20 and C22 polyunsaturated fatty acids. European Journal of Lipid Science Technologies **103,** 106–113.

Agarwal, A.K. (2007) Biofuels (alcohols and biodiesel) applications as fuels for internal combustion engines. Progress in Energy and Combustion **33**, 233–271.

Aguilar, P.S., and de Mendoza, D. (2006). Control of fatty acid desaturation: a Mechanism conserved from bacteria to humans. Molecular Microbiology **62,** 1507-1514.

Aitzetmüllera, K., Matthäus, B., Friedrich, H. A new database for seed oil fatty acids – the database SOFA. European Journal of Lipid Science Technologies **105** (2003) 92–103.

Altschul, S.F., Gish, W., Miller, W., Myers, E.W., Lipman, D.J. (1990). Basic local alignment search tool. Journal of Molecular Biology **215,** 403–410

Alves-Bezerra M., Majerowicz D., Grillo L.A., Tremonte H., Almeida C.B., Braz G.R., Sola-Penna M., Paiva-Silva G.O., Gondim K.C. (2010). Serotonin regulates an acyl-CoA-binding protein (ACBP) gene expression in the midgut of Rhodnius prolixus. Insect Biochemistry and Molecular Biology **40,** (2):119-25.

Andersen K.V., Ludvigsen S., Mandrup S., Knudsen J., Poulsen F.M. (1991). The secondary structure in solution of acyl-coenzyme A binding protein from bovine liver using ^{1}H nuclear magnetic resonance spectroscopy. Biochemistry **30**, 10654–10663.

Baud, S. and Lepiniec, L. (2010). Physiological and developmental regulation of seed oil production. Progress in Lipid Research **49,** 235-249.

Biermann, U., Friedt, W., Lang, S., Luhs, W., Machmuller, G., Metzger, J.O., Klaas, M.R., Schafer, H.J. and Schneider, M.P. (2000). New syntheses with oils and fats as renewable raw materials for the chemical industry. Angewandte Chemie International Edition England **39**, 2206–2224.

Bligh, E.G. and Dyer, W.J. (1959). A rapid method of total lipid extraction and purification. Canadian Journal of Biochemistry and Physiology **37**, 911–917.

Braun, S., Matuschewski, K., Rape, M., Thoms, S., and Jentsch, S. (2002). Role of The ubiquitin-selective CDC48(UFD1/NPL4)chaperone (segregase) in ERAD of OLE1 and other substrates. The EMBO Journal **21,** 615-621.

Brown, K., Keeler, W. (2005). The History of Tung Oil. Wildland Weeds **9** (1): 4–24.

Browse, J., McConn, M., James, D., Jr., and Miquel, M. (1993). Mutants of *Arabidopsis* deficient in the synthesis of alpha-linolenate. Biochemical and genetic characterization of the endoplasmic reticulum linoleoyl desaturase. The Journal of Biological Chemistry **268,** 16345-16351.

Browse, J., and Sommerville, C. (1991). Glycerolipid synthesis: biochemistry and regulation. Annual Reviews in Plant Physiological Plant Molecular Biology **42,** 467-506.

Burton, M. Rose, T.M., Faergeman, N.J., Knudsen, J. (2005). Evolution of the acyl-CoA binding protein (ACBP). Biochemistry Journal **392,** 299–307.

Cahoon, E.B., Dietrich, C.R., Meyer, K., Damude, H.G., Dyer, J.M. and Kinney, A.J. (2006). Conjugated fatty acids accumulate to high levels in phospholipids of metabolically engineered soybean and Arabidopsis seeds. Phytochemistry, **67**, 1166–1176.

Cahoon E.B., Shockey J.M., Dietrich C.R., Gidda S.K., Mullen R.T., Dyer J.M. (2007). Engineering oilseeds for sustainable production of industrial and nutritional feedstocks: solving bottlenecks in fatty acid flux. Current Opinions in Plant Biology **10,** (3):236-44.

Chen, Q.F., Xiao, S., Chye, M.L. (2008). Overexpression of the *Arabidopsis* 10-Kilodalton acyl-CoA-binding protein ACBP6 enhances freezing tolerance. Plant Physiology **148,** 304–315.

Christie, W.W. (1986). The positional distributions of fatty acids in triglycerides. In: The Analysis of Oils and Fats, pp. 313-339.

Christie, W.W. (1993). Preparation of ester derivatives of fatty acids for chromatographic analysis. Advances in Lipid Methodology **2**, 69-111.

Chye, M.L. (1998). *Arabidopsis* cDNA encoding a membrane-associated protein with an acyl-CoA binding domain, Plant Molecular Biology **38,** 827–838.

Chye, M.L., Huang, B.Q., Zee, S.Y. (1999). Isolation of a gene encoding *Arabidopsis* membrane-associated acyl-CoA binding protein and immunolocalization of its gene product. Plant Journal **18,** 205–214.

Chye, M.L., Li H.Y., Yung, M.H. (2000). Single amino acid substitutions at the acyl-CoA-binding domain interrupt ^{14}[C]palmitoyl-CoA binding of ACBP2, an *Arabidopsis* acyl-CoA-binding protein with ankyrin repeats. Plant Molecular Biology **44,** 711–721.

Chye, M.L., Xiao, S., Li, H.Y. (2008). Light-regulated expression of mRNAs encoding cytosolic acyl-CoA-binding proteins, ACBP4 and ACBP5. 18th International Symposium on Plant Lipids, Bordeaux, France, pp. 71.

Clough, S.J. and Bent, A.F. (1998). Floral dip: a simplified method for *Agrobacterium*-mediated transformation of *Arabidopsis thaliana.* Plant Journal **16**, 735–743.

Coleman, R.A. and Lee, D.P. (2004). Enzymes of triacylglycerol synthesis and their regulation. Progressions in Lipid Research, **43**, 134-176.

Cuperus, F.P., Boswinkel, G. and Derksen, J.T.P. (1996). The processing of new oilseed crops – an economic evaluation. Journal of the American Oil Chemical Society **73**, 1635–1640.

Dahlqvist, A., Stahl, U., Lenman, M., Banas, A., Lee, M., Sandager, L., Ronne, H. and Stymne, S. (2000). Phospholipid:diacylglycerol acyltransferase: an enzyme that catalyzes the acyl-CoA-independent formation of triacylglycerol in yeast and plants. Proceedings of the National Academy of Sciences USA **97**, 6487–6492.

Das, U.N. (2006). Essential fatty acids – a review. Current Pharmaceutical Biotechnology **7**, 467–482.

Deane, C.M., Salwiński, L., Xenarios, I., and Eisenberg, D. (2002). Protein Interactions: Two Methods for Assessment of the Reliability of High Throughput Observations. Molecular and Cellular Proteomics **1**, 349-356.

DeDuve, C., Baudhuin, P., Mueller, M., Poole, B., (1965). Non-Mitochondrial Oxidizing Particles (Microbodies) in Rat Liver and Kidney and in *Tetrahymena pyriformis.* Biochemical Biophysics Research Community **20**:53-9.

Drexler, H., Spiekermann, P., Meyer, A., Domergue, F., Zank, T., Sperling, P., Abbadi, A. and Heinz, E. (2003). Metabolic engineering of fatty acids for breeding of new oilseed crops: strategies, problems and first results. Journal of Plant Physiology **160**, 779–802.

Dugail, I. and Hajduch, E. (2007). A new look at adipocyte lipid droplets: towards a role in the sensing of triacylglycerol stores? Cellular and Molecular Life Sciences, **64**, 2452-2458.

Duke, J.A. (1979). Ecosystematic data on economic plants. Quarterly Journal of Crude Drug Research. **17** (3–4):91–110.

Duke, J.A. (1983). Handbook of Energy Crops. Unpublished.

Durrett, T., Benning, C. and Ohlrogge, J. (2008). Plant triacylglycerols as feedstocks for the production of biofuels. Plant Journal **54**, 593–607.

Dyer, J.M., Chapital, D.C., Kuan, J.C., Mullen, R.T., Turner, C., McKeon, T.A. and Pepperman, A.B. (2002). Molecular analysis of a bifunctional fatty acid conjugase/desaturase from tung: implications for the evolution of plant fatty acid diversity. Plant Physiology **130**, 2027–2038.

Dyer, J.M. and Mullen, R.T. (2008). Engineering plant oils as high-value industrial feedstocks for biorefining: the need for underpinning cell biology research. Plant Physiology **132**, 11–22.

Dyer, J.M., Stymne, S., Green, A.G., Carlsson A.S. (2008). High-value oils from plants. The Plant Journal **54,** 640-655.

Engeseth, N.J., Pacovsky, R.S., Newman, R., Ohlrogge, J.B. (1996). Characterization of an acyl-CoA-binding protein from *Arabidopsis thaliana*. Archives of Biochemistry and Biophysics **331,** 55–62.

Faergeman, N.J., Knudsen, J. (2009). Role of long-chain fatty acyl-CoA esters in the Regulation of metabolism and in cell signaling. Biochemistry Journal **323,** (1997) 1–12.

Faergeman N.J., Sigurskjold B.W., Kragelund B.B., Andersen K.V., Knudsen J. (1996). Thermodynamics of ligand binding to acyl-coenzyme A binding protein studied by titration calorimetry. Biochemistry **35**, 14118–14126.

Færgeman, N.J., Wadum, M., Feddersen, M., Burton, M., Birthe, B., Kragelund F., and Knudsen, J. (2007). Acyl-CoA binding proteins; structural and functional conservation over 2000 MYA. Molecular and Cellular Biochemistry **299,** 55–65, 2007.

FAOSTAT (2007). ProdSTAT: Crops. Rome: Food and Agriculture Organization of the United Nations.

Feddersen S., Neergaard T.B., Knudsen J., Faergeman N.J. (2007). Transcriptional regulation of phospholipid biosynthesis is linked to fatty acid metabolism by an acyl-CoA-binding-protein-dependent mechanism in *Saccharomyces cerevisiae*. The Journal of Biochemistry **407**(2):219-30.

Gao, W., Xiao, S., Li, H.Y., Tsao, S.W., Chye, M.L. (2006). *Arabidopsis* acyl-CoA-binding Protein ACBP2 interacts with a heavy-metal-binding protein *At*FP6. New Phytology **181,** 89–102.

Gersuk, V.H., Rose, T.M., Todaro, G.J. (1995). Molecular cloning and chromosomal localization of a pseudogene related to the human acyl-CoA binding protein/diazepam binding inhibitor. Genomics **25,** 469–476.

Gietz, R.D., Triggs-Raine, B., Robbins, A., Graham, K., Woods, R. (1997). identification of proteins that interact with a protein of interest: Applications of the yeast two-hybrid system. Molecular and Cellular Biochemistry **172**, 67–79

Graham, I.A., Larson, T. and Napier, J.A. (2007). Rational metabolic engineering of transgenic plants for biosynthesis of omega-3 polyunsaturates. Current Opinions in Biotechnology **18**, 142–147.

Gunstone, F.D., Alander, J., Erhan, S.Z., Sharma, B.K., McKeon, T.A. and Lin, J.-T. (2006). Nonfood uses of oils and fats. In The Lipid Handbook, 3rd edn. (Gunstone, F.D., Harwood, J.L. and Dijkstra, A.J., eds). Boca Raton, FL: Taylor & Francis Group, pp. 591–636.

Gunstone, F.D. and Harwood, J.L. (2006). Occurrence and characterization of oils and fats. In The Lipid Handbook, 3rd edn (Gunstone, F.D., Harwood, J.L. and Dijkstra, A.J., eds). Boca Raton, FL: Taylor & Francis Group, pp. 37–142.

Gurr M.I., Harwood, J.L. and Frayn, K.N. (2002). Lipid Biochemistry (Fifth Edition) (Blackwells Publishing, Oxford).

Hamilton, J.A. (2007). New insights into the roles of proteins and lipids in membrane transport of fatty acids. Prostaglandins, Leukotrienes, and Essential Fatty acids **77**, 355-361.

He, X., Chen, G.Q., Lin, J.T. and McKeon, T.A. (2004). Regulation of diacylglycerol acyltransferase in developing seeds of castor. Lipids **39**, 865–871.

Heinz, E. (1993). Biosynthesis of polyunsaturated fatty acids. In Lipid Metabolism in Plants, T.S. Morre, Jr., ed. (BocaRaton, FL: CRC Press), 33-90.

Hills, M.J., Dann, R., Lydiate, D., Sharpe, A. (1994). Molecular cloning of a cDNA from *Brassica napus L.* for a homologue of acyl-CoA-binding protein. Plant Molecular Biology **25,** 917–920.

Hu, F.B., Stampfer, M.J., Manson, J.E., Rimm, E., Colditz, G.A., Rosner, B.A., Hennekens, C.H., and Willett, W.C. (1997). Dietary fat intake and the risk of coronary heart disease in women. The New England Journal of Medicine **337,** 1491-1499.

Hugly, S., Kunst, L., Somerville, C. (1991). Linkage relationships of mutations that affect fatty acid composition in *Arabidopsis.* Journal of Heredity **82**:484-488.

ISTA Mielke GmbH Hamburg (2002). The revised oil world 2020: supply, demand and prices.

IUPAC Compendium of Chemical Terminology 2nd Edition (1997). International Union of Pure and Applied Chemistry.

Ivell, R., Pusch, W., Balvers, M., Valentin, M., Walther, N., Weinbauer, G. (2000). Progressive inactivation of the haploid expressed gene for the sperm-specific endozepine-like peptide (ELP) through primate evolution. Gene **255,** 335–345.

Jaworski, J., and Cahoon, E.B. (2003). Industrial oils from transgenic plants. Current Opinions in Plant Biology **6,** 178-184.

Kader, J.C. (1996). Lipid-transfer proteins in plants. Annual Review of Plant Physiology and Plant Molecular Biology **47**, 627-654.

Knudsen, J., Neergaard, T.B., Gaigg, B., Jensen, M.V., Hansen, J.K. (2000). Role of acyl-CoA binding protein in acyl-CoA metabolism and acyl-CoA-mediated cell signaling. Journal of Nutrition **130,** (2S Suppl.) 294S–298S.

Knudsen, J., Fiergeman, J., Skott, H., Hummel, R., Borsting, C., Rose, T.M., Skorstensgaard, J., Andersen, T., Hojrup, P., Roepstorff, P., Kridtiansen, K. (1994). Yeast acyl-CoA-binding protein: acyl-CoA-binding affinity and effect on intracellular acyl-CoA pool size. The Journal of Biochemistry **302**, 479-485.

Kohlwein, S.D. (2010). Triacylglycerol homeostasis: insights from yeast. The Journal of Biological Chemistry **285**, 15663-15667.

Kragelund, B. B., Andersen, K. V., Madsen, J. C., Knudsen, J., and Poulsen, F. M. (1993). Three-dimensional structure of the complex between acyl-coenzyme A binding protein and palmitoyl-coenzyme A. Journal of Molecular Biology **230,** 1260–1277.

Kragelund, B.B., Knudsen, J., Poulsen, F.M. (1999). Acyl-coenzyme A binding protein (ACBP). Biochimical Biophysics Acta **1441,** 150–161.

Kragelund B.B., Poulsen K., Andersen K.V., Baldursson T., Kroll J.B., Neergard T.B., Jepsen J., Roepstorff P., Kristiansen K., Poulsen F.M., Knudsen J. (1999). Conserved residues and their role in the structure, function, and stability of acyl-coenzyme A binding protein. The Journal of Biochemistry **38**, 2386–2394.

Kroon, J.T., Wei, W., Simon, W.J. and Slabas, A.R. (2006). Identification and functional expression of a type 2 acyl-CoA:diacylglycerol acyltransferase (DGAT2) in developing castor bean seeds which has high homology to the major triglyceride biosynthetic enzyme of fungi and animals. Phytochemistry, **67**, 2541–2549.

Leung, K.C., Li, H.Y., Mishra, G., Chye, M.L. (2004). ACBP4 and ACBP5, novel *Arabidopsis* acyl-CoA-binding proteins with kelch motifs that bind oleoyl-CoA. Plant Molecular Biology **55,** 297–309.

Larsen, M.K., Tuck, S., Faergeman, N.J., Knudsen, J. (2006). MAA-1, a novel acyl-CoA binding protein involved in endosomal vesicle transport in *Caenorhabditis elegans.* Molecular Biology of the Cell **17,** 4318–4329.

Leung, K.C., Li, H.Y., Mishra, G., Chye, M.L. (2004). ACBP4 and ACBP5, novel *Arabidopsis* acyl-CoA-binding proteins with kelch motifs that bind oleoyl-CoA. Plant Molecular Biology **55,** 297–309.

Leung, K.C., Li, H.Y., Xiao, S., Tse, M.H., Chye, M.L. (2006). *Arabidopsis* ACBP3 is an extracellularly targeted acyl-CoA-binding protein. Planta **223,** 871–881.

Li-Beisson, Y., Shorrosh, B., Beisson, F., Andersson, M.X., Arondel, V., Bates, PD., Baud, S., Bird, D., DeBono, A., Durrett, T.P., Franke, R.B., Graham, I.A., Katayama, K., Kelly, A.A., Larson, T., Markham, J.E., Miquel, M., Molina, I., Nishida, I., Rowland, O., Samuels, L., Schmid, K.M., Wada, H., Welti, R., Xu, C., Zallot, R. and Ohlrogge, J. Acyl-lipid metabolism. In: The Arabidopsis Book, published online (http://www.bioone.org/doi/pdf/10.1199/tab.0133).

Li, H.Y., Chye, M.L. (2003). Membrane localization of *Arabidopsis* acyl-CoA binding protein ACBP2. Plant Molecular Biology **51,** 483–492.

Li, H.Y., Chye, M.L. (2004). *Arabidopsis* acyl-CoA binding protein ACBP2 interacts with an ethylene-responsive element binding protein AtEBP via its ankyrin repeats. Plant Molecular Biology **54,** 233–243.

Li, H.Y., Xiao, S., Chye, M.L. (2008). Ethylene- and pathogen-inducible *Arabidopsis* acyl-CoA-binding protein 4 interacts with an ethylene-responsive element binding protein. Journal of Experimental Botany **59**, 3997–4006.

Li, W., Li, M., Zhang, W., Welti, R., Wang, X. (2004). The plasma membrane-bound phospholipase Dd enhances freezing tolerance in *Arabidopsis thaliana.* Biotechnology **22,** 427–433.

Mackay, I. M. (2007). Real-Time PCR in Microbiology. Caister Academic Press.

Mandrup S., Hojrup P., Kristiansen K., Knudsen J. (1991). Gene synthesis, expression in Escherichia coli, purification and characterization of the recombinant bovine acyl-CoA-binding protein. The Journal of Biochemistry **276**, 817–823.

Mandrup, S., Hummel, R., Ravn, S., Jensen, G., Andreasen, P.H., Gregersen, N., Knudsen, J., Kristiansen, K. (1992). Acyl-CoA-binding protein/diazepam-binding inhibitor gene and pseudogenes. A typical housekeeping gene family. The Journal of Molecular Biology **228,** 1011–1022.

McDonough, V.M., Stukey, J.E., Martin, C.E. (1992). Specificity of unsaturated fatty acid regulated expression of the *Saccharomyces* Cerevisiae OLE1 gene. The Journal of Biological Chemistry **267,** 5931–5936.

Metzger, J.O. and Bornscheuer, U. (2006). Lipids as renewable resources: current state of chemical and biotechnological conversion and diversification. Applied Microbiology and Biotechnology **71**, 13–22.

Metzner, M., Ruecknagel, K.P., Knudsen, J., Kuellertz, G., Mueller-Uri, F., Diettrich, B. (2000). Isolation and characterization of two acyl-CoA-binding proteins from proembryogenic masses of *Digitalis lanata.* Planta **210**: 683-685.

Meza, T.J., Stangeland, B., Mercy, I.S., Skårn, M., Nymoen, D.A., Berg, A., Butenko, M.A., Håkelien, A.M., Haslekås, C., Meza-Zepeda, L.A., Aalen, R.B. (2002). Analyses of single-copy *Arabidopsis* T-DNA-transformed lines show that the presence of vector backbone sequences, short inverted repeats and DNA methylation is not sufficient or necessary for the induction of transgene silencing. Nucleic Acids Research **30**(20): 4556–4566.

Mielewski, D.F., Flanigan, C.M., Perry, C., Zaluzec, M.J. and Killgoar,P.C. (2005). Soybean oil auto applications: developing flexible polyurethane foam formulations containing functionalized soybean oil for automotive applications. Industrial Biotechnology. **1**, 32–34.

Mogensen I.B., Schulenberg H., Hansen H.O., Spener F., Knudsen J. (1987). A novel acyl-CoA binding protein from bovine liver: effect on fatty acid synthesis. The Journal of Biochemistry **241**, 189–192.

Mount, D.W. (2004). Bioinformatics: Sequence and Genome Analysis. Cold Spring Harbor Press.

Moreau, P., Bessoule, J.J., Mongrand, S., Testet P., Vincent, Cassagne, C. (1998). Lipid trafficking in plant cells. Progress in Lipid Research **37,** 371–391.

Mu, H. and Høy, C.E. (2004). The digestion of dietary triacylglycerols. Progress in Lipid Research **43**, 105-133.

Murphy, D.J. (2001). The biogenesis and functions of lipid bodies in animals, plants and microorganisms. Progress in Lipid Research **40**, 325-438.

Napier, J.A. (2007). The production of unusual fatty acids in transgenic plants. Annual Review of Plant Biology **58**, 295–319.

Ohlrogge, J.B., Browse, J. (1995). Lipid biosynthesis. Plant Cell **7** 957–970.

Post-Beittenmiller, D., Roughan, P.G. and Ohlrogge, J.B. (1992). Regulation of plant fatty acid biosynthesis. Analysis of acyl-CoA and acyl-ACP substrate pools in spinach and pea chloroplasts. Plant Physiology **100**, 923-930.

Rasmussen, J. T., Faergeman, N. J., Kristiansen, K., and Knudsen, J. (1994). Acyl-CoA-binding protein (ACBP) can mediate intermembrane acyl-CoA transport and donate acyl-CoA for b-oxidation and glycerolipid synthesis. The Journal of Biochemistry **299,** 165–170.

Rasmussen, J.T., Rosendal, J., Knudsen, J. (1993). Interaction of acyl-CoA binding protein (ACBP) on processes for which acyl-CoA is a substrate, product or inhibitor. The Journal of Biochemistry **292,** 907–913.

Rigaudy, J., Klesney, S.P. (1979). *Nomenclature of Organic Chemistry*.

Ruuska, S.A., Girke, T., Benning, C., Ohlrogge, J.B. (2002). Contrapuntal Networks of Gene Expression during *Arabidopsis* Seed Filling. The Plant Cell **14**, 1191–1206.

Sakurai, H. and Pokorny´, J. (2003). The development and application of novel vegetable oils tailor-made for specific human dietary needs. European Journal of Lipid Science and Technology **105**, 769–778.

Sargent, J.R. and Tacon, A.G.J. (1999). Development of farmed fish: a nutritionally necessary alternative to meat. Proceedings of the Nutrition Society **58**, 377–383.

Schittmayer, M. and Birner-Gruenberger, R. (2009). Functional proteomics in lipid research: Lipases, lipid droplets and lipoproteins. The Journal of Proteomics **72**, 1006-1018.

Schjerling, C.K., Hummel, R., Hansen, J.K., Borsting, C., Mikkelsen, J.M., Kristiansen, K., Knudsen, J. (1996). Disruption of the gene encoding the acyl-CoA binding protein (ACB1) perturbs acyl-CoA metabolism in *Saccharomyces cerevisiae*, The Journal of Biological Chemistry **271,** 22514–22521.

Scheideler, M.A. and Bell, R.M. (1989). Phospholipid dependence of homogeneous, reconstituted sn-glycerol-3-phosphate acyltransferase of Escherichia coli. The Journal of J Biological Chemistry **264** (21):12455-61.

Schneider, M.P. (2006). Plant-oil-based lubricants and hydraulic fluids. The Journal of the Science of Food and Agriculture **86**, 1769–1780.

Shockey, J.M., Gidda, S.K., Chapital, D.C., Kuan, J.C., Dhanoa, P.K., Bland, J.M., Rothstein, S.J., Mullen, R.T. and Dyer, J.M. (2006). Tung tree DGAT1 and DGAT2 have nonredundant functions in triacylglycerol biosynthesis and are localized to different subdomains of the endoplasmic reticulum. Plant Cell, **18**, 2294–2313.

Smith, D.R., Kahng, M.W., Quintanilla-Vega, .B, Fowler, B.A. (1998). High-affinity renal lead-binding proteins in environmentally-exposed humans. Chemical Biology Interactions **115,** 39–52.

Taskinen, J.P., van Aalten, D.M., Knudsen, J., and Wierenga, R.K. (2007). High Resolution Crystal Structures of Unliganded and Liganded Human Liver ACBP Reveal a New Mode of Binding for the Acyl-CoA Ligand. PROTEINS: Structure, Function, and Bioinformatics **66**, 229–238.

Thelan, J.J. and Ohlrogge, J. (2002). Metabolic engineering of fatty acid biosynthesis in plants. Metabolic Engineering **4**, 12-21.

Voelker, T. and Kinney, A.J. (2001). Variations in the biosynthesis of seed-storage lipids. Annual Reviews in Plant Physiology, **52**, 335-361.

Walz, C., Giavalisco, P., Schad, M., Juenger, M., Klose, J., Kehr, J. (2004). Proteomics of curcurbit phloem exudate reveals a network of defence proteins. Phytochemistry **65,** (2004) 1795–1804.

Watt, M.J. and Steinberg, G.R. (2008). Regulation and function of triacylglycerol lipases in cellular metabolism. The Journal of Biological Chemistry **414**, 313-325.

Weber, A.P.M., Weber, K.L., Carr, K., Wilkerson, C., and Ohlrogge, J.B. (2007). Sampling the Arabidopsis Transcriptome with Massively Parallel Pyrosequencing. Plant Physiology **144**, 32–42.

Weselake, R.J., Nykiforuk, C.L., Laroche, A., Patterson, N.A., Wiehler, W.B., Szarka, S.J., Moloney, M.M., Tari, L.W., Derekh, U. (2000). Expression and properties of diacylglycerol acyltransferase from cell-suspension cultures of oilseed rape. Biochemical Society Transactions **28**, part 6.

Whittle E., Cahoon E.B., Subrahmanyam S., Shanklin J. (2005). A multifunctional acyl-acyl carrier protein desaturase from *Hedera helix L.* (English ivy) can synthesize 16- and 18-carbon monoene and diene products. The Journal of Biological Chemistry **31**, 28169-76.

Xiao, S., Chye, M.L. (2009). An Arabidopsis family of six acyl-CoA-binding proteins has three cytosolic members. Plant Physiology and Biochemistry **47,** 479–484.

Xiao, S., Gao, W., Chen, Q.F., Ramalingam, S., Chye, M.L. (2008). Overexpression of membrane-associated acyl-CoA-binding protein ACBP1 enhances lead tolerance in *Arabidopsis.* Plant Journal **54,** 141–151.

Xiao, S., Li, H.Y., Zhang, J.P., Chan, S.W., Chye, M.L. (2008*). Arabidopsis* acyl-CoA-binding proteins ACBP4 and ACBP5 are subcellularly localized to the cytosol and ACBP4 depletion affects membrane lipid composition. Plant Molecular Biology **68,** 571–583.

Yang, P., Li, X., Shipp, M.J., Shockey, J.M., Cahoon, E.B. (2010). Mining the Bitter Melon (*Momordica charantia* L.) Seed Transcriptome by 454 Analysis of Non-Normalized and Normalized cDNA Populations for Conjugated Fatty Acid Metabolism-Related Genes.

Ye, Y., Shibata, Y., Yun, C., Ron D., and Rapoport T. (2004). A membrane protein Complex mediates retro-translocation from the ER lumen into the cytosol. Nature **429,** 841-847.

Yurchenko, O.P., Nykiforuk, C.L., Moloney, M.M., Stahl, U., Banas, A., Stymne, S., Weselake R.J. (2009). A 10-kDa acyl-CoA-binding protein (ACBP) from *Brassica napus* enhances acyl exchange between acyl-CoA and phosphatidylcholine. Plant Biotechnology Journal **7**, 602–610.

Zammit, V.A., Buckett, L.K., Turnbull, A.V., Wure, H. and Proven, A. (2008). Diacylglycerol acyltransferases: Potential roles as pharmacological targets. Pharmacology and Therapeutics **118**, 295-302.

Zechner, R., Kienesberger, P.C., Haemmerle, G., Zimmermann, R. and Lass, A. (2009). Adipose triglyceride lipase and the lipolytic catabolism of cellular fat stores. The Journal of Lipid Research **50**, 3-21.

Vita

Steven Pastor was born in Metairie, Louisiana in 1982. He graduated from Ridgewood Preparatory School in 2001. He enrolled at the University of New Orleans in 2001, and earned his Bachelor of Science Degree in Biological Sciences in May of 2008. He entered the Master of Science program at the University of New Orleans in August of 2008 and performed his thesis research at the United States Department of Agriculture under the direction of Dr. Jay Shockey. In May 2011, he received his Master of Science degree in Biological Sciences from the University of New Orleans.